ДОКЛАДЫ
АКАДЕМИИ НАУК СССР

PROCEEDINGS OF THE ACADEMY OF SCIENCES

OF THE USSR

Physical Chemistry Section

(DOKLADY AKADEMII NAUK SSSR)

IN ENGLISH TRANSLATION

VOL. 115 NOS. 1-6

CONSULTANTS BUREAU, INC.
227 WEST 17TH STREET, NEW YORK 11, N. Y.

an agency for the interpretation of international knowledge

PROCEEDINGS OF THE ACADEMY OF SCIENCES OF THE USSR

(DOKLADY AKADEMY NAUK SSSR)

Section: PHYSICAL CHEMISTRY

Volume 115, Issues 1-6

July-August, 1957

(A Publication of the Academy of Sciences of the USSR)

IN ENGLISH TRANSLATION

CONSULTANTS BUREAU, INC.

227 West 17th Street

New York 11, N. Y.

Printed in the United States

Annual Subscription	$160.00
Single Issue	35.00

SIGNIFICANCE OF ABBREVIATIONS MOST FREQUENTLY ENCOUNTERED IN SOVIET PERIODICALS

FIAN	Phys. Inst. Acad. Sci. USSR.
GDI	Water Power Inst.
GITI	State Sci.-Tech. Press
GITTL	State Tech. and Theor. Lit. Press
GONTI	State United Sci.-Tech. Press
Gosenergoizdat	State Power Press
Goskhimizdat	State Chem. Press
GOST	All-Union State Standard
GTTI	State Tech. and Theor. Lit. Press
IL	Foreign Lit. Press
ISN (Izd. Sov. Nauk)	Soviet Science Press
Izd. AN SSSR	Acad. Sci. USSR Press
Izd. MGU	Moscow State Univ. Press
LEIIZhT	Leningrad Power Inst. of Railroad Engineering
LET	Leningrad Elec. Engr. School
LETI	Leningrad Electrotechnical Inst.
LETIIZhT	Leningrad Electrical Engineering Research Inst. of Railroad Engr.
Mashgiz	State Sci.-Tech. Press for Machine Construction Lit.
MEP	Ministry of Electrical Industry
MES	Ministry of Electrical Power Plants
MESEP	Ministry of Electrical Power Plants and the Electrical Industry
MGU	Moscow State Univ.
MKhTI	Moscow Inst. Chem. Tech.
MOPI	Moscow Regional Pedagogical Inst.
MSP	Ministry of Industrial Construction
NII ZVUKSZAPIOI	Scientific Research Inst. of Sound Recording
NIKFI	Sci. Inst. of Modern Motion Picture Photography
ONTI	United Sci.-Tech. Press
OTI	Division of Technical Information
OTN	Div. Tech. Sci.
Stroiizdat	Construction Press
TOE	Association of Power Engineers
TsKTI	Central Research Inst. for Boilers and Turbines
TsNIEL	Central Scientific Research Elec. Engr. Lab.
TsNIEL-MES	Central Scientific Research Elec. Engr. Lab.–Ministry of Electric Power Plants
TsVTI	Central Office of Economic Information
UF	Ural Branch
VIESKh	All-Union Inst. of Rural Elec. Power Stations
VNIIM	All-Union Scientific Research Inst. of Meteorology
VNIIZhDT	All-Union Scientific Research Inst. of Railroad Engineering
VTI	All-Union Thermotech. Inst.
VZEI	All-Union Power Correspondence Inst.

Note: Abbreviations not on this list and not explained in the translation have been transliterated, no further information about their significance being available to us. – Publisher.

ON THE THEORY OF ORDERING IN ALLOYS

I. L. Aptekar

(Presented by Academician G. V. Kurdyumov, January 24, 1957)

As is known, in an examination of long-range order in mixed alloys all lattice points of the lattice are divided into two classes (1 and 2). The presence of long-range order is thus characterized by the fact that the probability of finding an atom of kind A in lattice points of one of the classes (say, 1) is larger than that of finding it in lattice points of the second class. For the description of long-range order a parameter is introduced

$$\eta = P_A^{(1)} - P_A^{(2)} \tag{1}$$

Here $P_A^{(1)}$ and $P_A^{(2)}$ are the probabilities that an atom of kind A be found in a lattice point of classes 1 and 2, respectively.

The presence of long-range order as a rule leads to a change in the mutual relationship of the atoms. This change can be described with the help of the parameter of short-range order:

$$\sigma = \frac{N_{AA}^0 - N_{AA}}{N_{AA}^0 - N_{AA}^1}. \tag{2}$$

Here N_{AA}^0 is the number of pairs of type AA in the case of complete disorder, N_{AA} in the actual condition observed, and N_{AA}^1 in the case of complete order.

If there is no local order, i. e., if the probability of finding an atom in a given lattice point depends only on the class of the lattice point and not on the relative number of atoms of kinds A and B surrounding this lattice point, then σ is a single-valued function of η.

It can be shown, for example, that for the biatomic case with equal numbers of the two kinds of atoms and a lattice in which lattice points of class 1 are surrounded only by lattice points of class 2 and vice versa, the simple relation exists:

$$\sigma = \eta^2. \tag{3}$$

However, in the general case of an alloy characterized by the parameter of long-range order, η replaces the local order. Such cases are actually found experimentally [1, 2]. If at a given η in the absence of local order $N_{AA} = N_{AA}^1$, then in the presence of local order and at the same η $N_{AA} \neq N_{AA}^1$. Let us accept that in the general case $N_{AA} = N_{AA}^1 (1 - x)$, where x is the parameter of local order. For these cases, if the relation (3) is true, we obtain on the basis of (2):

$$\sigma = \eta^2 + x(1 - \eta^2). \tag{4}$$

We shall illustrate the above graphically in order to make it clear. We select a linear chain of lattice points in an alloy, in which lattice points of classes 1 and 2 alternate. We plot the probability of finding an atom of kind A at any point against the distance of that point from a lattice point of class 1 occupied by an atom of kind A. In this way we may compare schematically the three cases, long-range order without local order ($\eta \neq 0$, $x = 0$); long-range order with local order ($\eta \neq 0$; $x \neq 0$) and short-range order ($\eta = 0$; $x = \sigma$) as has been shown in graphs a, b, c, corresponding to these cases, respectively, in Figure 1.

From graphs b and c it is evident that the distribution of the atoms in the immediate neighborhood of a given atom will be identical for both $\eta = 0$ and $\eta \neq 0$ (if $r < r_0$). The effect of the long-range order alone (in the absence of local order) is apparent at distances greater than the "radius" of action of local order r_0. It is assumed in the following in any discussion of long-range order that the volume of the alloy is large relative to r_0.

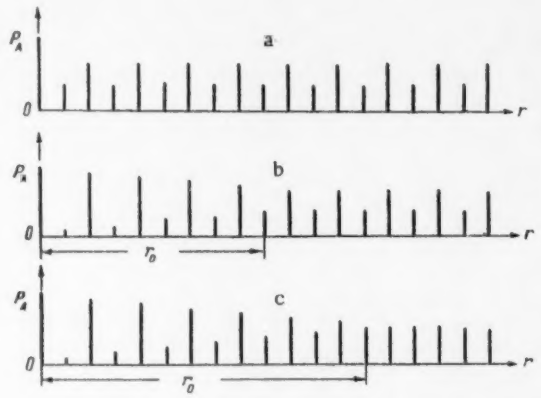

Fig. 1

In the majority of theoretical studies devoted to processes of ordering, the energy is considered to be approximately equal to the sum of the interactions of nearest neighbors. In this approximation the configuration energy of fusion has the form:

$$E = E_0 + V\sigma. \tag{5}$$

Here E_0 is a term which is not dependent on order and

$$V = NK\left(V_{AB} - \frac{V_{AA} + V_{BB}}{2}\right)$$

where N is the total number of atoms; K is a constant dependent on the structure and coordination number; V_{AA}, V_{AB}, and V_{BB} are the energy of pairs of the type AA, AB, and BB respectively.

It is evident from Equation (4) that various values of the parameter η may correspond to the same degree of short-range order (σ = const.), including the case $\eta = 0$. For this reason, it is clear that the value of the parameter σ is not sufficient to specify uniquely long-range order. Consequently, it is doubtful whether long-range order in alloys can be described by means of an expression for energy which is simply a function of σ [see relation (5)].

Moreover, in the nearest neighbor approximation for any σ = const, the state having the lowest free energy is that in which there is no long-range order. Thus, for any given short-range order, the equilibrium state of fusion will be a state having no long-range order. Indeed, it is at once obvious that the additional requirement imposed by the condition $\eta \neq 0$ leads to a decrease in the entropy of fusion. For constant σ and E the free energy $F = E - TS$ is thus smaller at $\eta = 0$ than at $\eta \neq 0$ in this approximation. We note that

inclusion of sums of interactions of atoms present in several spheres around the given atom and not only in the first sphere does not introduce anything basically new into our argument.

For the sake of clarity we shall treat a concrete example. Let us consider the quasi-chemical theory of ordering of Fowler and Guggenheim [3] which has been greatly elaborated in past years. In this theory, separate pairs of atoms are considered as independent units, so that the number W of various configurations of a system is assumed to be proportional to the number of ways in which it is possible to obtain any given number of pairs AA, AB, BA, and BB from the total number of pairs in the system. After some additional assumptions, W is given by the relation:

$$W(\sigma, \eta) = \frac{N^{(1)}!}{(N^{(1)}P_A^{(1)})!\,(N^{(1)}P_B^{(1)})!} \cdot \frac{N^{(2)}!}{(N^{(2)}P_A^{(2)})!\,(N^{(2)}P_B^{(2)})!} \times$$
$$\times \frac{\left(\frac{N_{A'B}}{Z/2}\right)!\left(\frac{N_{B'A}}{Z/2}\right)!\left(\frac{N_{A'A}}{Z/2}\right)!\left(\frac{N_{B'A}}{Z/2}\right)!}{\left(\frac{N_{AB}}{z/2}\right)!\left(\frac{N_{BA}}{z/2}\right)!\left(\frac{N_{AA}}{z/2}\right)!\left(\frac{N_{BB}}{z/2}\right)!} \tag{6}$$

Here $N^{(1)}$ and $N^{(2)}$ are the corresponding number of lattice points of classes 1 and 2, and z is the coordination number; the first line in the product on the right-hand side refers to the case in which no local order is present ($x = 0$).

It is easy to show that if σ = const., the number of configurations W increases with decreasing values of the parameter of long-range order η. Therefore, $W(\sigma, 0) > W(\sigma, \eta)$ and as a result $S(\sigma, 0) > S(\sigma, \eta)$. Thus even in the given case we arrive at $F(\sigma,0) < F(\sigma, \eta)$.

On the basis of the above, the general conclusion can be drawn that it is fundamentally impossible to describe the appearance of long-range order (for $\sigma \neq 1$ and sufficiently large volumes of an alloy) by approximations considering solely the direct interaction of nearest neighbors.

The origin of long-range order is in reality a cooperative phenomenon associated with the alloy as a whole. The cooperative nature of the energy of ordering was observed by Slater [4]. This author attributes the energy gain of long-range order to the decrease of Fermi energy (the energy of generalized electrons) together with the appearance of new Brillouin zones. An approach of this sort enables him to explain the origin of long-range order in the case of alloys of CuPt, in which long-range order does not lead to changes in the region of the first coordination sphere.

It is important to stress that theories taking account only of the energy of close interactions ignore fundamentally not only the electron theory of metals but also the general thermodynamic considerations of Landau [5] regarding the role of symmetry in ordering processes. A consideration which takes account of specific energies of long-range order can be closely associated with the electron theory of metals as well as with the theory of Landau.

It is necessary to note that in the first works on ordering [6, 7] the energy of fusion was given as a function of the parameter of long-range order only:

$$E = E_0 + U\eta^2. \tag{7}$$

However, after the work of Bethe, Equation (5) became widely used for energy.

Since in the general case of fusion it is required that one take into account the energy contribution of both short-range and long-range order, the expression for the total energy must be considered a function of the parameters σ and η.

If it is assumed that the energy contribution of long-range order is independent of local order and if relation (5) and (7) are employed, then the following expression may be written for the total energy of fusion:

$$E = E_0 + U\eta^2 + V\sigma. \tag{8}$$

Institute of Precision Fusion of the
Central Research Institute of Ferrous Metals

Received January 21, 1957

LITERATURE CITED

[1] G. Cowly, Phys. Rev., 77, 669 (1950).

[2] D. R. Chipman, J. Appl. Phys., 27, 739 (1956).

[3] R. H. Fouler, E. A. Gugenheim, Statistical Thermodynamics, Cambridge, 1939.

[4] J. C. Slater, Phys. Rev., 84, 179 (1951).

[5] L. D. Landau, Sow. Phys., 11, 546 (1937).

[6] W. S. Gorsky, Zs. Phys., 50, 64 (1928).

[7] W. L. Bragg, E. J. Williams, Proc. Roy. Soc., A 145, 699 (1934).

[8] H. A. Bethe, Proc. Roy. Soc., A 150, 552 (1935).

THE THEORY OF FORCE INTERACTION OF RESTING DROPLETS AT ANY DISTANCE AT PSYCHROMETRIC TEMPERATURE

S. S. Dukhin and Corresponding Member of Acad. Sci. USSR B. V. Deryagin

In a former paper [1] we have studied, to a first-order approximation, the diffusion interaction of droplets so distant from each other that each droplet may be regarded as present in a uniform diffusion field of the other. The ratio of the partial density of the steam ρ' to the partial density of the air ρ'' occurs as a parameter which is small in this theory

$$\lambda = \rho'/\rho'' \ll 1. \tag{1}$$

Below we treat the analogous case of the interaction of resting droplets at any* distance in stationary and adiabatic flow during phase transition with a calculation of first- and second-order terms of λ. By taking advantage of the similarity of the processes of heat transfer and diffusion, it is not difficult to demonstrate that, during the adiabatic flow of phase transition, i. e. in the absence of heat sources or sinks in the droplet, the temperature T under the surface of the droplet does not vary and equals the psychrometric temperature. This will simplify our treatment, since any kind of specificity of interaction will be dependent on this fact.

1. From the previously obtained results [1], we write the equations and boundary conditions describing the velocity and flow fields in diffusion during phase transition at the surfaces of two spherical particles (droplets) 1 and 2 of radii R_1 and R_2, respectively; we assume the steam-air medium to be isothermal and at rest (of infinite extent) and define two systems of spherical coordinates having their origins at the centers of the two particles, respectively:

$$\rho(\mathbf{v}\nabla)\mathbf{v} = -\operatorname{grad} p + \eta\Delta\mathbf{v} + (\zeta + \eta/3)\operatorname{grad}\operatorname{div}\mathbf{v}; \tag{2}$$

$$\operatorname{div}\rho\mathbf{v} = 0; \tag{3}$$

$$\operatorname{div}[\rho''\mathbf{v} + D(\rho'' + \rho')\nabla\rho'/(\rho'' + \rho')] = 0; \tag{4}$$

$$p = RT(\rho''/\mu'' + \rho'/\mu'); \tag{5}$$

$$v|_{r\to\infty} = 0; \tag{6}$$

$$\rho'|_{r\to\infty} = \rho'_\infty = \text{const}; \tag{7}$$

$$\rho'(R_1) = \rho'_s[T(R_1)],\ \rho'(R_2) = \rho'_s[T(R_2)]; \tag{8}$$

$$\left[\rho'' v_2 + D(\rho'' + \rho')\nabla\frac{\rho'}{\rho'' + \rho'}\right]\Big|_{r_1=R_1} = 0,$$

$$\left[\rho'' v_2 + D(\rho'' + \rho')\nabla\frac{\rho'}{\rho'' + \rho'}\right]\Big|_{r_2=R_2} = 0; \tag{9}$$

$$v_{0_1}(R_1, \vartheta_1) = 0, \quad v_{0_2}(R_2, \vartheta_2) = 0, \tag{10}$$

* When the distance between the surfaces of two droplets is very small the pressure in the steam-air space between them increases greatly [2] causing the form of the droplets to deviate from the spherical, in which case the present theory is no longer applicable.

where $\underline{v}$ is the velocity of the particles of the mixture, $\underline{p}$ is pressure, η and ζ are the coefficients of the usual and volumetric viscosity for air, $\rho = \rho'' + \rho'$, μ' and μ'' are the molecular weights of steam and air, D is the diffusion coefficient of steam in air, and $\rho_s'(T)$ is the density of steam in the saturated mixture at temperature T.

The character of the boundary conditions (6) - (10) suggests that the following relation should exist between the velocity and partial-concentration fields:

$$v = -D(1 + \rho'/\rho'')\nabla\frac{\rho'}{\rho'' + \rho'}. \tag{11}$$

We see that in this case Condition (9) and Equation (4) will be simultaneously satisfied, Condition (6) will be fulfilled because of (7), and Conditions (10) will be fulfilled because of the isothermal conditions at the surface following from (8) and from the insignificance of variations in ρ'' from constant value at the surface as concluded from evaluation of variations in the pressure from constant value employing (2), (5), (6), and (10). Relation (11) has a simple and important physical significance: the total flow of air at each point in space (i. e. not only at the surface boundaries as already follows from (9) and (10)) is equal to zero; the steam diffuses through motionless air. Since the right-hand side of (11) is equal to the gradient of the potential φ, where

$$\varphi = -D\ln(1 + \rho'/\rho''), \tag{12}$$

it is noted that Stefanov laminar flow (Re << 1) of a viscous medium is found to be a potential.* This considerably lightens the task of calculating the diffusion forces, since instead of the exceedingly complicated system of equations and boundary conditions (2-10), it is sufficient to consider the equation for φ.

2. It is convenient to transform the equation for φ obtained from (3) by substitution for ρ and $\mathbf{v}$ by their respective expressions in φ to a function of a new variable $\chi = (\varphi - \varphi|_{r\to\infty})/D$, which function under conditions (1), if only first- and second-order terms in λ are retained, takes the form:

$$\Delta\chi + (1 - \mu''/\mu')(\Delta\chi)^2 = 0. \tag{13}$$

At infinity χ becomes zero; on the surfaces of droplets it has the constant values

$$\chi(R_1, \theta_1) = \tau_1 = \delta\rho_1'/\rho'' + 0(\lambda^2),\ \chi(R_2, \theta_2) = \tau_2 = \delta\rho_2'/\rho'' + 0(\lambda^2), \tag{14}$$

where

$$\delta\rho_1' = \rho'(R_1) - \rho_\infty';\ \delta\rho_2' = \rho'(R_2) - \rho_\infty'.$$

We expand χ as a power series in powers of λ: $\chi = \chi_1 + \chi_2 + \ldots$, where χ_1 is of the order of λ and χ_2 of the order of λ^2. For the determination of χ_1 and χ_2 we obtain the equations

$$\Delta\chi_1 = 0; \tag{15}$$

$$\chi_1(R_1) = \tau_1,\quad \chi_1(R_2) + \tau_2.\quad \chi_1|_{r\to\infty} = 0; \tag{16}$$

$$\Delta\chi_2 + (1 - \mu''/\mu')(\nabla\chi_1)^2 = 0; \tag{17}$$

$$\chi_2(R_1) = 0,\ \chi_2(R_2) = 0,\ \chi_2|_{r\to\infty} = 0. \tag{18}$$

* Nonvortical motion does not give the hydrodynamic solution for a viscous fluid because, although it does satisfy the fundamental equations, it does not satisfy the boundary conditions. The relationship with the Stefanov-flow potential arises from the nature of the boundary conditions at the surfaces of the phase transition.

Since χ_1 is a harmonic function, $(\mu''/\mu'-1)\ \chi_1^2/2$ will be a particular solution of (17); thus, if we neglect the terms higher than order two in λ, we obtain

$$\chi = \chi_1 + \psi + (\mu''/\mu' - 1)\chi_1^2/2, \tag{19}$$

where ψ is a harmonic function.

3. From (15), (16), and (19) mixed tensors of viscous stress may be written directly as functions of χ_1, expressing p as a function of χ_1 by means of (2) after transformation by permutation of the differential operators and subsequent integration. Then by means of elemental, but rather cumbersome transformations, we obtain, using (19), the expression for the resultant force of droplet 1 on droplet 2

$$F = 2\pi R_2^2 \int_0^\pi (p_{rr}\cos\theta_2 - p_{r\theta}\sin\theta_2)\sin\theta_2\, d\theta_2 =$$

$$= 4\pi R_2^2 D\eta \left\{ [1 + (\mu''/\mu' - 1)\chi_1(R_2)]\, I_1(\chi_1) + I_1(\psi) + \right.$$

$$\left. + \frac{1}{2}\left[\left(\frac{4}{3} - \zeta/\eta\right)(\mu''/\mu' - 1) + D/2\nu\right] I_1(\chi_1)\right\}, \tag{20}$$

where

$$I_1(\chi_1) = \int_0^\pi \left[\cos\theta_2 \frac{\partial^2\chi_1}{\partial r_2^2} - \sin\theta_2 \frac{\partial}{\partial r_2}\left(\frac{1}{r_2}\frac{\partial\chi_1}{\partial r_2}\right)\right]\Bigg|_{r_1=R_1} \sin\theta_2\, d\theta_2,$$

$$I_2(\chi_1) = \int_0^\pi \left(\frac{\partial\chi_1}{\partial r_2}(R_2)\right)^2 \cos\theta_2 \sin\theta_2\, d\theta_2.$$

4. As is known(D'Alambert paradox)a body in motion in an ideal incompressible fluid does not encounter resistance. Even though the potential of Stefanov flow has a laminar viscous character, it can also be shown for it that the resultant force acting on the droplet* in a viscous medium is equal to zero if the potential of the velocities is a harmonic function and if the inert term which in this case is a second-order term, may be neglected. Since after these limitations the resultant force contains only the terms with $I_1(\chi_1)$ and $I_1(\psi)$, the principle formulated above follows from the equality of $I_1(\psi)$ to zero, where φ is an arbitrary harmonic function. With the calculation of the second-order approximation

$$F = \varkappa 2\pi R_2^2 \int_0^\pi \left(\frac{\partial\chi_1}{\partial r_2}\Big|_{r_1=R_1}\right)^2 \Big/ 2\cos\theta_2 \sin\theta_2\, d\theta_2, \tag{21}$$

where

$$\varkappa = 2D\eta\left[\left(\frac{4}{3} - \zeta/\eta\right)(\mu''/\mu' - 1) + \frac{D}{2\nu}\right],$$

it is natural to define κ as a constant of diffusion interaction. Thus in the first-order approximation and at $Re \ll 1$, the interaction of the droplets over all distances is zero. This conclusion, obtained on the basis of a general consideration of the problem, agrees very well with the result of direct calculation of the interaction of droplets over large distances which vanished in the first-order approximation.

* Not only of spherical but also of arbitrary shape and size.

5. A remarkable analogy between diffusion interaction and electrostatic interaction follows from Equation (21) since the total electrostatic force acting on a conducting sphere is expressed as a function of the potential of the electrostatic field V analogous to χ_1 ; in this, the dielectric constant ϵ can be compared with the constant of diffusion interaction. The value of this analogy increases considerably in view of the fact that χ_1 and V both satisfy the Laplace equation and assume a constant value at the surface boundaries. This* permits the direct expression of the force of diffusion interaction by means of the equation for the electrostatic interaction of conducting spheres, replacing ϵ with κ and the values of V at the surfaces of the spheres with those of χ_1 at the surfaces of the droplets

$$F = \frac{\varkappa}{2\varepsilon(\rho'')^2}\left[\frac{\partial c_{11}}{\partial h}(\delta\rho_1')^2 + 2\frac{\partial c_{12}}{\partial h}\delta\rho_1'\delta\rho_2' + \frac{\partial c_{22}}{\partial h}(\delta\rho_2')^2\right],$$

where $\underline{h}$ is the distance between the centers of the droplets, and C_{11}, C_{12}, and C_{22} are the capacities calculated for the cases of interactions of spheres in [3] and where, after substitution of (14), the terms of order three and higher were neglected.

We shall state the expression for the interaction of droplets over large distances obtained directly from Coulomb's law:

$$F = 4\pi\varkappa\left(\frac{\delta\rho_1'}{\rho''}\right)\left(\frac{\delta\rho_2'}{\rho''}\right)\frac{R_1R_2}{h^2}.$$

Although the absolute magnitude of the diffusion force for a relatively small concentration gradient of steam is small, its slow decrease, inversely proportional to the square of the distance, is essential. The sign of the diffusion force is determined by the agreement or difference in the direction of the phase transition at the surface of the droplets and also by the sign of κ, the qualitative composition of the steam-air mixture. In an interaction of water droplets in air $\mu'' > \mu', \zeta/\eta < \frac{4}{3}$, so that κ is positive. In this system, two droplets will repel each other if the direction of the phase transition at their respective surfaces is the same, i. e. if evaporation (or condensation) is occurring at both surfaces, and will attract each other if the directions are opposed.

Received January 29, 1957

LITERATURE CITED

[1] B. V. Deryagin, S. S. Dykhin, Proc. Acad. Sci. USSR, 106, 851 (1956).

[2] B. V. Deryagin, P. S. Prokhorov, Proc. Acad. Sci. USSR, 54, 511 (1946).

[3] W. Smythe, Static and Dynamic Electricity (Foreign Lit. Press, 1954) **

* If the influence of diffusion on the process of heat transmission is calculated the similarity of the fields of temperature and concentration is no longer valid as a result of which a change of temperature below the surface of the droplet takes place. This variation of the temperature within the droplets, the disturbance of their isothermal nature, leads to some deviation of the Stefanov flow from a potential. In view of the small magnitude of this effect, the correction of the error arising from it in section 5 presumably should not be significant. A strict consideration of this problem presents large mathematical difficulties. It should be pointed out that the deviation from isothermal nature of the temperature field of the droplet is a second-order effect and could influence the results stated in sections 1-4 which are based on the consideration of the Stefanov flow in the first-order approximation.

** [Russian Translation].

ABSORPTION SPECTRA OF SOME TETRAVALENT URANIUM COMPOUNDS AT LIQUID NITROGEN TEMPERATURE

V. T. Aleksanyan

(Presented by Academician A. N. Frumkin, February 7, 1957)

1. The series of features of the absorption spectra of lanthanide compounds in the solid and liquid state, for example the extremely narrow absorption bands, have been explained by the presence of unbounded electrons in the 4f orbit of these elements, and the bands in the infrared, visible, and near ultraviolet regions have been interpreted as transitions within the 4f orbit [1]. Apparently, such also is the nature of the absorption spectra of compounds of the actinide series, which bear considerable similarity to the spectra of the lanthanide compounds [2]. But, judging from numerous experimental data, this similarity is not so striking for the first elements of the actinide series, particularly uranium, which differs considerable in physical and chemical properties from the elements located closer to the middle of the actinide series [2].

Most of the spectral data for compounds of trivalent and tetravalent uranium (for which, respectively, three and two unbounded electrons can be expected in the 5f orbit) relate to solutions, where the bands are considerably broader. For the solid state, there have been investigated only the reflection spectra of UF_4, UCl_4, UBr_4, K_2UF_6, K_2UCl_6, $U(SO_4)_2$, $U(SO_4)_2 \cdot 4H_2O$, $U(SO_4)_2 \cdot 8H_2O$, and UCl_3 [3] and the absorption spectra of UF_4, $NaUF_5$, KUF_5, Na_2UF_6 (two modifications), UCl_3, and UCl_4 [4-6].

2. In connection with the above, we resolved to investigate the absorption spectra of U(IV) compounds in the solid state at a low temperature in order to clarify to what extent these spectra can be connected to the possible presence of the remaining two valence electrons in the 5f orbit which are not participating in bonds. In the present work are presented the results of an investigation of the absorption spectra in the visible region of seven compounds of U(IV):* $U(SO_4)_2 \cdot 8H_2O$, $U(C_2O_4)_2 \cdot 6H_2O$, $K_4[U(C_2O_4)_4] \cdot 5H_2O$, $K_2Sr[U(C_2O_4)_4] \cdot 8H_2O$, $Ca_2[U(C_2O_4)_4] \cdot 6H_2O$, $Ba_2[U(C_2O_4)_4] \cdot 8H_2O$ and $Na_4[U(P_2O_7)_2] \cdot 8H_2O$, of which $Ca_2[U(C_2O_4)_4] \cdot 6H_2O$ was prepared for the first time.

3. The spectra obtained differed rather considerably in character from each other. Certain of them (the spectra of $Na_4[U(P_2O_7)_2] \cdot 8H_2O$, and $U(SO_4)_2 \cdot 8H_2O$) consisted of very diffuse and broad bands with weak indications of structure. On the other hand, the bands of $U(C_2O_4)_2 \cdot 6H_2O$, $K_2Sr[U(C_2O_4)_4] \cdot 8H_2O$ and, especially, $Ca_2[U(C_2O_4)_4] \cdot 6H_2O$ and $Ba_2[U(C_2O_4)_4] \cdot 8H_2O$, which are broad at room temperature, were, at −196°, broken up into a large number of preeminently narrow bands grouped in separate regions of the spectrum. We observed three such groups: in the regions from 6900-6700 to 6300-6200 A (I), from 5700-5500 to 5400-5300 A (II), and from 5200-5150 to 5050-4900 A (III). It can be assumed that there is a fourth group of bands in the region 8000-8500 A, which was observed in the spectrum of $U(C_2O_4)_2 \cdot 6H_2O$. The wave lengths found for these groups of bands are in agreement with data on the broad bands in the absorption spectra of solutions [3, 7, 8]. Beginning at 4900-4800 A, the character of the spectra change markedly. The bands become more diffuse and broader, and the number of details of fine spectra decreases significantly. One more group of several broad bands in the region 4450-4250 A, also observed in the spectra of solutions [8], was observed in this part of the spectra.

* The author expresses his deep appreciation to the staff of the Laboratory of Chemical Analysis of the Institute of Organic Chemistry of the Academy of Sciences USSR for their determination of the content of carbon and water of crystallization in the compounds synthesized.

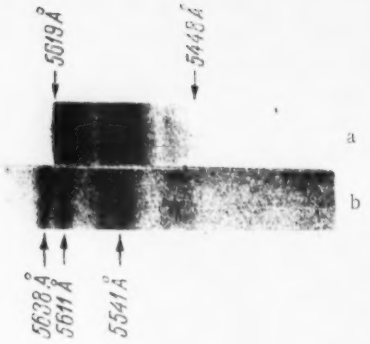

Fig. 1. Second group of bands in the absorption spectra of thin layers of $Ba_2[U(C_2O_4)_4] \cdot 8H_2O$ (a) and $Ca_2[U(C_2O_4)_4] \cdot 6H_2O$ (b).

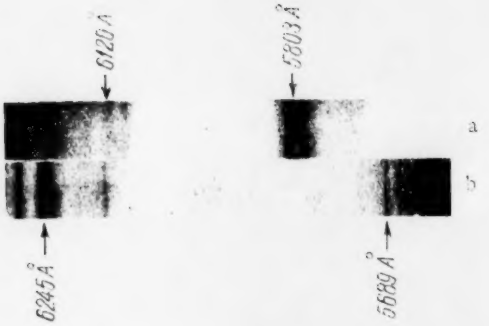

Fig. 2. Absorption region between the first and second groups of bands in the spectra of $U(C_2O_4)_2 \cdot 6H_2O$ (a) and $Ba_2[U(C_2O_4)_4] \cdot 8H_2O$ (b).

TABLE 1

Found ν_{vib} in cm^{-1}		Frequencies of bands in infrared absorption spectrum *
$Ca_2[U(C_2O_4)_4] \cdot 6H_2O$	$Ba_2[U(C_2O_4)_4] \cdot 8H_2O$	$(NH_4)_4[U(C_2O_4)_4] \cdot 6H_2O$
499±5	500±2	—
—	—	670 (w.)
810±3	—	790 (str.)
—	—	900 (str.)
1165±4 (?)	—	—
1308±4	1293±4	1320 (w.)
1430±1 (?)	—	—
1650±6	1630±4	1630 (str.)

* Evaluated from the graphical data cited in [11]; region to 600 cm^{-1} not investigated.

TABLE 2

Interpretation version	Expected ratio $P_I : P_{II} : P_{III}$		
	In a field with cubic symmetry	In a field with hexagonal symmetry	In a field with tetragonal symmetry or less
First	2 : 1 : 2	2 : 1 : 2	9 : 5 : 9
Second	1 : 6 : 2	2 : 9 : 3	3 : 13 : 5

Each group consists of several intense and, for the most part, sharp bands located in the center (Figure 1), a large number of weak, but also predominately sharp, bands in the long wave length region, and comparatively broad bands in the background of considerable intensity in the short wave length region. In those cases where the structure of the individual groups of bands is poor or altogether unresolved, in the short wave length groups in place of individual bands there is a long "dress train" slowly diminishing in intensity. During the photographing of thick layers of the compounds, there was observed between the basic groups of bands a significantly large number of weak bands, the intensity of which gradually diminished in the direction of shorter wave lengths (Figure 2). These features were very characteristic of the spectra investigated.

4. We assume that the most intense bands in each group correspond to purely electronic transitions from the basic state of the uranium ion. In addition, the accompanying long-wave bands of each group can be interpreted as pure electronic transitions from excited sub-levels of the basic state of the uranium ion, arising as a consequence of the removing of the degeneracy with respect to J in the field of the crystal lattice. In the spectrum of $Ca_2[U(C_2O_4)_4] \cdot 6H_2O$, such long-wave members of the intense bands of the group are removed from the latter by 157 ± 4 cm^{-1}, in the spectrum of $Ba_2[U(C_2O_4)_4] \cdot 8H_2O$ by 104 ± 4 cm^{-1} and 225 ± 4 cm^{-1}, with the average accuracy of determination of the position of the narrow and broad bands equal, respectively, to $\pm$ 2-4 cm^{-1} and $\pm$ 5-7 cm^{-1}. The weak bands intermediate the individual groups, also duplicating the intense bands of the groups, can be related to transitions of the type $\nu_{el} + \nu_{vib}$, where ν_{vib} is the vibrational frequency of $C_2O_4^{-2}$, $P_2O_7^{-4}$, SO_4^{-2}, and, possibly, H_2O. Such transitions have also been observed in the absorption spectra of compounds of the lanthanides [9]. In fact, the found values of ν_{vib} in the spectra of $Ca_2[U(C_2O_4)_4] \cdot 6H_2O$ and $Ba_2[U(C_2O_4)_4] \cdot 8H_2O$ agree satisfactorily with data from the infrared absorption spectrum of the related compounds $(NH_4)_4[U(C_2O_4)_4] \cdot 6H_2O$ [10] (see Table 1).

In view of the great diffuseness of the other spectra, data from their analysis is less reliable, and we have not presented them. The bands and the background in the short-wave parts of the groups can apparently be related to combinations of electronic shifts with extraneous vibrations of the crystal lattice.

5. According to the calculations of Jorgensen [8], the appearance of bands in the red, green, and blue regions of the spectra of U(IV) solutions (Groups I, II, and III in the spectra of crystals) are connected with transitions from the basic level $^3H_4$ U (IV) $5f^2$ to excited levels corresponding to $^3F_4$ (or $^1G_4$), $^1D_2$, and $^1G_4$ (or $^3F_4$) with the same configuration. Jorgensen [8] also presented the results of another calculation, one based on the hypothesis of Gruen [12]. In this case, bands I, II, and III are interpreted as the transitions $^3H_4 \rightarrow {}^3P_1$, $^3H_4 \rightarrow {}^1I_6$ and $^3H_4 \rightarrow {}^1D_2$. Our data are undoubtedly subject to both versions of interpretation. As is well known [11], in a crystal field, depending on its symmetry degeneration of the levels with respect to J is partially or completely removed. The number of sublevels, P_J formed in this manner was determined for fields of various symmetries by the method of group theory [11]. In Table 2 is presented the expected ratio $p_I : p_{II} : p_{III}$ in fields of various symmetries for both versions of the interpretation of the spectrum of U(IV).

The number of sublevels in the higher states of U(IV) can be judged by the number of intense bands in the corresponding groups of bands. According to our data, $p_I : p_{II} : p_{III} \approx 2:2:1$, which contradicts both versions of interpretation.

In the present communication, we limit ourselves to a statement of the discrepency between our data and the attempts in the literature to interpret the absorption spectra of U(IV) on the basis of the $5f-5f$ hypothesis. Possible reasons will be presented after publication of the experimental data at our disposition.

The author is glad to have this opportunity to express his deep appreciation to his scientific leader Associate Member Acad. Sci. USSR Ya. K. Syrkin for aid during the course of completing the present work and to Kh. E. Sterin for valuable counsel during the preparation of the present article. The author also acknowledges with appreciation the aid of Academician G. S. Landsberg for a number of valuable comments on the present work.

Note in proof. After submission of the manuscript to the editor, there appeared in the literature a description of the synthesis of $Ca_2[U(C_2O_4)_4] \cdot 6H_2O$ [13].

Commission on Spectroscopy with the Division
of Physical-Mathematical Sciences
Academy of Sciences USSR

Received February 6, 1957

LITERATURE CITED

[1] M. A. Elyashevich, Spectra of the Rare Earths,* 1953.

[2] The Actinide Elements, edited by G. Seaborg and J. Katz, Foreign Lit. Press, 1956. (Translation).

* In Russian.

[3] F. Ephraim and M. Mezener, Helv. Chim. Acta, 16, 1257 (1933).

[4] S. Freed and F. J. Leitz, J. Chem. Phys. 17, 540 (1949).

[5] K. Sancier and S. Freed, J. Chem. Phys. 20, 349 (1952).

[6] D. M. Gruen, J. Am. Chem. Soc. 76, 3850 (1954).

[7] T. Dreisch and O. Kallscheuer, Zs. Phys. Chem. B45, 19 (1939).

[8] C. K. Jorgensen, Dan. Mat. Fys. Medd. 29, No. 7 (1955).

[9] H. Ewald, Ann. Phys. 34, 209 (1939).

[10] Landolt-Börnstein, 1, T, 4, Berlin, 1951.

[11] H. Bethe, Ann. Phys., (5), 3, 133 (1929).

[12] D. M. Gruen, J. Chem. Phys. 20, 1818 (1952).

[13] A. A. Grinberg and G. I. Petrzhak, Trans. Radium Inst. Acad. Sci. USSR 7, 15 (1956).

RELATION OF THE ADSORPTION OF CATIONS TO THE POTENTIAL OF THE HYDROGEN ELECTRODE

N. A. Balashova, V. A. Ivanov and V. E. Kazarinov

(Presented by Academician A. N. Frumkin, March 8, 1957)

For the majority of metals, the study of the adsorption of cations on their surface is complicated by the phenomenon of exchange between the metal cations and the same or foreign ions in the solution. Such exchange has not been observed on platinum [1], the electrochemical and adsorption properties of which compare favorably. Until recently, there were no specific investigations on the adsorption of cations on platinum. The particular results of the work of Erbacher [2] and of Lorenz [3] relating to the adsorption of ions on platinum did not permit conclusions as to the connection between the phenomenon of adsorption and the structure of the electrical double layer on the surface of the metal. From work with the mercury electrode it follows that inorganic cations, with the exception of the thallium ion [4], do not exhibit specific adsorptivity. It has been shown that univalent cations even exhibit a certain adsorption on mercury when the adsorption is from concentrated solutions [5]. Only for the polyvalent cations of lanthanum and thorium was there observed, by capacity measurements, excess adsorption with respect to the weak negative charge, this effect being explained by the formation of anion-cation pairs adsorbed on the mercury surface in a manner such that the anion was exposed to the solution [6].

In a study of the electrical double layer on metals, it was of interest to clarify the relationship between the adsorption of cations and the potential of a platinized platinum electrode, which was done in the present work through the use of tagged atoms. Cation adsorption was measured by measuring the radioactivity of the solution which was tagged by means of the appropriate radioactive isotope. The method was similar to that

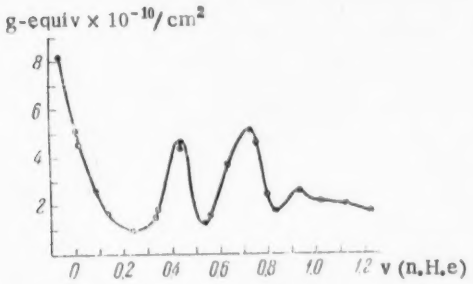

Fig. 1. Variation in adsorption of cesium cations with potential. Cs_2SO_4 solution ($2 \cdot 10^{-1}$ N, pH 2.5).

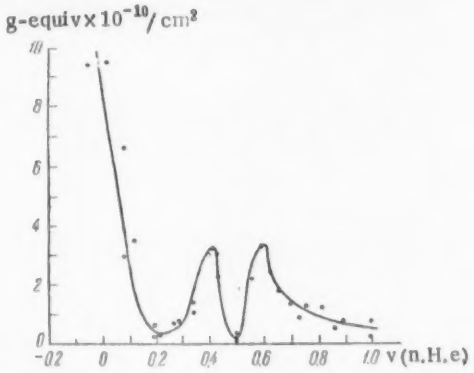

Fig. 2. Variation in adsorption of strontium cations with potential. $Sr(ClO_4)_2$ solution ($5 \cdot 10^{-3}$ N, pH 1.85).

described in reference [7]. The electrode potential was varied in the range from the value of the reversible hydrogen electrode to that of the air electrode by means of polarization. The electrode was maintained at each potential value for 10 minutes. The experiments were carried out in cesium, lanthanum, and strontium salt solutions acidified with perchloric and sulfuric acids. Radioactive isotopes of cesium, Cs^{-134}, strontium, Sr^{-89}, and lanthanum, La^{-140}, served as indicators. The solutions were prepared from doubly distilled acids and recrystallized salts. In the present work, the

conditions of all previous operations during the preparation of the electrodes were taken strictly into account, since reproducibility of results is strongly dependent thereon. The electrodes were platinized by the method described in reference [8]. All experiments were carried out at room temperature and with agitation provided by purified nitrogen.

In Figure 1 is presented a typical curve showing the variation in adsorption of cesium cations from sulfuric acid solution ($2 \cdot 10^{-2}$ N Cs_2SO_4, pH 2.5) with potential of the platinum. All potentials are referred to the normal hydrogen electrode. Adsorption is expressed in gram-equivalents per square centimeter of actual surface, which was determined in each experiment by a comparison of the length of the hydrogen part of the polarization curves with the corresponding value for smooth platinum, the roughness coefficient of which was taken as 1.5. In Figure 2 is presented a similar curve for strontium cations adsorbed from perchlorate solution.

It is known from literature data that the point of zero charge of unoxidized platinum lies at 0.11-0.27 v [8, 10]. Consequently, electrostatic adsorption of cations caused by attraction by charges on the surface of the platinum should be observed only with a negatively charged surface.

The results presented show that the variation in cation adsorption with potential has a more complex form than corresponds to such a simple idea. As seen from Figures 1 and 2, in the most negative region there is a maximum value of cation adsorption which, even without taking into account possible H^+-ion adsorption, apparently somewhat exceeds the value required for the formation of a double layer on the surface, calculated as explained above. With a shift in potential in a positive direction, there is observed a rapid diminution in cation adsorption corresponding to the decrease in the negative charge of the surface; however, the adsorption of cations is not zero at the zero potential point. In the potential region from 0.20 to 0.45 v, corresponding to an increase in the positive charge of the surface, an increase in cation adsorption is observed.

The dependence of cation adsorption on the potential of the platinum observed in this region can be explained by taking into account the adsorption of anions. We explained the adsorption of cations on the positively charged platinum by the adsorption of SO_4^{2-} and ClO_4^- anions in excess of equivalent amounts at these potentials, which has been shown with SO_4^{2-} using tagged atoms [11]. This same work also showed that there is appreciable adsorption of anions with no charge and with the platinum charged negatively. With the surface charged negatively, the presence of specifically adsorbed anions would lead to cation adsorption exceeding that corresponding to the negative charge of the surface. As is well known, adsorption of anions in excess of equivalence leads, in the case of mercury also [5], to the adsorption of cations on a positively charged surface. At not too high concentrations and in the vicinity of zero charge, the adsorption of cations in the presence of a majority of anions proceeds through a minimum [12].

The course of Curves 1 and 2 at potentials more positive than 0.45 v is connected, in all probability, with the appearance of adsorbed oxygen on the surface. As was shown earlier [8, 11], with the initiation of oxygen adsorption on the platinum, desorption of anions adsorbed when the surface was positively charged is observed, and is explainable by the appearance of negative charges due to oxygen-platinum dipoles disposed with their negative ends toward the solution. According to the above, desorption of anions must lead to a decrease in the adsorption of cations so long as the surface remains negatively charged. In this manner it is possible to explain the decrease in cation adsorption in the potential interval 0.45-0.55 v. With a further increase in the amount of adsorbed oxygen, the surface of the platinum becomes negatively charged, and electrostatic adsorption of cations increases. After reaching a potential of 0.7 v, the increase in the amount of adsorbed oxygen cannot compensate for the effect of the rapidly increased positive potential, and the adsorption of cations again begins to decrease. At more positive potentials, still further maxima and minima can be observed on the adsorption curves; this is possibly connected with the appearance of surface oxides, studied by V. I. Veselovsky [13]. However, it is impossible to form definite conclusions as to this behavior, since, with the rapid change in potential occurring in our work, poorly reproducible results were obtained with oxidized platinum, this being connected, probably, with the nonequilibrium state of the surface. A special study of the adsorption properties of oxidized platinum is required, and this has not yet been carried out.

Some results with regard to the adsorption of cations on oxidized platinum at high anode potentials were obtained in the present work. In acid solutions of various concentrations, it was possible to observe, at potentials above 1.9 v, practically complete desorption of Cs^+ and Sr^{2+} cations adsorbed when the platinum

was negatively charged. Adsorption of these cations was not observed at 1.9 v. On the basis of these results, it can be assumed that at potentials close to that at which oxygen is liberated, the surface of the platinum is charged positively. Lanthanum and yttrium cations are not, however, desorbed completely under these conditions. This presumably can be explained by their adsorption on the platinum oxides, which is confirmed by the increase in desorption of these cations during cathode polarization, which decomposes the platinum oxides.

The high values for cation adsorption obtained at all potentials is connected, in all probability, with the penetration of ions into the depths of the platinum in pores and microcrevices, and their adsorption on the surface is greater than determined by the polarization curve. Penetration into the depths of the platinum has been demonstrated by means of tagged atoms for the anions SO_4^{2-} [11], I^-, and Br^-.

We express our deep appreciation to A. N. Frumkin for valuable counsel during consideration of the results of this work.

Received March 8, 1957

LITERATURE CITED

[1] J. Palacios and B. Baptista, Nature, 170, 665 (1952).

[2] O. Erbacher, Zs. Phys. Chem. 182, 253 (1938).

[3] W. Lorenz and H. Muhlberg, Zs. Elektrochem. 59, 736 (1955).

[4] A. Frumkin and A. Titievskaya, J. Phys. Chem. 31, No. 2 (1957).

[5] A. N. Frumkin and Z. A. Iofa, J. Phys. Chem. 18, 932 (1939); Z. A. Iofa, B. Ustinsky and F. Eiman, J. Phys. Chem. 18, 934 (1939).

[6] M. A. Proskurin and M. A. Vorsina, Proc. Acad. Sci. USSR, 24, 915 (1939); M. A. Vorsina and A. N. Frumkin, Proc. Acad. Sci. USSR, 24, 918 (1939); J. Phys. Chem. 17, 255 (1943).

[7] N. A. Balashova and N. S. Merkulova, Coll. New Methods of Investigation,* Trans. Institute of Phys. Chem., Moscow, 1957.

[8] A. I. Shlygin and A. N. Frumkin, Acta physicochim. URSS, 3, 791 (1935); A. I. Shlygin, A. N. Frumkin and V. I. Medvedovsky, Acta Physicochim. URSS, 4, 911 (1936); A. N. Frumkin and A. I. Shlygin, Bull. Acad. Sci. USSR, Ser. Chem. 773 (1936).

[9] B. V. Ershler, Acta Physicochim. URSS, 7, 327 (1937).

[10] A. V. Gorodetskaya and B. N. Kabanov, J. Phys. Chem. 4, 529 (1933).

[11] N. A. Balashova, Proc. Acad. Sci. USSR, 103, No. 4, 639 (1955).

[12] D. Grahame, J. Am. Chem. Soc. 76, 4819 (1954).

[13] V. I. Ginzburg and V. I. Veselovsky, J. Phys. Chem. 24, 366 (1950); L. E. Elina, T. I. Borisova and Ts. I. Zalkind, J. Phys. Chem. 28, 785 (1954); K. I. Rozental and V. I. Veselovsky, J. Phys. Chem. 27, 1163 (1953).

* In Russian.

THE EFFECT OF THE CHEMICAL NATURE OF THE SOLVENT ON THE OXIDATION OF RUBBER IN SOLUTIONS

T. G. Degteva and A. S. Kuzminsky

(Presented by Academician P. A. Rebinder, February 21, 1957)

Many investigators [1-5] have used solutions of rubber in simulating oxidation processes which occur in rubber in the solid state. In such cases, attention is directed mainly to the conversion of the polymers themselves. As regards the solvent,* its role in the process of the oxidation of rubber in solutions has not been considered at all. Moreover, participation of the solvent in this process ensues from the presently generally acknowledged radical-chain mechanism of the oxidation of hydrocarbons.

The problem of the present investigation came down to a study of the effect of the chemical nature of the solvent on the oxidation of rubber in solutions.

Purified, sodium-polymerized butadiene rubber was investigated. Aromatic (benzene, toluene, xylene, ethylbenzene, and isopropylbenzene), naphthenic, and naphthenic-aromatic (decalin and tetralin) hydrocarbons were used as solvents. The hydrocarbons chosen differed in reactivity with respect to oxidation.

For oxidation of the rubber solutions, and also of the solvents, a special apparatus was constructed in which vigorous agitation was provided during the course of the reaction in order to eliminate delay in the diffusion of oxygen.

The kinetic curves for the oxidation of 1% solutions of rubber, which are presented in Figure 1, show that the rate of oxidation of the solutions increases in the following order of solvents: toluene < xylene < decalin < ethylbenzene < isopropylbenzene < tetralin. With respect to the rate of oxidation of the solvents themselves, the aromatic hydrocarbons may be arranged in the same order: toluene < xylene < ethylbenzene < isopropylbenzene.**

In a separate series of experiments*** it was shown that a 1% solution of rubber in benzene oxidizes at a lower rate than does a toluene solution (Figure 2).

The observed difference in the oxidation rates of the rubber solutions could be due only to an unequal effect of the solvent on the development of the radical-chain process of rubber oxidation.

The question arises as to what elemental acts in the oxidation of rubber most essentially affect the solvent, and how its chemical nature is manifested in this.

---

* By the term "solvent" is to be understood the various low molecular weight hydrocarbons in which rubber dissolves.

** This is in agreement with the generally known thesis [6] that in the oxidation of hydrocarbons, in the majority of cases, a tertiary C–H bond is most subject to attack by oxygen, a secondary bond is less subject to attack, and a primary carbon atom is least of all subject to attack.

*** Owing to the considerable vapor pressure of benzene at 90°, observation of the oxidation processes was carried out not by absorption of oxygen, but by means of the accumulation of peroxide compounds.

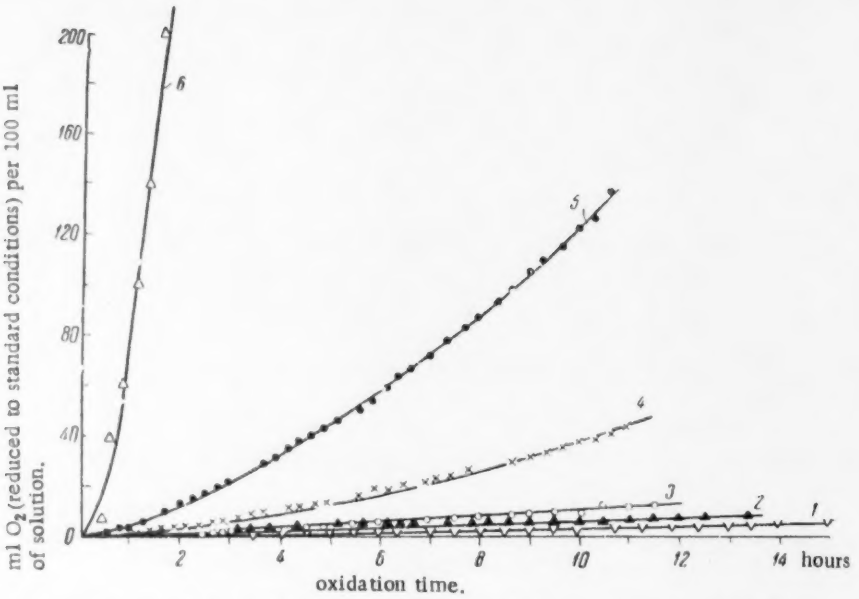

Fig. 1. Kinetics of the oxidation of 1% solutions of sodium-polymerized butadiene rubber at 90°: 1) in toluene, 2) in xylene, 3) in decalin, 4) in ethylbenzene, 5) in isopropylbenzene, 6) in tetralin.

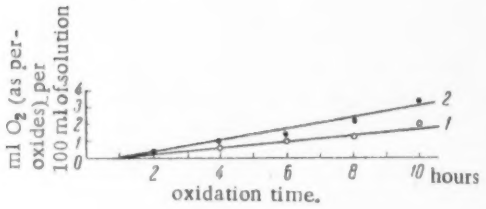

Fig. 2. Kinetics of the accumulation of peroxides in the course of the oxidation of 1% solutions of sodium-polarized butadiene rubber at 90°: 1) in benzene, 2) in toluene.

During the course of the reaction initiating the oxidation chain in the rubber, $R-H^{*} + O_2 \rightarrow HO_2^{\cdot} + R^{\cdot}$ [1], radicals, $R^{\cdot}$, arise which can either add oxygen with the formation of peroxide radicals, $ROO^{\cdot}$, or react with the solvent molecule.* If the radicals are able to split off an H-atom from a solvent molecule, this must result in the formation of new radicals with which oxygen can react and thereby transfer the chain from the rubber macromolecule to a solvent molecule.

Frank [7] has indicated the course of the chain transfer reaction during the oxidation of a mixture of two low molecular weight hydrocarbons. However, a solvent can serve not only as a chain transfer agent, but certain of them, as, for example, aromatic hydrocarbons (benzene, toluene, xylene, etc.), display a tendency toward the addition of radicals [11]. Thus, Stockmayer and Peebles [11] have shown that retardation of the polymerization of vinyl acetate in benzene is associated with the addition of the latter to a polymer radical according to the reaction:

$$R\,(CH_2CHOAc)_x + C_6H_6 \rightarrow R\,(CH_2CHOAc)_x\text{–}C_6H_5$$

In the opinion of these authors, deactivation of the radicals proceeds under the influence of oxygen during precipitation and solution of the polymer.

* We have in mind the abstraction of hydrogen at an α-methylene carbon atom.

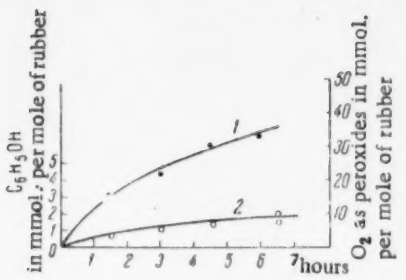

Fig. 3. Accumulation of phenol during the course of the oxidation of a 4% solution of sodium polymerized butadiene rubber in benzene at 110°: 1) peroxide, 2) phenol.

According to the concept developed in reference [8], stabilization of the relatively unreactive radical

$R(CH_2CHOAc)_x-\underset{H}{\overset{}{\langle\bigcirc\rangle}}\cdot$ can occur through the

splitting off of a hydrogen from it by any other radical present in the system according to the reaction:

$$R(CH_2CHOAc)_x-\underset{H}{\overset{}{\langle\bigcirc\rangle}}\cdot + R_1^{\cdot} \longrightarrow$$

$$\longrightarrow R_1H + R(CH_2CHOAc)_x-\langle\bigcirc\rangle$$

where $R_1^{\cdot}$ is a polymer radical.

In a similar manner, the radicals R•, formed during the course of the reaction initiating the oxidation chain in the rubber in solution, can be captured by the molecules of aromatic hydrocarbons, as:

$$R^{\cdot} + \langle\bigcirc\rangle \rightarrow \underset{H}{\overset{R}{\langle\bigcirc\rangle}}\cdot \xrightarrow{X^{\cdot}} XH + R-\langle\bigcirc\rangle,$$

where X• can be R•, ROO•, RO•, •OH, etc.

If the radical R• can react with oxygen, then the resulting peroxide radical can either isomerize* with decomposition of the molecular chain of the rubber, which may be detected by the decrease in relative viscosities of the oxidized solutions, or it can be stabilized. The probability of the stabilization of the radical ROO• depends on the chemical nature of the solvent and on the concentration of rubber in the solution. In the oxidation of rubber in benzene, the ROO• radical cannot split off an H-atom from a molecule of solvent, since this cannot be done by the even more reactive radical $\dot{C}H_3$ [8]. Therefore, stabilization of the peroxide radical can take place either through its capture by a molecule of benzene with the formation of, in the end, the stable peroxide $ROO-\langle\bigcirc\rangle$, or by splitting off a hydrogen from a molecule of rubber with the formation of the hydroperoxide ROOH and a free radical. The latter case explains why the rate of oxidation of a solution increases with an increase in the concentration of rubber in the solution.

During the course of oxidation of the solution, the rubber hydroperoxides ROOH can decompose with the formation of the reactive radicals RO• and •OH, which, as a result of their capture by benzene molecules, can form certain compounds which we may indicate by $RO-\langle\bigcirc\rangle$ and $HO\langle\bigcirc\rangle$. In fact, during the oxidation of a 4% solution of rubber in benzene at 110°, the formation of phenol was observed (Figure 3). It should be noted that the formation of phenol can be visualized as occurring also through the decomposition of the peroxide $ROO-\langle\bigcirc\rangle$.

Thus, the capture of the radicals R• and ROO• by molecules of benzene must lead to breaking of the primary oxidation chain, and the capture of the radicals RO• and •OH must lead to the breaking of the secondary chain.

On changing from benzene to toluene, a new possibility for the stabilization of the polymer radical ROO•

* We have in mind here the transfer of a free valence within the radical similar to that which takes place in the oxidation of low molecular weight hydrocarbons [12].

appears – by the splitting off of a hydrogen atom from the methyl group of toluene [12] with the formation of the relatively inactive benzyl radical according to the reaction:

The benzyl radical can react comparatively easily with oxygen, forming the radical 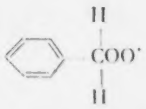

This radical, if only it does not capture a molecule of toluene, can stabilize by splitting off hydrogen either from a rubber molecule or from a molecule of solvent with the formation of toluene hydroperoxide 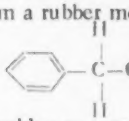 . The occurrence of a reaction transferring the oxidation chain from a macromolecule of rubber to a molecule of solvent leads to an increase in the length of the oxidation chain.

On going from toluene to xylene, ethylbenzene, and isopropylbenzene, the mobility of the hydrogen in the side chain is increased.

This factor favors still more the occurrence of the oxidation chain transfer reaction, which leads to an increase in the rate of oxidation of the rubber solutions in this series of solvents (see Figure 1).

The effect of the different chemical nature of the solvent molecules also appears during the oxidation of solutions of rubber in tetralin and decalin. Owing to the ease with which a hydrogen atom is split off from a molecule of tetralin, intermediate products – solvent and rubber peroxide molecules – accumulate comparatively rapidly in the solution. Under the influence of the free radicals available in the system, these products decompose, promoting the development of an autocatalytic process of oxidation of tetralin solutions of rubber. The course of autocatalysis is favored by the lower thermal stability of tetralin hydroperoxide in comparison with isopropylbenzene hydroperoxide.

In decalin at 90°, the oxidation of rubber develops at a very low rate, because the peroxide radicals are not able to split off an H-atom from the solvent molecule. These radicals can be stabilized with continuation of the chain by splitting off hydrogen from the rubber macromolecules, but in dilute solution the probability of this occurring is small. With an increase in temperature to 100°, a sharp jump in the rate of oxidation of rubber in decalin is observed, which can be explained by the possibility of chain transfer involving solvent molecules under these conditions.

Consequently, during the oxidation of rubber in solution, the solvent can slow down (Curves 1, 2 in Figure 1), accelerate (Curves 4-6), or even not participate in the process – appearing in the role of a diluent. The solvents used by us can be arranged in the following order of accelerating effect: tetralin > isopropylbenzene > ethylbenzene; in order of retarding effect: benzene > toluene > xylene.

Scientific-Research Institute
of the Rubber Industry

Received February 6, 1957

LITERATURE CITED

[1] H. Farmer, Rub. Chem. and Techn. 16, 17 (1943).

[2] J. Lacau and M. Magat, Disc. Farad. Soc. No. 2, 388 (1947).

[3] J. Cortil-Lacau, Rev. Gen. Caoutchouc, 30, No. 11, 819 (1953).

[4] I. I. Zhukov, V. A. Komarov and G. N. Sibiryakova, Syn. Rubber, No. 3, 4 (1935).

[5] B. Dolgoplosk, E. Tinyakova and V. Reikh, Trans. of the Conference on Rubber Vulcanization,* Moscow, 1954.

* In Russian.

[6] K. I. Ivanov, Intermediate Products and Intermediate Reactions in the Autooxidation of Hydrocarbons,* Moscow, 1949.

[7] C. E. Frank, Chem. Rev. No. 1, 46, 155 (1950).

[8] M. T. Jagniss and M. Szwarc, Nature, 170, 312 (1952).

[9] D. H. Hey, A. Nechvatal and T. F. Robinson, J. Chem. Soc. 1951, 2892; 1952, 2094; 1953, 45.

[10] W. A. Waters, The Chemistry of Free Radicals, Foreign Lit. Press, 1948. (Translation).

[11] W. H. Stockmayer and L. H. Peebles, J. Am. Chem. Soc. 75, 2278 (1953).

[12] N. N. Semenov, On Some Problems of Chemical Kinetics and Reactivity,* Izd. An SSSR, 1954.

* In Russian.

THE HEAT OF ADSORPTION OF BENZENE AND HEXANE VAPORS ON CALCINED AND HYDRATED SILICAS

A. A. Isirikyan and A. V. Kiselev

(Presented by Academician M. M. Dubinin, December 25, 1956)

In a number of works it has been shown that changing the chemical composition of silica gel surfaces by subjecting the surfaces to chemical reactions, dehydration [1, 2], esterification [3, 4], halogenation [5-7], very sharply changes their adsorption properties with respect to substances which are adsorbed, not only by universal dispersion interactions, but also by more intimate reactions, for example reactions of the acid-base type [1, 8, 9]. The effect of the degree of dehydration of the silica gel surface on the adsorption of methanol and benzene vapors has been particularly studied in reference [10], where it was shown that thermal dehydration of silica gel leads to a decrease in the magnitude of the adsorption of these vapors in the initial part of the isotherm. In references [9, 11] it was shown, on the other hand, that the adsorption of vapors of a saturated hydrocarbon (n-pentane) on silica gel dehydrated by heating at from 200 to 400° is not changed.

The effect of the degree of hydration of the silica gel surface on the magnitude of the differential heat of adsorption of benzene and hexane vapors was investigated in the present work. The amount of adsorption was measured in an improved version of the apparatus described in reference [11]. The heat of adsorption was measured in an automatic calorimeter with constant heat exchange similar to that described in reference [12]. The high purity benzene and hexane were obtained from E. A. Mikhailova, and were redistilled in a column and introduced into the apparatus through a silica gel column. Their vapor pressures at 20° were 75.25 and 121.7 mm Hg, respectively. All experiments were carried out at 20°.

The original silica adsorbent was prepared by G. V. Vinogradov* as a "white carbon black" by combustion of organosilicon compounds in a muffle furnace and subsequent calcination of the fine powder at 800-1000°. Such method of preparation excluded the possibility of forming on the surface a compact layer of hydroxyl groups of silicic acid (in contrast to silica gel prepared from the hydrogel [1, 13]). The hydrated samples were prepared from this original material by holding it under liquid water for 7 months and subsequently drying at 120°. Before the heat of adsorption measurements, both of these samples were degassed in the calorimeter case at 200°. The specific surfaces of both samples after degassing at 200° were determined by E. V. Khrapova by nitrogen adsorption, and were 185 sq. m/g for the original and 135 sq. m/g for the hydrated sample. The reduction in surface of the highly dispersed silica on lengthy treatment with water probably occurred similarly to that in reference [14]. The original sample retained about 0.58% "structural water;" i.e., it contained 3.5μ mole of OH per m^2 of surface. The hydrated sample retained 1.32% "structural water;" i.e., it contained μ moles of OH per sq. m. This value is close to the limiting value of OH on the surface of hydrated quartz and of silica gel: 12.8μ moles per sq. m., as calculated in references [15, 16].

In Figure 1 are presented the complete isotherms for the adsorption of benzene vapors on the original and hydrated silica samples. It is seen from the figure that the samples are porous; this porosity is associated with a certain amount of sintering occurring during the heating of the original sample to 1000° after preparation. In Figure 1 are presented curves showing the distribution of pore volume with throat diameter of the pores, calculated from the desorption branches of the isotherms (without correction for the thickness of the adsorbed

* The authors avail themselves to this opportunity to express their deep appreciation to E. A. Mikhailova and G. V. Vinogradov.

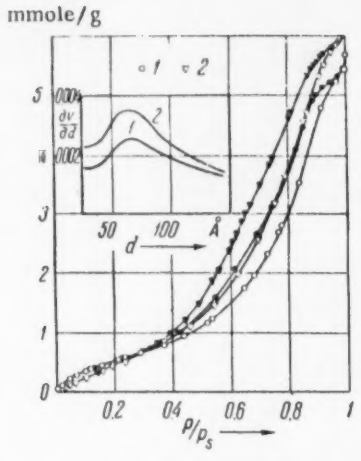

Fig. 1. Adsorption isotherms for benzene vapors on the hydrated (1) and the calcined (2) silica samples. Black points – desorption. Above – distribution curves for pore volume as a function of dimensions.

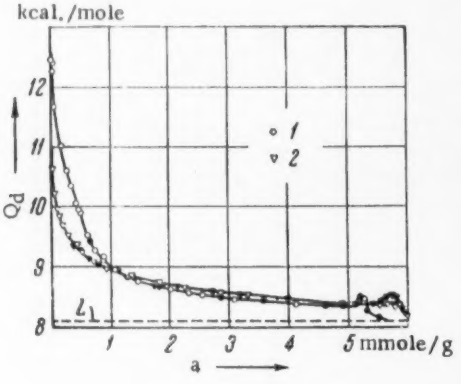

Fig. 2. Variation in differential heat of adsorption of benzene vapors, Q_a, with amount adsorbed, a, for the hydrated (1) and the calcined (2) silica samples. L – heat of condensation. Black points – desorption.

layer). Both samples belong to the fourth structural type; i.e., they are heterogeneous adsorbents [17] with an insignificant predominance of pores with throat diameters around 60-70 A. It is also seen from Figure 1 that there is some reduction in pore volume during hydration [14].

The isotherms for the two samples are very similar in the capillary condensation region, but in the initial, purely adsorption, region, the isotherm for the hydrated sample is significantly higher in spite of the lower specific surface. The increase in adsorptive capacity for benzene as a result of hydration of the silica surface is clearly seen from Figure 2, in which is shown the relation of the differential heat of adsorption of benzene on the original and hydrated samples to the amount of adsorption up to saturation. In the initial part of the curves, as in the case of silica gel, the heats fall sharply owing to the considerable heterogeneity of the silica surfaces [18]. In the broad region of capillary condensation, the curves for both samples differ little, and exceed the heat of condensation of the normal liquid by only 0.5-0.3 kcal/mole. Owing to the heterogeneous porosity of these samples, in both cases capillary condensation in the vicinity of saturation is concluded with weakly expressed maxima of heat of adsorption in contrast to homogeneous silica gel [18]. Measurement of the adsorption isotherms and differential heats of adsorption in the capillary condensation region permits calculation of the sizes of the adsorbed films, s', by thermodynamics [17]. These values of s' were 172 sq. m/g for the original sample and 134 sq. m/g for the hydrated sample; i.e., they are close to the corresponding values of s which indicate the availability of the surfaces of these samples for the adsorption of these hydrocarbons.

In Figure 3 are presented the differential heats of adsorption of benzene and hexane on calcined and hydrated silica gel samples as functions of the absolute amount of adsorption, α, (μ moles/sq. m.) in the monolayer region. The heat of adsorption of hexane vapors is only slightly sensitive to an abrupt change in the degree of hydration of the surfaces of these samples. The heat of adsorption of benzene is very sensitive to a change in the hydration of the surfaces. It is seen from Figure 3 that in the midst of completion of the monolayer (close to $\theta = 0.5$), the standard [19] heat of adsorption of benzene vapor increases by approximately 1.0 kcal/mole as a result of the increase in the content of silicic acid hydroxyls on the surface from 3.5 to 10.8 μ moles/sq. m. Taking into account the amount of surface occupied by a planar oriented benzene molecule on the surface of the hydrated silica, $\omega_0 = 49$ A^2 [9], and the amount of surface required by one hydroxyl, we may ascribe this 1.0 kcal/mole increase in the heat of adsorption of benzene to the energy of formation of π-complexes [8, 9] between the benzene molecule and two or three silicic acid hydroxyls. Clarification of the nature of the bonds in these π-complexes, evaluation of the relative role of polarization or deeper chemical interactions, requires, however, further investigation, and such clarification is to be found in connection with the general development of the concept of the hydrogen bond or similar bonds in molecular complexes of the donor-acceptor type.

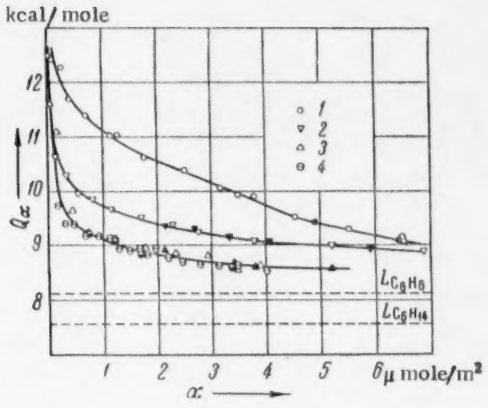

Fig. 3. Variation in the differential heat of absorption of benzene (1, 2) and of hexane (3, 4) with the absolute amount of adsorption, α, for the hydrated (1, 3) and calcined (2, 4) silica samples. Black points – desorption.

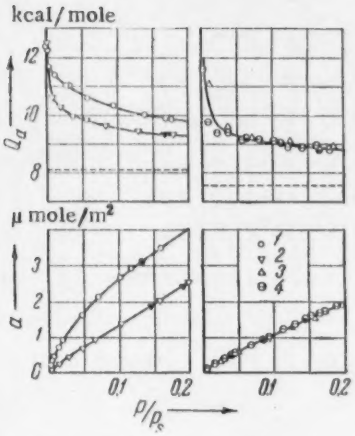

Fig. 4. Isotherms showing the adsorption, α, and differential heat of adsorption, Q_a, of benzene (1, 2) and hexane (3, 4) as functions of the relative pressure, p/p_s, for the hydrated (1, 3) and calcined (2, 4) silica samples. Black points – desorption.

The values obtained for the differential heats of adsorption of these hydrocarbons and their relationship to surface hydration show that the basic interactions with the silica gel surface are nonpolar, van der Waals interactions, the energy of which, however, is less than in the case of adsorption on graphite [19] owing to the significantly less frequent disposition of force centers in the quartz lattice. The absence of a sharp effect of an increase in concentration of hydroxyls on the silica surface on the heat of adsorption of hexane indicates the small contribution of the energy of ordinary inductive interactions. In the case of the adsorption of benzene on the hydrated surface, the formation of π-complexes with silicic acid, while increasing the total heat of adsorption of benzene, Q_a, by only 10%, nevertheless increases greatly the net heat of adsorption, $Q_a - L$ (by approximately a factor of 2 close to $\theta = 0.5$), which very greatly changes the form of the adsorption isotherm of benzene vapors. This is clearly seen from Figure 4, in which both the heat of adsorption and the absolute amount of adsorption for hexane and benzene are plotted as functions of the relative pressure p/p_s.

M. V. Lomonosov Moscow State University

Received December 19, 1956

LITERATURE CITED

[1] A. V. Kiselev, Coll. Surface Chemical Compounds and Their Role in Adsorption Phenomena,* Izd. MGU, 1957, pp. 90, 199.

[2] S. P. Zhdanov, Proc. Acad. Sci. USSR, 68, 99 (1949).

[3] O. M. Dzhigit, A. V. Kiselev, N. N. Mikos-Avgul and K. D. Shcherbakova, Proc. Acad. Sci. USSR, 70, 441 (1950).

[4] K. V. Topchieva and A. P. Ballod, Proc. Acad. Sci. USSR, 75, 247 (1950).

[5] A. P. Ballod and A. V. Topchiev, Coll. Surface Chemical Compounds and Their Role in Adsorption Phenomena,* Izd. MGU, 1957, p. 146.

[6] I. E. Neimark, R. Yu. Sheinfein and L. G. Svintsova, Proc. Acad. Sci. USSR, 108, 871 (1956).

[7] K. D. Shcherbakova and K. I. Slovetskaya, Proc. Acad. Sci. USSR, 111, 855 (1956).

* In Russian.

[8] A. V. Kiselev, Proc. Acad. Sci. USSR, 100, 1046 (1956).

[9] A. V. Kiselev, Prog. Chem. 25, 705 (1956).

[10] A. V. Kiselev, K. G. Krasilnikov and L. N. Soboleva, Proc. Acad. Sci. USSR, 94, 85 (1954).

[11] A. V. Kiselev and Yu. A. Eltekov, J. Phys. Chem. 31, 250 (1957).

[12] A. V. Kiselev, V. F. Kiselev, N. N. Mikos, G. G. Muttik, A. D. Runov and K. D. Shcherbakova, J. Phys. Chem. 23, 577 (1948).

[13] A. V. Kiselev, Coll. J. 2, 17 (1936).

[14] A. V. Kiselev, E. A. Leontyev, V. M. Lukyanovich and Yu. S. Nikitin, J. Phys. Chem. 30, 2149 (1956).

[15] L. D. Belyakova, O. M. Dzhigit and A. V. Kiselev, J. Phys. Chem. 31, No. 7 (1957).

[16] A. V. Kiselev and S. P. Zhdanov, J. Phys. Chem. 31 (1957).

[17] A. V. Kiselev, J. Phys. Chem. 23, 452 (1949).

[18] A. A. Isirikyan and A. V. Kiselev, Proc. Acad. Sci. USSR, 110, 1009 (1956).

[19] N. N. Avgul, G. I. Berezin, A. V. Kiselev and I. A. Lygina, J. Phys. Chem. 30, 2106 (1956).

A KINETIC METHOD OF INVESTIGATING PROPANE CRACKING USING LABELED ATOMS

M. B. Neiman, N. I. Medvedeva and E. S. Torsueva

(Presented by Academician V. N. Kondratyev, Jan. 30, 1957)

According to contemporary ideas thermal decompositions of hydrocarbons are chain reactions, proceeding by means of free radicals.

Methane, ethylene, hydrogen and propylene are known to be the main products of propane cracking; ethane is formed in smaller amounts. According to Rice's theory [1] on the decomposition of organic compounds, these products are formed by the following scheme:

a) $CH_3CH_2CH_3 \rightarrow \dot{C}H_3 + \dot{C}_2H_5$;

b) $\dot{C}H_3 + CH_3CH_2CH_3 \rightarrow CH_4 + \dot{C}H_2CH_2CH_3$;

c) $\dot{C}H_2CH_2CH_3 \rightarrow C_3H_4 + \dot{C}H_3$;

d) $\dot{C}_2H_5 \rightarrow C_2H_4 + \dot{H}$;

e) $\dot{H} + CH_3CH_2CH_3 \rightarrow H_2 + CH_3\dot{C}HCH_3$;

f) $CH_3\dot{C}HCH_3 \rightarrow C_3H_6 + \dot{H}$;

g) $\dot{C}H_3 + \dot{C}H_3 \rightarrow C_2H_6$.

An answer to the problem of whether the above products of propane cracking are the end products or whether they undergo further conversion can be found by using labeled atoms in investigating cracking. Some conclusions may be drawn on the cracking mechanism by introducing into the initial propane a minute quantity of one of the reaction products, labeled with the radioactive carbon isotope C^{14}, and by observing the activity in the different reaction products.

The purpose of the present work was to study the behavior of ethylene, formed by propane cracking. A kinetic method of applying labeled atoms [2, 3], developed by one of the authors, was used in the work. This method makes it possible to determine the order of formation of particular products from others, to calculate the formation and consumption rates of separate reaction products, and also to evaluate the concentrations of intermediate products and radicals from the rates of the elementary processes.

We studied propane cracking under static conditions in a quartz reaction vessel of 725 ml capacity, over a temperature range of 530-580°. We synthesized propane from propyl bromide via the organomagnesium compound. After purification the propane contained 0.5% ethane and 1-1.5% propylene. 1% of labeled ethylene $C_2^{14}H_4$, prepared from $BaC^{14}O_3$ [4], was added to the starting propane. The specific activity of the ethylene introduced was 38.8 μ C/mmole. The starting pressure of the mixture in the reaction vessel was the same in all experiments – 354 mm.

The cracking products were isolated by chromathermography [5, 6] and were burned to CO_2, which was trapped in barium hydroxide solution. Samples for measuring the activity with an end-window counter were

prepared from the barium carbonate. The kinetic decomposition curves of propane containing 0.5% ethane and 1% labeled ethylene at different temperatures are shown in Fig. 1.

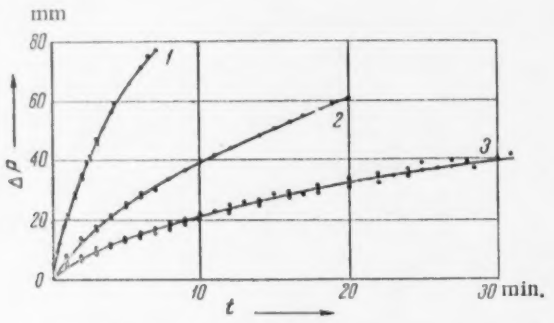

Fig. 1. Kinetic curves of the thermal decomposition of propane: 1) 580°; 2) 554°; 3) 532°.

The activation energy of the overall cracking process varies from 68,000 cal/mole for 3% propane conversion, up to 72,500 cal/mole for 14% conversion.

Radiometric analysis of the cracking products showed that, besides ethylene, ethane had a high specific activity. Figure 2 gives the change in specific activity of ethylene (1) and ethane (2) with degree of conversion for 3 series of experiments at different temperatures. The specific activity of ethylene α falls due to dilution of labeled ethylene with inactive ethylene formed during cracking. The specific activity of ethane β at the starting moment is equal to zero, as the starting mixture contains unlabeled ethane; then β increases, passing through a maximum. The maximum of the specific activity of ethane lies on the curve of the change in specific activity of ethylene; according to the general theory on the kinetic method this indicates that ethane is formed directly from ethylene.

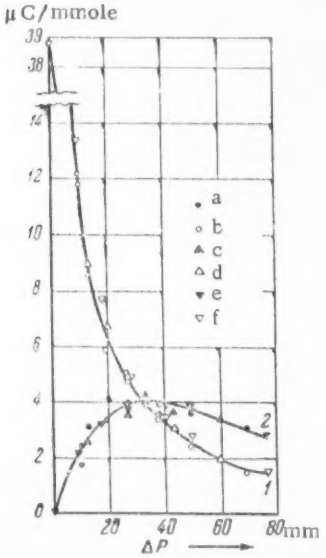

Fig. 2. The change in specific activity of ethylene (1) and ethane (2) during the reaction; a and b) T = 532°; c and d) 554°; e and f) 580°; a, c and e) C_2H_6, b, d and f) C_2H_4.

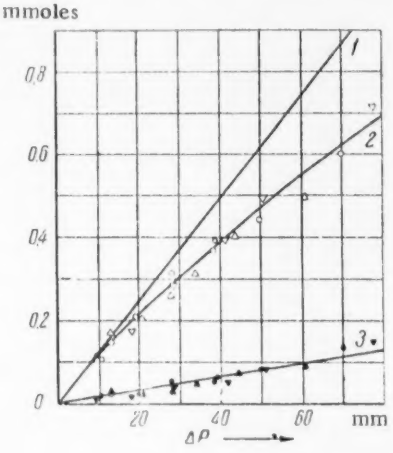

Fig. 3. Ethylene consumption and ethane formation during propane cracking: 1) The amount of ethylene formed (neglecting its consumption); 2) ethylene accumulation; 3) ethane accumulation during the reaction. The conventional symbols are the same as in Fig. 2.

Figure 3 shows the relation between the amount of ethylene converted during the reaction and the amount of ethane formed. The amount of ethylene formed C', neglecting its consumption (1), may be calculated by the kinetic method from the formula

$$C' = \int C \, d \ln \alpha, \tag{1}$$

where C is the ethylene concentration during the reaction, corresponding to the specific activity of ethylene α.

Curve 2 shows the accumulation of ethylene, measured during the experiments; curve 3 – the accumulation of ethane during the reaction. The amount of ethylene reacting – the difference between curves 1 and 2 – corresponds to the amount of ethane formed, within the limits of accuracy with which the amounts of ethane and ethylene were measured, and the activity of the ethylene introduced balances with that of the active cracking products. This confirms the fact that during propane cracking, ethane is mainly formed from ethylene, and not by recombination of methylene radicals as was formerly supposed. It should be noted that with an increase in the degree of reaction the difference between the amounts of reacted ethylene and ethane formed is greater than the error of measurements. This indicates the possibility of the formation of other products from ethylene in the more advanced cracking stages.

On the basis of the radical-chain scheme of hydrocarbon cracking, the following course for ethane formation from ethylene may be given:

$$C_2^{14}H_4 + \dot{H} \rightarrow \dot{C}_2^{14}H_5; \tag{2}$$

$$\dot{C}_2^{14}H_5 + C_3H_8 \rightarrow C_2^{14}H_6 + \dot{C}_3H_7; \tag{3}$$

$$\dot{C}_2^{14}H_5 + H_2 \rightarrow C_2^{14}H_6 + H. \tag{4}$$

Reaction (2) proceeds readily with an activation energy of $E \leq 5000$ cal/mole [7]. Further conversion of ethyl radicals occurs by reactions of $\dot{C}_2H_5$ abstracting H atoms from the saturated C_3H_8 or H_2 molecules.

Knowledge of the rate w_2 of the elementary process (2), or, what amounts to the same, the rate of ethylene accumulation makes it possible to evaluate the concentration of H atoms in the region of the thermal decomposition of propane. We determined w_2 as the difference in the rate of ethylene formation w_1 and the overall ethylene accumulation with time $\frac{d(C_2H_4)}{dt}$.

$$w_2 = -[C_2H_4]\frac{d \ln \alpha}{dt} - \frac{d[C_2H_4]}{dt}, \tag{5}$$

where

$$w_1 = -[C_2H_4]\frac{d \ln \alpha}{dt}. \tag{6}$$

However, it can be seen from Equation (5) and Fig. 3 that the calculation of w_2 values using the difference between two rates, similar in magnitude cannot be carried out with sufficient accuracy, although the rates of ethylene consumption obtained by this method are similar in magnitude to the formation rate of ethane from ethylene, as was to be expected from the above discussion on the relation between the amount of reacted ethylene and the ethane formed.

Considering that the rate of ethane consumption under our experimental conditions was small, by using the kinetic method we can calculate the formation rate of ethane from ethylene

$$w_{C_2H_6} = \frac{1}{\alpha}\frac{dI_{C_2H_6}}{dt}, \tag{7}$$

where $I_{C_2H_6} = \beta [C_2H_6]$ is the total ethane activity.

The mean value of $w_{C_2H_6}$ is close to the rate of formation of ethane which can be obtained from the slope of the experimental curve of ethane accumulation. By using the rate of formation of ethane $w_{C_2H_6}$ for evaluating the concentration of H atoms by reaction (2)

$$w_2 = w_{C_2H_6} = fk_0 e^{-E/RT} [C_2H_4] [H] \tag{8}$$

and substituting f = 0.01, $k_0 = 10^{-10}$ cm^3 · sec^{-1} · molecule^{-1} and E = 5000 cal/mole, we obtained the values for [H], given in Table 1.

To evaluate the concentrations of normal propyl radicals we used the rates of formation of ethylene w_1, calculated by formula (6). By Rice's scheme, normal propyl radicals decompose with the formation of ethylene and a methyl radical

$$n\,\dot{C}_3H_7 \xrightarrow{w_1} C_2H_4 + \dot{C}H_3. \tag{9}$$

The rate of this process, equal to the rate of formation of ethylene, may be written as:

$$w_1 = k_0 e^{-E/RT} [n\,\dot{C}_3H_7]. \tag{10}$$

We took the value E = 28,000 cal/mole to calculate [n-$\dot{C}_3H_7$]. The concentration values obtained are given in Table 2.

TABLE 1

Concentration of H atoms during propane cracking, T = 580°

Propane conversion, %	[H] · 10^{-10}, atom/cm^3
3.5	4.2
6	2.9
8	2.3
10	2
13	1.6
16	1.3
18	1.2
20	1.1

TABLE 2

Concentration of n-C_3H_7 radicals during propane cracking, T = 580°

Conversion, %	[n-C_3H_7] · 10^{-10}, molecules/cm^3
2	4.9
3.5	4.1
6	2.6
10	2.0
13	1.7
16	1.6

The calculations of radical and atom concentrations in the reaction region, carried out in this work using the kinetic method, indicate the possibility of further developing this method for studying the elementary stages of complex processes.

In conclusion the authors would like to thank L. Ya. Margolis, N. P. Keier and O. A. Golovina for consultation and help in synthesizing labeled ethylene.

Institute of Chemical Physics
Academy of Sciences USSR

Received January 29, 1957

LITERATURE CITED

[1] F. O. Rice, J. Am. Chem. Soc., 53, 1959 (1931).

[2] M. B. Neiman, J. Phys. Chem., 28, 1235 (1954).

[3] A. F. Lukovnikov, M. B. Neiman, J. Phys. Chem., 29, 1410 (1955).

[4] L. Ya. Margolis, B. V. Klimenok, O. A. Golovina, Proc. Acad. Sci., 86, 313 (1952).

[5] A. A. Zhukhovitsky, O. V. Zolotareva, V. A. Sokolov, N. M. Turkeltaub, Proc. Acad. Sci., 77, 435 (1951).

[6] N. I. Medvedeva, E. S. Torsueva, Proc. Com. on Anal. Chem., 6, 88 (1955).

[7] E. W. R. Steacie, Atomic and Free Radical Reactions, N. Y., 1954, p. 435.

THE MECHANISM OF SORPTION OF DIPOLAR IONS BY IONITES

G. V. Samsonov and N. P. Kuznetsova

(Presented by Academician P. A. Rebinder, February 6, 1957)

Dipolar ions (amino acids, polypeptides and proteins in solutions of certain acidity) carry positive and negative charges at the same time. This property is bound to affect the process of their sorption by ionites, which is based on the electrostatic interaction of the ions with the ionite.

In the case of the sorption of dipolar ions, in contrast to the sorption of ions with single charges, an electrostatic repulsion should be observed together with an electrostatic attraction. Up to now, no attention has been paid to this phenomenon. The usual ideas on the mechanism of ion sorption, making no allowance for the peculiarity of dipolar ions, were used in the most important investigations in this field [1, 2], in which the dynamic sorption of amino acids by ion-exchange resins was studied and the aim was to establish the order of displacement of amino acid ions from ionites.

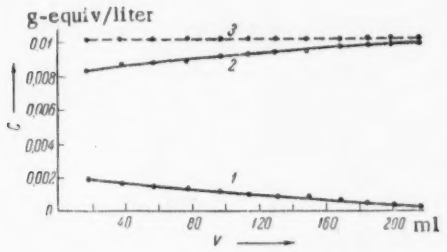

Fig. 1. The equivalence of the exchange of alanine cations with hydrogen ions on the resin SDV-3 on displacing alanine with a 0.01 N solution of HCl. 1) concentration of alanine cations; 2) concentration of hydrogen ions; 3) total concentration of alanine cations and hydrogen ions.

As a result of our investigations we were able to show that the sorption of dipolar ions proceeds according to a law, which differs considerably from the laws of sorption of ions carrying charges of one sign. Experiments were carried out with amino acids. The concentrations of amino acids were determined with ninhydrin. The concentrations of sodium ions were determined by the uranyl acetate method and hydrogen ions with a glass electrode.

First of all, experiments were carried out to investigate the equivalence of exchange. The amino acids glycine, alanine and leucine were sorbed under dynamic conditions on the sulfonate resin SDV -3 (in the H-form). In each experiment 1 g of resin was taken; the concentration of the initial solutions of amino acids was 0.01 N. In all the experiments it was established that in the sorption of amino acids by the hydrogen form of the sulfonate resin liberation of hydrogen ions into the solution did not occur and that the acidity of the solution did not change.

The equivalence of the exchange was also studied in the reverse process – in the displacement of amino acids with a 0.01 N solution of HCl. As Fig. 1 shows, in this case complete equivalence was observed between the amount of hydrogen ion absorbed and the amount of alanine ions displaced (in this case we have to consider only that part of the alanine which is found in the solution as cations).

The results obtained make it possible to put forward a hypothesis on the sorption mechanism of dipolar ions on H-exchangers. The sorption occurs according to the scheme

$$RSO_3^-H^+ + NH_3^+R_1COO^- \rightleftarrows RSO_3^-NH_3^+ + R_1COOH;$$

R is the radical of the cationite polymer; R_1 is the radical of the dipolar ion.

This scheme presupposes that the hydrogen ion is not liberated into the solution, but migrates to the negatively charged end of the dipolar ion, as a result of which the dipolar ion is converted into a cation and is sorbed without electrostatic interference.

The reverse process, the displacement of an amino acid, proceeds in the following way:

$$RSO_3^-NH_3^+R_1COOH + H^+ \rightleftarrows RSO_3^-H^+ + NH_3^+R_1COOH.$$

Here the amino acid appears in solution as a cation as the solution is quite acid and essentially the equivalence concerns only the process given here. The part of the alanine, which is converted into the dipolar ion (the closeness of pH and pK) should not be considered.

Neutralization of the carboxyl group of the dipolar ion, attached to the ionite, is quite probable, despite the high pH value (7), as interaction with the ionite markedly changes the properties of the ion. However, neutralization of the carboxyl group charge is naturally impossible on using the sodium or any salt form of the resin as the salt of a carboxylic acid is always dissociated. Due to this the dipolar ions must be sorbed with greater difficulty on the sodium form of the resin because of the competition of the electrostatic attraction and repulsion. The results given in Table 1 completely confirm this. The sodium forms of the sulfonate resins SDV-3 and SBS-2 sorb much smaller amounts of amino acids than the hydrogen form of the same resins. Here and below the sorption capacity was determined by the dynamic method.

TABLE 1

Sorption Capacity of Sulfonate Resins in the Hydrogen and Sodium Forms for Amino Acids

Resins	Amino acids	Sorption capacity in mg-equiv/g	
		H-form of the resin	Na-form of the resin
SDV-3	Glycine	2,2	0,02
SDV-3	Alanine	1,75	0,011
SDV-3	Leucine	1,92	0,08
SBS-2	Glycine	1,2	0,044

TABLE 2

Sorption Capacity of the Sulfonate Resin SNF (Na) and the Carboxylic Resin KFU (Na) for Amino Acids From Water and Aqueous Acetone Solutions

Resins	Amino acids	Sorption capacity in mg-equiv/g	
		from aqueous solution	from 75% acetone solution
KFU	Glycine	0,14	0,82
KFU	Alanine	0,086	0,67
SNF	Glycine	0,098	0,62
SNF	Alanine	0,054	0,286

The effect of the negative charge of the carboxyl group on the sorption of dipolar ions may be reduced to a known extent by using solutions of increased ionic strength, as a result of screening the charge of the carboxyl group. Experiments to study the sorption of alanine on the sodium form of the resin SDV-3 from a solution containing alanine at a concentration of 0.01 N and sodium chloride at various concentrations, confirmed these considerations. As Fig. 2 shows, on increasing the concentration of sodium chloride the sorption capacity for alanine first increases and then decreases. The increase in the capacity is due to screening of the carboxyl group charge and the decrease is from the competing effect of the sodium ions. It must be emphasized that in the sorption of ions with charges of one sign an increase in the concentration of a competing ion can only lead to a decrease in the sorption capacity.

A second method of reducing the effect of the carboxyl group on the sorption of amino acids is the use of acetone as a solvent, as in acetone solutions the carboxyl group of an amino acid is not dissociated [3]. In Table 2 we give the results of determining the sorption capacity of the carboxylic resin KFU and the sulfonate resin SNF (both resins in the Na-form) for glycine and alanine from 0.01 N solutions of the amino acids in 75% acetone and in water. The amino acids were absorbed quite insignificantly from aqueous solution. On changing to aqueous acetone solution, the sorption capacity increased significantly.

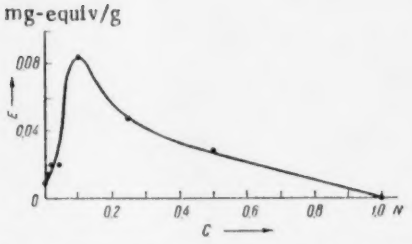

Fig. 2. The relation between the completely dynamic sorption capacity of the resin SDV-3 for alanine and the NaCl concentration. The initial concentration of alanine was 0.01 N. C is the concentration of NaCl (in normality).

The effect of the carboxyl group on the sorption of amino acids by cationites also should apparently be weaker on increasing the distance between the amino and carboxyl groups. To study this effect, we determined the sorption capacity of the resin SBS-2 in the Na-form for an amino acid (glycine), a dipeptide (diglycine) and a tripeptide (leucylleucylglycine). The sorption capacity for glycine was 0.044 mg-equiv/g, the dipeptide 0.208 mg-equiv/g and the tripeptide 0.214 mg-equiv/g, which confirms the importance of the distance between the positive and negative charges in the sorption of dipolar ions on the salt form of the resin.

The results obtained raise the question of reexamining all the systems of interpreting the sorption of amino acids, peptides and proteins and open up new possibilities of selective separations of dipolar ions from all other ions, for example, with the use of two filters with resins in salt and hydrogen forms. In this system of purification the cations are collected on the first filter and only the dipolar ions on the second. Here is one example of a practical application of the sorption mechanism of dipolar ions, established by us. On the basis of the ideas developed it is possible to suggest a large number of variants of the method of selectively sorbing dipolar ions.

We would like to thank R. B. Ponomareva, who participated in serveral experiments.

The High Molecular Compound Institute
of the Academy of Sciences of the USSR

Received July 7, 1956

LITERATURE CITED

[1] S. M. Partridge, G. R. Westall, Biochem. J., 44, 418 (1949); S. M. Partridge, Biochem. J., 45, 459 (1949); S. M. Partridge, R. C. Brimley, Biochem. J., 44, 513 (1949); 48, 313, (1951); 49, 153 (1951).

[2] C. N. Davies, Biochem. J., 45, 38 (1949).

[3] K. Linderstrom-Lang, Hoppe Seylers Zs. Physiol. Chem., 173, 32 (1928).

THE RELATION OF THE HEATS AND THE FREE ENERGIES OF FORMATION OF ZIRCONIUM NITRIDES TO THE COMPOSITION AND STRUCTURE

E. I. Smagina, V. S. Kutsev and B. F. Ormont

(Presented by Academician V. A. Kargin, April 25, 1957)

In the literature it has been accepted that zirconium nitride has a constant phase composition and a formula with integral coefficients has been ascribed to it [1-10]. In accordance with this, data obtained in thermochemical and thermodynamic investigations of zirconium nitride referred to the integral composition ZrN [5, 6, 11-14, 22].

Using methods of precision X-ray and chemical analysis, in the present work we showed that the composition ZrN applied only in a particular case. Hence, it is important to examine the relation of the change in the heat of formation to the composition and the structure of zirconium nitride.

EXPERIMENTAL

The starting materials were zirconium containing 1% hafnium (according to spectrographic analysis) and carefully purified nitrogen. The nitrides were synthesized in a furnace with a tungsten heater which we constructed [15], at an initial vacuum of 10^{-4} mm Hg and temperatures up to 2500° K. Equilibrium of the components was attained by fixing the equilibrium pressure of the nitrogen over the nitride phase. Chemical and X-ray analyses were performed on the products obtained. The heats of formation were determined by thermochemical combustion in a microbomb in an isothermal calorimeter. The heat value (992.3 cal/deg) was determined from standard benzoic acid with a heat of combustion of 6329 cal/g (Leningrad Metrology Institute).

The best combustion of the nitrides occurred at an oxygen pressure of ~16 atm. At higher pressures the products were atomized. A lining of fused ZrO_2 was used to prevent possible reaction between the burning sample and the quartz crucible (the nitride sample was of the order of 600 mg). The initial and final combustion periods were 10 minutes, the main period was 8-10 minutes, the increase in temperature was ~1.2°. Corrections were made for the exposed mercury column of the Beckmann thermometer, for the calorimeter's loss of heat to the outer medium and for the Joule effect, produced on passing an electric current through the platinum wire (on igniting the preparation). The combustion products were also analyzed by chemical and X-ray phase analysis. Corrections were made for the uncombusted nitride and for the carbon from the thin, cotton fabric igniter [16] found by analysis (10-15 mg and 1-2 mg respectively). Traces of nitric acid were found but corrections for it were beyond the limits of accuracy. No traces of CO or nitric oxide were found in the gas phase. The solid combustion products were identical with monoclinic ZrO_2.

RESULTS OF THE INVESTIGATIONS

A series of zirconium nitrides were obtained with compositions from $ZrN_{0.56}O_{0.02}$ to $ZrN_{1.0}O_{0.04}$. In this range all the compositions have a face-centered cubic lattice with a repeating unit of $4.586_6 \pm 0.001$ A. This shows that constancy of the lattice period cannot always serve as proof of a constant composition phase. The heats of formation of nitrides (see Table 1) were calculated by the equation

$$ZrN_xO_y + \left(1 - \frac{Y}{2}\right)O_2 = ZrO_2 + \frac{x}{2}N_2. \qquad (1)$$

The value of ΔH^0_{298} for ZrO_2 was taken as -261.5 ± 0.2 kcal/mole [17].

TABLE 1

Nitrile formula	Lattice period, A	Heat of form., kcal/mole	Heat of form. (oxygenless), kcal/mole	Change in entropy ΔS^0_{298} by Equation (2)	S^0_{298} ZrN_x	Free energy of samples ΔF^0_{298} for oxygenless nitrides, kcal/mole	Part. molar free energy $\overline{F}_i = \left(\frac{\partial \Delta F^0_{298}}{\partial N_i}\right)_{N_k, P, T}$ kcal/mole	Part. molar free energy $\overline{F}_k = \left(\frac{\partial N F^0_{298}}{\partial N_k}\right)_{N_i, P, T}$ kcal/mole
$ZrN_1O_{0.04}$	4.587_3	90.7 ± 0.2	87.9	−22.9	9.3	−81.1	−81	
$ZrN_{0.89}O_{0.03}$	4.588_0	84.5 ± 0.5	82.4	−20.4	9.3	−76.3	−82	−30
$ZrN_{0.74}O_{0.00}$	4.586_3	72.2 ± 0.9	72.2	−16.5	9.7	−67.3	−84	−18
$ZrN_{0.69}O_{0.00}$	4.587_3	68.7 ± 1.8	68.7	−15.4	9.7	−64.1	−88	−10
$ZrN_{0.56}O_{0.02}$	4.585	57.5 ± 0.7	56.1	−12.7	9.4	−52.3	−95	−2

The mean value for each composition from three determinations is given in Table 1. As can be seen in the table, the heats of formation vary a great deal: from 57,500 to 90,700 cal/mole, i. e. by 33,000 cal/mole in changing x from 0.56 to 1. This effect has a much greater value (~ twofold), than in the case of the carbide systems [16, 20]. As a result of this the use of the values of ΔQ^0_{298} for "ZrN", given in the literature (+82200 cal/mole [5], 87300 cal/mole [19]), may lead to serious errors (up to 30,000 cal/mole).

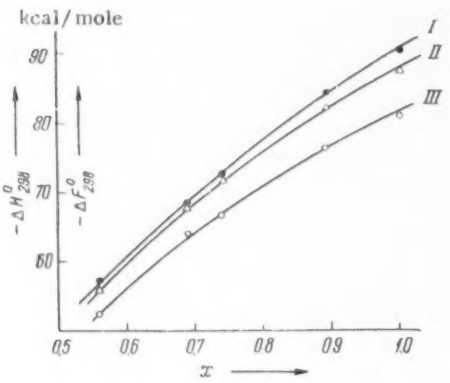

Fig. 1. Curves of the relation: $-\Delta H^0_{298} = f_1(x)$ for ZrN_xO_y (I); $-\Delta H^0_{298} = f_2(x)$ for ZrN_x (II); $-\Delta F^0_{298} = f_3(x)$ for ZrN_x (III).

According to the data from chemical analysis Y reached 0.04 g-atom of oxygen. According to data in the literature, $Q^0_{298} = 80.4 \pm 0.27$ kcal/mole for TiN [21], $Q^0_{298} = 224.89 \pm 0.06$ kcal/mole for TiO_2; Q^0_{298}/x is the mean heat of solution of oxygen in the lattice going from $TiO_{0.871}$ to $TiO_{1.009}$ changes in value from 60.18 to 62.88 kcal/g-atom [24]; for $ZrNO_{0.04}$ $Q^0_{298} = 90.7 \pm 0.24$ kcal/mole (our data); for ZrO_2 $Q^0_{298} = 261.5$ kcal/mole [17]. Using Kireev's law, which is well satisfied in this case, we obtain the mean heat of solution of oxygen in a cubic lattice equal to 70 kcal/g-atom O.

The graph in Fig. 1 gives the curves of the relation of the heats of formation of zirconium nitrides to composition for the preparations obtained and the calculated curve for oxygen-less nitrides. To plot the latter, the value calculated above for the heat of solution of oxygen in a cubic nitride lattice was used. The 1% Hf content was accounted for in calculating the heats of formation. The correction was introduced by the equation:

$$Q_{p\,(Zr+Hf)\,N_x} \cong Q_{p\ ZrN_x} + [Q_{p\,(HfN)} - Q_{p\,(ZrN)}] \cdot \frac{1}{100}.$$

The value of the heat of formation of hafnium nitride was taken as equal to 88.34 kcal/mole [18]. It follows from this that $Q_{p\,(ZrN_x)} \cong Q_{p\,(Zr+Hf)\,N_x}$ within the limits of experimental error. Thus the 1% Hf content could be neglected in investigating the heats of formation.

The amount of oxygen and hafnium impurities were not determined in the papers cited above and the data on heats of formation are given without corrections. From the data on Q^0_{298} in Table 1 for pure nitrides (after

correcting for the heat introduced by the oxygen), obtained from the graph in Fig. 1 and from the data in the literature for standard entropies: $S^0_{298N_2}$ = 45,767 entropy units [28], S^0_{298} = 9.28 ± 0.08 entropy units, S^0_{298} = 9.29 ± ± 0.05 entropy units [22], we calculated the standard free energies of nitrides in relation to nitrogen content using the equation:

$$Zr + \frac{x}{2} N_2 = ZrN_x. \qquad (2)$$

As is shown the entropies of the solid phases differ only by 0.01 entropy units and compensate for each other in the calculation; the value of ΔS^0_{298} is determined from the large value of the entropy of nitrogen and the coefficient x in the equation (2).

To estimate the change in entropy in going from the literature value of $S^0_{298}ZrN$ to $S^0_{298}ZrNx$ we take the increment of nitrogen entropy for a series of nitrides, equal to 2.7-2.9 entropy units [27]; we obtain the increment of S^0_{298} for zirconium: 9.28-2.8 = 6.5 entropy units. Considering that in the first approximation the entropy introduced by each subsequent atom of nitrogen is the same, we obtain approximately:

$$S^0_{298ZrN_x} = 6.5 + 2.8\,x + S^{0h},$$

where S^{0k} is the configurational part of the entropy, which appears when $x < 1$. The latter is calculated by the equation: $S^{0k} = k \ln W$. We obtain a formula for face-centered cubic lattices of ZrN_x the same as for the entropy of mixing in a binary ideal solution [23], as in the occupation of the octahedral interstitial positions by nitrogen $N_i = x$, $N_h = 1 - x$ and $N_i + N_h = 1$.

$$S^{0h} = -R[x \ln x + (1-x)\ln(1-x)]^*.$$

By the well known graphic method [23], we calculated the values of the partial molar free energies of ZrN_x in relation to the number of lattice positions occupied and unoccupied by nitrogen, N_i and N_h.** As the number of Zr atoms in the lattice does not change or changes insignificantly in comparison with N_i and N_h, $\Delta\overline{F}^0_{298}$ depends only on N_i and N_h. The values of $\Delta\overline{F}^0_{298}$ are given in Table 1.

SUMMARY

1. The relation of the heats and free energies of formation of zirconium nitrides to the composition was investigated. In contrast to literature data it was established that zirconium nitride forms a phase of variable composition with a wide range of homogeneity. We prepared samples in the range from $ZrN_{1.0}O_{0.04}$, to $ZrN_{0.56}O_{0.02}$, whose heats and free energies of formation varied from 90.7 to 57.5 kcal/mole and from −81.1 to −52.3 kcal/mole respectively.

2. Despite the wide differences in the nitride compositions and heats and free energies of formation, the lattice period remains practically constant.

L. Ya. Karpov Physico Chemical Institute

Received January 18, 1957

LITERATURE CITED

[1] A. E. Arkel, Physica, 4, 286 (1924).

[2] E. Friederich, L. Sittig, Zs. anorg. allgem. Chem., 143, 293 (1925).

[3] R. Lorenz, J. Wootcock, Zs. anorg. Chem., 176, 289 (1928).

* The mixing entropy in the case of body centered lattices was calculated in [26].

** The consideration of lattice defects as independent variables in thermodynamic calculations was first introduced by Schottky and Wagner in their well known paper [25].

[4] G. Agte, K. Moers, Zs. anorg. Chem., 198, 233 (1931).

[5] B. Neumann, C. Kröger, H. Kunz, Zs. anorg. Chem., 218, 379 (1934).

[6] M. Hoch, D. Dingledy, L. Jonston, J. Am. Chem. Soc., 77, 304 (1955).

[7] G. Hägg, Zs. Phys. Chem., 6, 221 (1929).

[8] G. V. Samsonov, Proc. Acad. Sci., 86, 329 (1952).

[9] Matthews, J. Am. Chem. Soc., 20, 843 (1898).

[10] E. Wedekind, Lieb. Ann., 395, 177 (1913).

[11] L. Brewer, H. Haraldsen, J. Electr. Soc., 102, 399 (1955).

[12] K. K. Kelly, US Bur. Mines Bull., 8, 407 (1937).

[13] Selected Values of Chemical Thermodynamic Properties.Circular of the National Bureau of Standards, 500 (1952).

[14] National Nuclear Energy Series Manhatten Project Technical Section, Div. IV, 1913 (1950).

[15] E. I. Smagina, V. S. Kutsev, B. F. Ormont, Fact. Lab., No. 10, 1249 (1956).

[16] V. I. Smirnova, B. F. Ormont, J. Phys. Chem., 30, 1327 (1956).

[17] G. L. Humphrey, J. Am. Chem. Soc., No. 4, 76, 978 (1954).

[18] G. L. Humphrey, J. Am. Chem. Soc., No.6, 2806 (1953).

[19] A. D. Mah, N. L. Gellert, J. Am. Chem. Soc., 78, 3261 (1956).

[20] V. I. Smirnova, B. F. Ormont, Proc. Acad. Sci., 100, 127 (1955).

[21] G. L. Humprey, J. Am. Chem. Soc., 73, 2261 (1951).

[22] S. S. Todd, Bur. Mines, 11, No. 477 (1950).

[23] V. A. Kirillin, A. E. Sheindlin, The Thermodynamics of Solutions, Moscow, 1956.

[24] M. P. Morosova, E. Volf, S. M. Ariya, Bull. Leningrad State Univ. No.22, 4 (1956).

[25] C. Wagner, W. Schottky, Zs. phys. Chem., 11, 163 (1931).

[26] M. I. Temkin, L. A. Shvartsman, J. Phys. Chem., 23, 755 (1949).

[27] W. M. Latimer, J. Am. Chem. Soc., 73, 1480 (1951).

[28] Short Handbook Physical Chemical Values, Moscow, 1955.

TRUE AND FALSE EQUILIBRIA IN ION EXCHANGE PROCESSES ON CARBOXYL CATIONITES WITH THE STREPTOMYCIN ION

L. F. Yakhontova and B. P. Bruns

(Presented by Academician V. A. Kargin, March 9, 1957)

We showed in previous papers [1, 2] that the rates of ion exchange processes on carboxyl cationites, involving streptomycin ions (Str^{+3}), are determined by their rate of diffusion into the depth of the cationite grain.

On certain types of cationites the rate of penetration of Str^{3+} into the grain slows down after a certain quantity of it has been absorbed by the cationite, so that the course of the reaction practically stops and an apparent (false) equilibrium sets in. This phenomenon occurs in the sorption of Str^{3+} onto both the Na-form (RNa) and the H-form (RH) of the cationite, and in the latter case the existence of false equilibria are especially strongly expressed. Pulverization of the Na-form of the cationite and an increase in the sorption temperature promote a fuller replacement of Na^+ of the ionogenic groups of the resin by Str^{3+} and thus the system is brought closer to a state of true equilibrium. Further investigation of Str^{3+} sorption by carboxyl cationites showed that in changing the cationite-solution system from false to true equilibria, as well as the temperature and dispersion of the resin, the concentration of mineral ions in the solution is quite important. The present work was devoted to this problem.

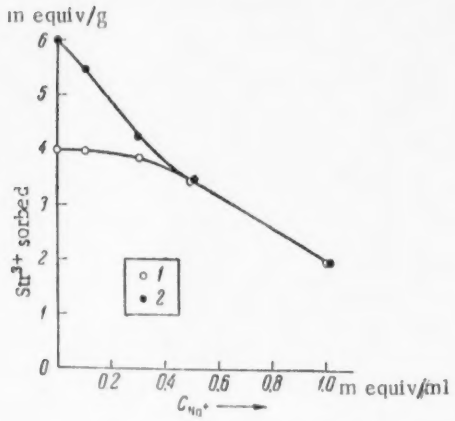

Fig. 1. The relation of Str^{3+} sorption by the Na-form of KB-4 cationite to C_{Na^+} in solution. Temperature was 25°; 1) the grain-size of the cationite was 0.25-0.50 mm, 2) 0.08-0.12 mm.

The investigation of the ion exchange processes was carried out, as in our previous work [1, 2], under static conditions with vigorous mixing of a streptomycin sulfate solution with the cationite. To maintain a constant pH value (~7) in sorption on the H-form of a cationite, an anionite (AOH) EDE-10 [1] was introduced into the solution. The investigation was carried out with two cationites —KFU and type II KB-4 [2].

Figure 1 shows the amount of Str^{3+} sorbed by the Na-form of resin KB-4, with two grain sizes, in relation to C_{Na^+} in the solution over 190 hours contact. The starting concentration of Str^{3+} was constant in all cases and equal to 0.026 N. The amount of Str^{3+} sorbed in 190 hours contact is practically saturation.

As seen in Fig. 1, an increase in the dispersion of the cationite affects the amount of Str^{3+} sorbed only with C_{Na^+} within the range 0 to 0.5 N. Starting from an Na^+ concentration equal to 0.5 N, Str^{3+} sorption does not depend on the size of the cationite grain. This indicates that the unequal distribution of Str^{3+} along the radius of the grain, determining the difference in behavior of the differently dispersed cationites, practically disappears at higher values of C_{Na^+} Thus, false equilibria in the system $Str^{3+} - Na^+ -$ cationite KB-4 are found only when C_{Na^+} is lower than 0.5 N.

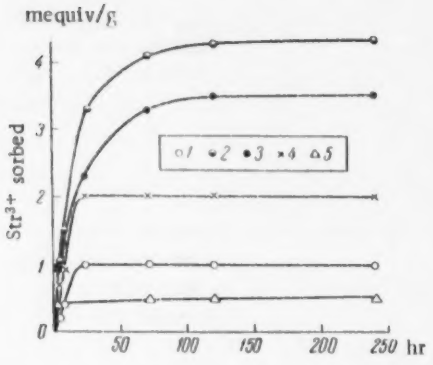

Fig. 2. The kinetics of Str^{3+} sorption by the H-form of KB-4 cationite to C_{Na^+} in the solution. Grain size 0.25-0.50 mm. Temperature 29°. C_{Na+}: 1) 0; 2) 0.03 N; 3) 0.3 N; 4) 1.0 N; 5) 2.0 N.

The effect of the sodium concentration in the solution is very noticeable in changing from false to true equilibria in the sorption of Str^{3+} by the H-form of a cationite. In a previous paper [1] it was shown that the introduction of sodium sulfate into an Str solution, in contact with the H-form of KFU, results in a sharp increase in Str^{3+} sorption. Here, the saturation sorption of Str^{3+} does not depend on the form of the cationite (H- or Na-form) introduced into the solution. Thus, one could assume that in this case true equilibrium had been produced in the system.

We investigated the ion exchange process in the system of H-form KB-4 – streptomycin sulfate with different sodium sulfate concentrations in the solution. The data obtained are shown in Fig. 2, which shows that in the absence of Na^+ the cationite sorbed only 1 mequiv/g of Str^{3+}, and that the process was complete in 24 hours.

The introduction of sodium sulfate, to give a 0.03 N concentration, leads to a sharp increase in ion exchange, with an increase in the time required to reach the saturation value for sorption to 124 hours. An increase of C_{Na^+} to 0.3 N results in yet greater Str^{3+} sorption. Further increase of C_{Na^+} to 1 N and 2 N causes a decrease in sorption. Here, the time required for completion of the ion exchange process becomes much shorter. This data is illustrated more clearly if the amount of Str^{3+} sorbed is plotted on the ordinate for different time periods, with C_{Na^+} along the abscissa, as in Fig. 3. The saturation amount of Str^{3+} sorbed, as can be seen in the figure, passes through a maximum which corresponds to C_{Na^+} close to 0.3 N.

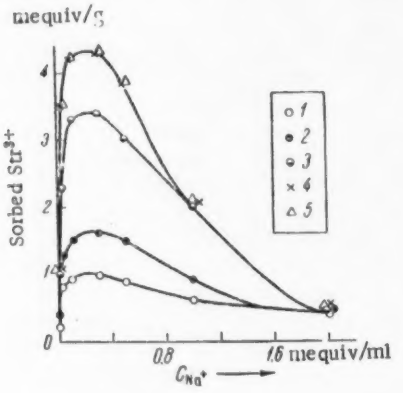

Fig. 3. The relation of Str^{3+} sorption by the H-form of KB-4 cationite to C_{Na^+} in the solution. Grain size 0.25-0.50 mm. Temperature 29°. Contact time: 1) 3 hrs, 2) 6 hrs, 3) 24 hrs, 4) 120 hrs., 5) 240 hrs.

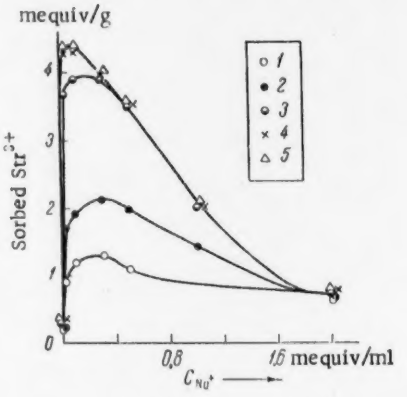

Fig. 4. The relation of Str^{3+} sorption by the H-form of KFU cationite to C_{Na^+} in the solution. Grain size 0.25-0.50 mm. Temperature 29°. Contact time: 1) 3 hrs., 2) 6 hrs., 3) 24 hrs., 4) 72 hrs., 5) 144 hrs.

As can be seen in Fig. 4, the condensation cationite KFU behaves completely analogously to KB-4 cationite. In this case the Str^{3+} sorption maximum is somewhat displaced towards the region of smaller C_{Na^+}.

From the data given, it can be clearly seen that at small C_{Na^+} in the solution no true equilibrium is reached in the streptomycin salt-cationite system. In this range of C_{Na^+} only false equilibria occur. At high values of

C_{Na^+}, a decrease in Str^{3+} sorption is observed with increase in C_{Na^+}, which is expected when true equilibrium is established in the system investigated. This explanation is in complete agreement with the data given in Fig. 1, which shows that for KB-4 resin Str^{3+} sorption depends on the grain size at a low C_{Na^+} in the solution and is independent of it with C_{Na^+} higher than 0.5 N. The existence of false and true equilibria may also be demonstrated very graphically in the system cationite-streptomycin solution, if one starts with the H- and Na-forms of cationite and introduces Na_2SO_4 into the system in such amounts that the Na^+ content remains constant. Table 1 gives data from four such experiments.

TABLE 1

System					
RH, g	RNa, g	AOH, g	Str^{3+}, mg/equiv	Na^+, mg/equiv	Str^{3+} sorbed, mequiv/g
0.5	—	0.75	5	3.5	3.10
—	0,5	—	5	3.5	4.35
0.5	—	0.75	5	200	2.06
—	0.5	—	5	203.5	1.97

As can be seen in Table 1, at low C_{Na^+} in the system, the amount of Str^{3+} sorbed by the Na-form is noticeably greater than in the case of the H-form. With a large amount of Na^+ introduced into the system, the final state does not depend on the form of the cationite. Consequently, it is reasonable to consider that in the first case the equilibrium is false and in the second – true.

It is still difficult at present to give a fully substantiated explanation of the effect of Na ions on the change in the system cationite-streptomycin from the false state of equilibrium to the true one. Hypotheses only may be put forward on this problem. The strong effect of cationite dispersion on the amount of Str^{3+} sorbed at low C_{Na^+} shows that, in this case, the exchange of resin Na^+ for Str^{3+} is limited to a small depth from the outer surface of the grain. At small values of C_{Na^+} a practically complete replacement of the resin Na^+ by Str^{3+} should take place in the case of true equilibrium. This, undoubtedly, does take place in the cationite layer directly in contact with the solution. The Str-form of cationite that is formed is almost impenetrable to Str^{3+} and acts something like a shielding film, preventing further penetration into the depth of the grain. The introduction of a considerable amount of Na^+ into the solution, naturally causes a partial replacement of the Str^{3+} by Na^+ in the outer layer of the cationite particle, which results in the formation of a mixed Str-Na-form. In this the diffusion rate of Str^{3+} increases considerably, making it possible for the Str^{3+} to be distributed equally through all the mass of the cationite grain.

The data given in this article are also unquestionably useful for the correct calculation of equilibrium constants in ion exchange reactions with Str^{3+}.

In papers of previous investigators [3], on equilibria in the carboxylic resin – Str^{3+} system, it was considered that there is in the cationite a definite amount of ionogenic groups, whose cations are completely incapable of being replaced by Str^{3+}. The inaccuracy of this supposition was made clear by the data given in our previous papers. The present investigation shows that it is impossible to determine the true capacity of a resin for Str^{3+} by lowering the C_{Na^+} in the solution for cationites with an average degree of cross-linking (5-10% DVB), as under these conditions, false equilibrium occurs with grain sizes of the order of 0.2-0.5 mm. The true value of the resin capacity for Str^{3+} can be determined for these cationites only with them highly dispersed. Thus, we may suppose that the capacity of the resin for Str^{3+} will be equal to the capacity for Na^+. The calculation of the exchange constants (K_{Na}^{Str}), possible only for the descending branch of the curve, which expresses the relation of Str^{3+} sorption to C_{Na^+} (Figs. 3 and 4), must be derived from a consideration of the weight of Na^+ introduced into the cationite.

All-Union Sci. Res. Antibiotics Inst.

Received March 8, 1957

LITERATURE CITED

[1] L. F. Yakhontova, E. M. Savitskaya, B. P. Bruns, Proc. Acad. Sci., 110, No. 2 (1956).

[2] L. F. Yakhontova, E. M. Savitskaya, B. P. Bruns, Proc. Acad. Sci., 111, No. 2 (1956).

[3] G. V. Samsonov, S. E. Bresler, Colloid J. 18, No. 3, 337 (1956).*

* Original Russian pagination. See C.B. Translation.

INVESTIGATION OF THE NATURE OF THE PRIMARY PHOTOREDUCED FORM OF CHLOROPHYLL AND ITS ANALOGS THROUGH THE USE OF D_2O

V. B. Evstigneev and V. A. Gavrilova

(Presented by Academician A. N. Terenin, March 2, 1957)

Data presented in previous communications [1, 2] support the proposition that the primary reduced form of chlorophyll and its analogs [1 b], which was discovered by us, represents the first stage of reduction of these pigments [3, 4], and is by nature a free radical – an ionized semiquinone – formed by the transfer of an electron from the reducing agent to a long-lived, excited biradical [5] of the pigment.

However, the question of whether the formation of the primary reduced form is actually the result only of the transfer of an electron to the pigment or whether a proton also participates in the process cannot be considered as definitely settled.

While realizing that it is a simplification, it is possible to visualize the following two series of reactions occurring during the photoreduction of chlorophyll and its analogs, the reactions including the formation of a primary product of reduction with the properties observed in the previous investigations:

$$\mathrm{Chl}^{\vee} + \mathrm{RH_2} \rightarrow \cdot\underline{\mathrm{Chl}}^{-} + \mathrm{RH_2^+} \rightarrow \cdot\underline{\underline{\mathrm{Chl\,H}}} + \cdot\mathrm{RH}, \tag{1}$$

$$\mathrm{Chl}^{\vee} + \mathrm{RH_2} \rightarrow \underline{\mathrm{Chl}}\,\mathrm{H}^{-} + \mathrm{RH}^{+} \rightarrow \underline{\underline{\mathrm{Chl\,H_2}}} + \mathrm{R}\cdot \tag{2}$$

where $\mathrm{Chl}^{\vee}$ represents chlorophyll in the biradical state, $\mathrm{RH_2}$ is the reducing agent, and the compounds underlined are the primary and secondary reduced forms.

For a definite anser to the question of to which of these series of reactions to give preference, at any rate with respect to the formation of the primary reduced form, we decided to use the kinetic method [6] already used in our laboratory [7] and based on the substitution of deuterium (D) for the labile hydrogen (H) in the reducing agent.

As is well known [6], in the case of reactions involving hydrogen transfer, a similar substitution usually leads to a slowing down of the course of the reaction, since the activation energy is thereby increased; apparent exceptions are explained by special features, especially by the multi-step nature of the given reaction [6]. Therefore, experiments on the effect of the substitution of D for H in one or several of the components of the reaction on the rate of this reaction can usually give an answer to the question of whether the hydrogen participates in the given reaction. In particular, the participation of hydrogen in photosynthesis [8], in the Hill reaction [7, 9], and in the photoreduction of chlorophyll [7] has been confirmed in a similar manner.

We were faced, then, with the problem of clarifying how the substitution of D for H affects the rate of formation of the primary reduced form of pigments. As in a series of previous investigations [1], the most convenient pigment for these experiments was pheophytin, the primary reduced form of which is most stable [1 c] and permits the carrying out of experiments which are impossible with the primary reduced form of chlorophyll owing to the very high rate of its reverse reactions.

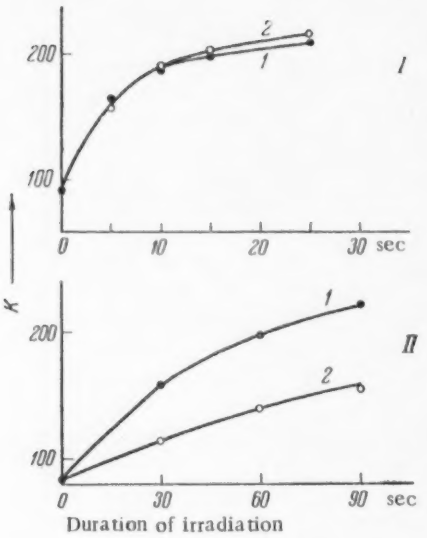

Fig. 1. Effect of the substitution of D for H in ascorbic acid on the rate of formation of the primary (I) and secondary (II) reduced forms of pheophytin a. 1) H_2O, 2) D_2O

The work was carried out under vacuum, in pyridine solution, and with the addition of 10% H_2O or D_2O. Pyridine is satisfactory in this case, because it does not contain labile H atoms which can be replaced by D. Therefore, the exchange of deuterium for hydrogen in the dissolved ascorbic acid is determined wholly by the ratio of the concentrations of this acid and the added D_2O. In our experiments, the concentration of D_2O (500 mg per 5 ml of solution) was 100 times higher than the concentration of ascorbic acid (5 mg per 5 ml); therefore, it can be assumed that in the experiments with D_2O, the equilibrium was almost completely shifted to the side of the formation of ascorbic acid with labile D atoms, and these atoms must have participated almost exclusively in the reduction reactions.

In Fig. 1 is shown the effect of the substitution of D for H in ascorbic acid on the rate of formation of the primary and secondary reduced forms of pheophytin a. The course of the formation of the primary reduced form was traced by measuring the absorption coefficient of the solution at 470 mμ [1c], irradiation of the solution being with red light at –40° [1]. The rate of formation of the secondary reduced form was measured by the change in the maximum at 525 mμ at room temperature.

As may be seen from the figure, the substitution of D for H in the reducing agent did not slow down the formation of the primary reduced form; on the contrary, after the lapse of a certain time, the curve obtained in the presence of D_2O begins to rise slightly higher than that obtained in the presence of H_2O, which can be explained by the limiting of the further rise of the latter curve by the more rapid secondary conversions of the primary form in the presence of H_2O.

In contrast to this, the substitution of D_2O for H_2O decreased to a considerable extent the rate of appearance of the red reduced form (525 mμ). The slowing down of the reduction of chlorophyll by a similar substitution has previously been shown [7], the course of the reaction in that case being determined by the decrease in the red maximum of chlorophyll under corresponding conditions. Again, the effect of D_2O on the reduction of chlorophyll was confirmed by us by measuring the rate of the increase of the red maximum at 525 mμ.

The decrease in the rate of the transition of the primary reduced product of pheophytin a into the secondary form was shown by us by a straightforward experiment, the results of which are presented in Fig. 2. A solution of the composition indicated above was irradiated at –40°, as a result of which the pheophytin a was almost completely reduced with the formation of the primary reduced form [1c]. The reaction tube was then introduced into the spectrophotometer, and the absorption coefficient at 525 mμ was measured [1]. On heating the solution in the dark, conversion of the primary reduced form to the secondary proceeded according to the extent of heating. Figure 2 shows that this conversion was strongly retarded by the substitution of D_2O for H_2O.

It is interesting to note that when using pheophytin a, in contrast to chlorophyll [7], the rate of the decrease of the red maximum (670 mμ) during irradiation differed little with D_2O or H_2O not only at low temperatures, but also at room temperature. However, the reduced solution obtained immediately after irradiation at room temperature differed in composition in the two cases. While in the presence of H_2O the solution contained almost exclusively the secondary form and possessed, in conformity with this, a red-violet color, in the presence of D_2O the color of the solution was tan-brown, and it contained a large amount of the primary form. This shows once again the considerably greater stability of the primary reduced form of pheophytin in comparison with that of chlorophyll. The use of D_2O can serve, consequently, as an additional method for retarding the transition of this form into the secondary.

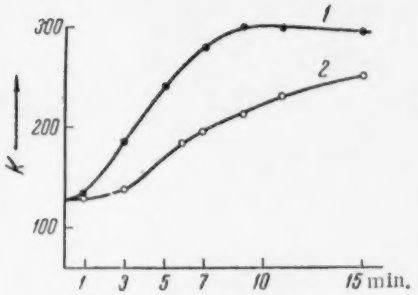

Fig. 2. Effect of the substitution of D for H in ascorbic acid on the rate of the conversion of the primary reduced form into the secondary. 1) H_2O, 2) D_2O.

Thus, the results of the experiments with D_2O are completely in support of the proposition that the proton does not participate in the formation of the primary reduced form of pigments, in contrast to the formation of the secondary reduced form. This form is formed as the result of a primary photochemical transfer of an electron from the reducing agent to the pigment in a long-lived excited state (see Equation 1). Apparently, the addition of the electron takes place at some place in the system of conjugated double bonds, as a result of which the absorption spectrum of the pigment changes sharply and becomes diffuse [1c]. The secondary reduced form is, apparently, the result of the subsequent addition of the proton. The absorption spectrum of the reduced pigment becomes more discrete, although it differs from the spectrum of the original pigment [1, 2].

The difference in the properties of the primary reduced forms of the various pigments of the chlorophyll group, particularly these forms of chlorophyll and pheophytin, is apparently explained by the different action on the conjugated system of double bonds of the positive atoms ($2H^+$ or Mg^{++}) in the center of the molecule. In the presence of $2H^+$ (pheophytin), the extraneous electron is received more readily and retained more stably than in the presence of a divalent metal, particularly Mg^{++} (chlorophyll). This also determines the considerable difference in stability of the electronic reduced forms of these pigments [1, 2].

Additional data on the effect of D_2O on the photoreduction of chlorophyll were obtained by a potentiometric method.

In Fig. 3 are presented curves showing the change in potential of a platinum electrode immersed in a solution of chlorophyll or pheophytin in pyridine in the presence of a reducing agent with added H_2O or D_2O during irradiation. In accordance with the effect previously shown [1a, 10], with irradiation in the presence of ordinary ascorbic acid (experiment with H_2O) the potential curve, which decreases at first, quickly bends upward as a result of further changes in the electrode-active primary reduced form, principally as a result of its conversion into the electrode-inactive secondary reduced form. The substitution of D for H in the ascorbic acid (experiment with D_2O), which retards this conversion (see Fig. 2), immediately changes the form of the curve. The drop proceeds farther, and the minimum is much lower. These data confirm once again that electrode activity is possessed only by the primary reduced form.

A picture similar to that described above of the effect of D_2O on the formation of the primary and secondary reduced forms of pigments was observed by us in certain other solvents incapable of rapidly exchanging their hydrogen for deuterium, particularly in acetone (with the addition of pyridine). In contrast to this, the addition of D_2O instead of H_2O to a methanol solution did not lead to a change in the rate of the photoreduction of chlorophyll or pheophytin, in accordance with the presence in the solvent molecule of a labile hydrogen capable of exchanging for D. In this solvent, the addition of D_2O converts ordinary ascorbic acid to the deuterated acid only to a slight extent insufficient to have an effect on the reaction rate.

The use of D_2O permitted confirmation once again that the red-violet reduced compound formed during the photoreduction of magnesium phthalocyanine [1e, 2], in spite of its instability, is the secondary reduced form, since the rate of its formation and, in particular, of the reverse reaction is reduced by the substitution of D for H in the reducing agent.

In conclusion, we express our appreciation to Academician A. N. Terenin and Professor A. A. Krasnovsky for their constant attention to and discussion of the work.

A. N. Bakh Institute of Biochemistry
Academy of Sciences USSR

Received February 22, 1957

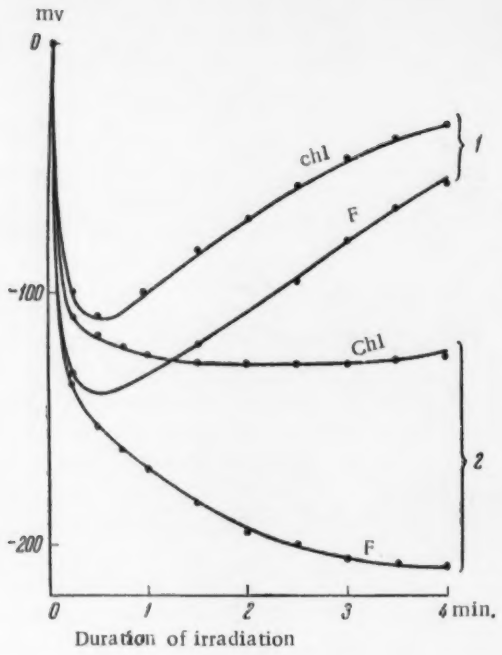

Fig. 3. Curves of the change in photopotential of pyridine solutions of pheophytin a (F) and chlorophyll a+b (Chl in the presence of H_2O (1) and D_2O (2).

LITERATURE CITED

[1] V. B. Evstigneev and V. A. Gavrilova, a) Proc. Acad. Sci. USSR, 92, 381 (1953); b) Proc. Acad. Sci. USSR, 95, 841 (1954); c) Proc. Acad. Sci. USSR, 96, 1201 (1954); d) Proc. Acad. Sci. USSR, 98, 1017 (1954); e) Proc. Acad. Sci. USSR, 103, 97 (1955).

[2] V. B. Evstigneev, Oxidation-Reduction Properties of Chlorophyll in Connection with Its Role in Photosynthesis*, Doctorate Thesis, A. N. Bakh Institute of Biochemistry Acad. Sci. USSR, Moscow, 1956.

[3] A. A. Krasnovsky, Proc. Acad. Sci. USSR, 60, 421 (1948); Bull. Acad. Sci. USSR, Ser. Biol., No. 2, 122 (1955); Coll. of Reports. Problems of Chemical Kinetics, Catalysis, and Reactivity*, Izd. AN SSSR, 1955.

[4] A. A. Krasnovsky et al, a) Proc. Acad. Sci. USSR, 63, 163 (1948); b) Proc. Acad. Sci. USSR, 66, 663 (1949); c) Proc. Acad. Sci. USSR, 69, 393 (1949); d) Proc. Acad. Sci. USSR, 81, 879 (1951); e) Proc. Acad. Sci. USSR, 89, 527 (1953).

[5] A. N. Terenin, The Photochemistry of Dyes*, Izd. AN SSSR, 1947.

[6] A. I. Brodsky, The Chemistry of Isotopes*, 1952.

[7] A. A. Krasnovsky and G. P. Brin, Proc. Acad. Sci. USSR, 96, 1025 (1954).

[8] I. Curry, S. F. Trelease, Science, 82, 18 (1935); E. N. Craig, S. F. Trelease, Am. J. Bot., 24, 332 (1937); R. Pratt, S. F. Trelease, Am. J. Bot., 25, 133 (1938).

[9] L. Horwitz, Bull. Math. Biophys., 16, 45 (1954).

[10] B. V. Evstigneev and V. A. Gavrilova, Proc. Acad. Sci. USSR, 114, No. 5 (1957).**

* In Russian.

** See C.B. translation.

INTERCRYSTALLITE LAYERS IN GYPSUM

V. A. Zolotov

(Presented by Academician P. A. Rebinder, April 29, 1957)

The majority of crystalline bodies used in engineering are aggregates consisting of individual, interconnected grains (crystallites). Numerous investigations, critically reviewed in detail by M. V. Klassen-Neklyudova and T. A. Kontorova [1], have shown that the boundaries between grains play a very essential role in a whole series of processes occurring in polycrystalline materials. The failure of metals and alloys under certain conditions proceeds along grain boundaries (hot-brittleness, creep); in other cases (lower temperature, different load conditions) the boundaries are, on the contrary, the strongest place in the metal. Intercrystallite boundaries change in a specific manner the nature of plastic deformation of crystals [2], they contribute to the development of diffusional processes in metallic alloys [3], they affect the electrical properties of the body [4], etc. Therefore, the specific study of the structure and properties of intercrystallite boundaries has acquired a very real significance.

At the present time, many investigators consider that the grains are separate from each other, being connected by their intercrystallite layer ("transition zone") which has a polyatomic thickness and a structure different from the structure of the grains themselves [5].

Another point of view is that there is no particular intermediate layer between grains, and the lattices of neighboring crystallites directly butt against each other forming a two-dimensional, not a three-dimensional, separation boundary [3].

Thus, in spite of the large amount of work (carried out, however, almost exclusively on metals), the question of the nature of intercrystallite bonding remains unanswered up to the present. This situation is explained partially by the fact that, owing to the small thickness of the layer, x-ray structural analysis cannot be used for their study. Moreover, intercrystallite boundaries in non-metals have been little studied; there has been almost no work at all carried out on transparent crystals. The large class of materials obtained by crystallization from solution has been studied very little in this regard. Furthermore, many important structural materials are polycrystals of precisely this form.

We considered it expedient, therefore, to undertake a study of the intercrystallite boundaries in polycrystalline gypsum dihydrate – a substance which satisfies the requirements indicated above and which finds wide use in structural practices. Satisfactorily pure fine-grained natural gypsum from the Peshelansky deposit of the Arzamas region served as the subject for investigation.

The following experiments were carried out.

1. From polycrystalline samples of the natural gypsum were prepared plane-parallel sections having a thickness of from 0.03 to 0.1 mm. Investigation of these sections under the polarizing microscope disclosed the presence along the grain boundaries of streaks 0.002-0.01 mm wide which did not change color and remained dark on rotation of the microscope stage. These streaks were observed in very thin sections, they remained visible at any rotation and inclination, and, therefore, they cannot be explained as merely the result of mutual overlap of the edges of neighboring grains. The presence of the dark streaks indicates the absence of a regular structure in the crystallites close to their boundaries; i. e., in other words, it indicates the presence in gypsum of special intercrystallite layers.

2. On the surfaces of samples which had been subjected to a 15-minute etching in HCl there appeared shallow furrows, easily observable under oblique illumination or by means of a binocular microscope, having a width up to 0.01 mm and proceeding along the grain boundaries, which indicates a higher solubility of the layer in comparison with the grains.

3. When the section was immersed for half an hour in an alcoholic solution of methyl violet and the upper surface ground a little or the excess dye washed off with alcohol, a more intense and deeper color was retained along the grain boundaries forming a characteristic network of intergranular boundaries.

4. Microscopic examination of the surface of a section heated in a special electric furnace mounted on the stage revealed the presence of turbidity in the crystallites when the section was heated to 80-100°, this turbidity beginning, as a rule, at the boundaries. These experiments provide a basis for the assumption that the process of dehydration in gypsum dihydrate begins initially in the intercrystallite layers.

5. During inspection under the microscope with reflected light of the surface of a fracture in the polycrystalline gypsum, it was observed that fracture of the individual grains proceeded primarily along the most perfect cleavage plane $\{010\}$, easily recognized by its characteristic luster; additionally, the pressure figure method was used to develop the fracture surface. However, a coarse surface of irregular form, rather than a smooth crystal face, appeared at many places, indicating, apparently, the presence in these places of disintegration along the boundaries of the crystalline grains.

6. Pieces of gypsum stone were pulverized at room temperature by various methods to a powder with a maximum particle size approximating the largest dimension of the crystallites in the given sample. Careful and repeated examination of the powder under crossed nicols did not disclose a single fragment which consisted of two, three, or more grains; all fragments appeared to be monocrystals. These experiments (just as those described in Paragraph 5) indicated the low strength of the intercrystallite layers in gypsum in comparison with the strength of the grains themselves. In this respect, gypsum behaves differently than, for example, metals, in which, as is well known, failure at room temperature proceeds by fracture or cleavage through the body of the grain. This same result was obtained in similar experiments repeated with gypsum powder prepared at +50° and −20°; under these conditions, it was not possible to detect any effect of temperature on the strength of the layer. All these experiments indicate the existence in natural gypsum of special, comparatively weak and porous intercrystallite layers, which could be sites of incomplete growth of the grains with an entrapped film of air between them. Undoubtedly, the peculiarities of such layers determine, in many respects, the mechanical strength of natural gypsum under different conditions (moisture, etc.).

When this work had been completed, there appeared in print an article by E. E. Segalova, V. N. Izmailova and P. A. Rebinder [6] in which was noted the significance of growth contacts of small crystals during the formation of a three-dimensional crystal structure (porous skeleton) in the process of crystallizing gypsum dihydrate from a supersaturated solution during the hardening of concentrated suspensions of gypsum hemihydrate.

In this connection, it would be of interest to study the change of conditions of growth during the origin of less and less porous natural gypsum and artificial gypsum stone.

Z. V. Sapazova and N. S. Igonina took part in carrying out the experiments.

Arzamas State
Pedagogical Institute

Received October 27, 1956

LITERATURE CITED

[1] M. V. Klassen-Neklyudova and T. A. Kontorova, Prog. Phys. Sci., 22, 249, 395 (1939).

[2] E. S. Yakovleva and M. V. Yakutovich, Proc. Acad. Sci. USSR, 90, 1027 (1953).

[3] S. M. Vinarov, J. Tech. Phys., 19, 243 (1949); 22, 335 (1952).

[4] A. I. Andrievsky, V. I. Voloshchenko and M. T. Mishchenko, Proc. Acad. Sci. USSR, 90, 521 (1953).

[5] V. I. Arkharov, J. Tech. Phys., 22, 332 (1952); Trans. Inst. of the Physics of Metals. Ural Branch Acad. Sci. USSR, No. 16, 7 (1955).

[6] E. E. Segalova, V. N. Izmailova and P. A. Rebinder, Proc. Acad. Sci. USSR, 110, 808 (1956).

THE FORMATION OF ACETYLENE DURING THE INCOMPLETE COMBUSTION OF METHANE IN OXYGEN

Z. V. Ievleva and P. A. Tesner

(Presented by Academician N. N. Semenov, February 28, 1957)

At the present time, one of the most effective methods for the production of acetylene from natural gas is oxidative pyrolysis, i. e., the incomplete combustion of natural gas in oxygen. Several commercial plants already operate by this method [1, 2]. However, the mechanism of the formation of acetylene in a flame remains almost completely unstudied. The work of Benedek and Laslo [3] and of Kydd [4], in which this question was recently considered, contain too few experimental data.

In the present work, the incomplete combustion of methane in oxygen was studied in a Bunsen type burner, samples of the gases being collected at various points in the flame. In order to decrease disturbance of the flame during collection of the samples, a watercooled gas collector with an internal diameter of 0.2-0.3 mm was used.

Temperature measurement was accomplished by means of three platinum—platinum-rhodium thermocouples with wire diameters of 0.04, 0.15, and 0.5 mm with subsequent extrapolation to zero wire diameter.

The collector and thermocouples were placed in the flame by means of an apparatus with a micrometer screw with which the distance could be read with an accuracy of 0.01 mm, thus providing for the construction of curves showing the distribution of composition and temperature in a zone 2-3 mm thick.

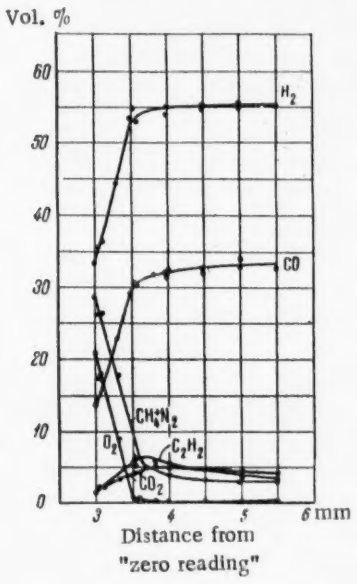

Fig. 1

Experiments were carried out with an open and with a divided flame with different ratios of methane to oxygen in the feed mixture, as well as experiments with the addition of propane to the methane.

In Fig. 1 are presented the results of analyses of combustion products taken along the vertical axis of the flame in the region of the apex of the inner cone while burning a mixture consisting of 43.5% O_2, 54.8% CH_4, and 1.7% N_2 in the burner with the divided flame. Division of the inner and outer cones was accomplished by means of a quartz hood with a diameter of 27 mm and a length of 70 mm. Feed rate of the combustible mixture was 2.2 liters/minute, giving a height of the inner cone of 12 mm.

Examination of the curves presented in Figure 1 shows that a large part of the methane and oxygen reacts in a very short region of the flame, from x = 3.0 to x = 3.5 mm (x is distance along the axis of the flame). In this region are formed basically all the reaction products, CO_2, C_2H_2, CO and H_2. In reality, the combustion zone apparently still exists here, since with the introduction of the sample tube into the flame there is inevitably some disturbance of the combustion front.

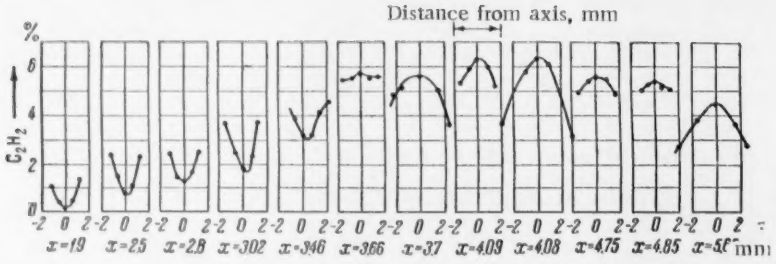

Fig. 2.

Similar results were obtained with a different feed mixture, an increase in oxygen content decreasing the acetylene concentration. In the combustion of a methane-propane mixture, the concentration of acetylene in the combustion products and the yield of acetylene based on the carbon in the influent gas increased.

In experiments with an undivided flame, considerable diffusion of outside air was observed, which led to an increased content in the gas of nitrogen and oxygen-containing components, distorting the results. Therefore, the acetylene concentration in undivided flame is lower and the hydrogen concentration passes through a maximum, while in a divided flame the hydrogen content increases continuously.

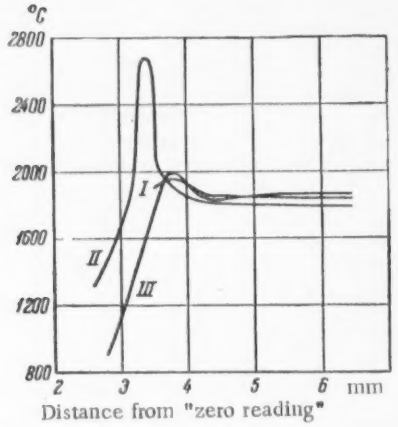

Fig. 3. I) Experimental curve, II) curve calculated from the water gas equilibrium, III) curve calculated by heat balance.

In Fig. 2 are presented curves of the acetylene content in eleven horizontal sections for various distances from the edge of the burner (from x = 1.90 to x = 5.65 mm). Samples of gas were taken at five points in each section. The curves of Fig. 2 show that above the apex of the inner cone, which occurs in the section x = 3.7 mm, the concentration of acetylene is a maximum along the axis, while below the apex it is a minimum. This is explained by the form of the inner cone, in which, in essence, the reaction forming acetylene takes place.

These experimental results show that the incomplete combustion of methane in oxygen, which is accompanied by the formation of significant amounts of acetylene, is completed, to all intents and purposes, in the apex zone in some tenths of a millimeter.

Beyond this zone and above the apex of the inner cone the reaction proceeds considerably more slowly. Beyond the oxygen zone, the acetylene content increases to a maximum, which occurs within a distance of 0.3-0.4 mm from the end of the oxygen zone. The acetylene content then begins to drop.

In order to study the initial stages of the reaction, experiments were conducted in which rapid and simultaneous ignition of the feed gas over the entire section was accomplished. For this purpose, a special spiral igniter, coiled from platinum foil and heated electrically to a temperature of 1100-1200°, was placed at the outlet of the burner. These experiments showed that at the beginning of the oxygen zone only CO, H_2O, and CO_2 are formed; the formation of acetylene and ethylene from the unburned portion of methane begins later. Thus, it can be concluded that the formation of acetylene proceeds chiefly in the end of the oxygen zone, and is concluded in the immediate vicinity of its end.

In Fig. 3 is presented a curve of the temperature distribution along the vertical axis of the flame (I) for a mixture containing 57% CH_4, 41.3% O_2, and 1.6% N_2. The temperature rises rapidly in the oxygen zone, and

then remains almost constant at approximately 1850°. In Fig. 3 are also presented two curves calculated using experimental data on the gas composition. Curve II was obtained from calculations based on the equilibrium among the components of the water gas reaction (the temperature was determined from tables of values of the ratio $\frac{p_{CO} \cdot p_{H_2O}}{p_{CO_2} \cdot p_{H_2}}$), and III was calculated from a heat balance without taking dissociation into account.

The considerable divergence between Curves I and II at values of $x<3.7$ shows that the components of the water gas reaction are not in equilibrium in the oxygen zone. Here primarily proceeds the formation of carbon monoxide and water, the content of which significantly exceeds the equilibrium content corresponding to the observed temperature. However, directly after this zone Curves I and II merge, which indicates establishment of equilibrium of the water gas reaction in the immediate vicinity of the oxygen zone. This result shows the applicability of the thermochemical method of calculation to the process of the formation of acetylene during incomplete combustion, taking into account the water gas equilibrium [5].

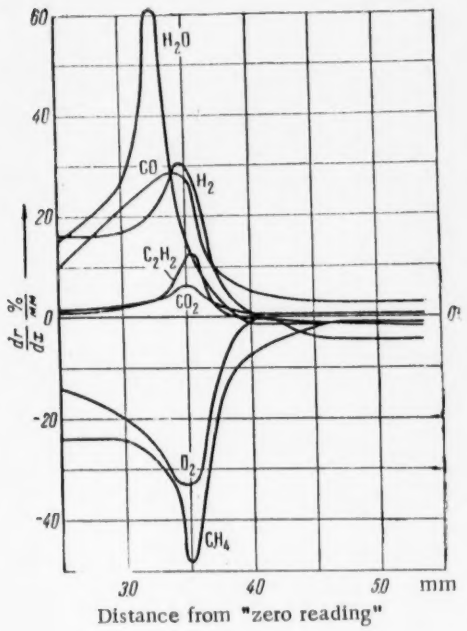

Fig. 4.

In order to evaluate the relative rates of formation of the various reaction products, values of the concentration gradients, $\frac{dr}{dx}$, were calculated on the basis of the experimental results obtained. In Fig. 4 are pictured the results relating to the change in concentration along the vertical axis of the flame. These results show that in the beginning of the oxygen zone the formation of carbon monoxide and water proceeds with the highest rate. The formation of acetylene attains an appreciable rate only in the end of the oxygen zone, and it is accompanied by an increase in the rate of formation of hydrogen.

This result refutes the mechanism proposed by Benedek and Laslo [3], according to which acetylene is formed by the reaction of formaldehyde and methyl alcohol. Apparently, the formation of acetylene, which is accompanied by the formation of hydrogen, has a purely thermal mechanism, and proceeds by the reaction of methane molecules or the corresponding hydrocarbon radicals upon attainment of a sufficiently high temperature by the combustion of part of the methane to CO, H_2O, and CO_2. Indeed, it must be considered that the increase in the rate of hydrogen formation in the end of the oxygen zone is also explained by the water gas reaction, which must proceed here in the direction $CO + H_2O \rightarrow CO_2 + H_2$. However, the concentration of CO_2 in the combustion products is somewhat less than the hydrogen concentration, so that this reaction alone cannot be responsible for all of the hydrogen formed.

All-Union Scientific-Research
Institute for Natural Gases

Received December 30, 1956

LITERATURE CITED

[1] H. Sachsse, Chem. Ing. Techn., 26, 245 (1954).

[2] E. Bartholome, Chem. Ing. Techn., 26, 253 (1954); Trans. of the 4th Petroleum Congress in Rome, 5, 1956.

[3] P. Benedek, A. Laslo, Magyar Kemiai Folyoirat, 57, 372 (1951).

[4] H. Kydd, J.Am. Chem. Soc., 74, 5536 (1952).

[5] P. A. Tesner, Proc. Acad. Sci. USSR, 95, 1275 (1954); Trans. All-Union Petroleum Gas Sci.- Res. Inst., No. 5 (1954).

ON THE MECHANISM OF THE HYDRATION OF OLEFINS IN AQUEOUS SOLUTIONS OF STRONG ACIDS

I. I. Moiseev and Associate Member Acad. Sci. USSR Ya. K. Syrkin

The hydration of isobutylene [1], triptene, trimethylethylene, and methylenecyclobutane [2] in 1-5 M solutions of HNO_3 obey a first-order equation. The following relationship exists between the reaction rate constant, k, and the acidity function of Hammett, H_0:

$$-\rho H_0 = \log k + \text{const}, \qquad (1)$$

in which the coefficient $\rho \approx 1$ (0.98–1.11). The applicability of this equation served as a basis for the following mechanism [1] for the hydration of olefins:

$$>C=C< + H_3O^+ \underset{\longleftarrow}{\xrightarrow{\text{fast}}} \left[>C\overset{\overset{H}{\uparrow}}{=}C<\right]^+ + H_2O \quad \text{(equilibrium)}$$

$$\left[>C\overset{\overset{H}{\uparrow}}{=}C<\right]^+ \underset{\longleftarrow}{\xrightarrow{\text{slow}}} -\overset{|}{\underset{H}{\underset{|}{C}}}-\overset{+}{C}< \quad \text{(limiting stage)}$$

$$-\overset{|}{\underset{H}{\underset{|}{C}}}-\overset{+}{C}< + 2H_2O \rightleftarrows \text{alc.} + H_3O^+ \quad \text{(equilibrium)}$$

The heat effect of the first stage may be evaluated by a summation of the heats of the following processes: a) desolvation of a proton, – 260 [3]; b) addition of the proton to the olefin with the formation of the π-complex, Q_X; c) solvation of the resulting π-complex, Q_Y; d) solution of the water molecule bonded to the proton, + 10 kcal. In order to calculate Q_X by the MO LCAO method it is necessary to know the value of the resonance integral, γ, of the bonds between the C and H atoms in the π-complex.

It is possible to evaluate γ by a method similar to that used by Simonetta and Winstein [4]. For this purpose, let us consider the change in the integral of the overlap of S during the approach of the proton to the π-electrons, which is described by pure p_z-functions.

Since the value of the p_z-functions is a maximum in the z-direction, the values of S' for each C...H distance obtained from the tables [5] were multiplied by cos θ (θ is the angle between the z-axis and the line joining the C and H atoms). The value of $S = S' \cos\theta$ increases with the approach of the proton, reaches a maximum value of 0.36 at $R_{CH'} = 1.13$ A, and decreases with a further decrease in R_{CH}, although the integral S' continues to increase. For the usual C – H bond, $\gamma_1 \approx 45$ kcal at $S_1 = 0.69$ [6]. Using these values in the formula [6] $\gamma = \gamma_1 [S/(1+S)] : [S_1/(1+S_1)]$, we find for S = 0.36 the value $\gamma = 29.3$ kcal. With this value of γ and with a value of the resonance integral for the π-bonds of >C = C< of 20 kcal, the energy of the two electrons in the field of the three nuclei becomes 103 kcal. The energy gain during the addition of a proton

to a double bond with the formation of a π-complex is, then, 103 − 40 = 63 kcal. This value is probably too low. An attempt to evaluate the upper limit of this value by the MO method, taking into account the difference in the ionization potentials of the olefin and hydrogen, led to a value of ~ 145 kcal for isobutylene. The heat of solvation of the π-complex formed from isobutylene is probably close to the heat of solvation of the cation $N(CH_3)_4^+$ (i. e., ~32 kcal [3]), in which the positively charged atom is surrounded by hydrophobic CH_3 groups.

Approximate calculations of this quantity by different methods [7, 8], lead to values from 20 to 39 kcal. Thus, the heat effect of the first stage is − 80 − 180 + 145 + 39 + 10 = − 66 kcal. For a solution to the problem of the heat effect of the second stage, it is necessary to know the heat of formation of a carbonium ion from isobutylene and a proton. With this same approximation, it can be shown that the complex of olefin and proton in which the proton is displaced toward one of the carbon atoms of the >C = C< bond is more favored than the symetrical π-complex, and the conversion of the second into the first is accompanied by an energy gain of more than 30 kcal. According to thermochemical data [9-11], the heat of addition of an unsolvated proton to gaseous isobutylene with the formation of a carbonium ion is 194 ± 2 kcal.• Thus, the carbonium ion is more stable than the π-complex, and conversion of the first into the second is accompanied by the absorption of ~50 kcal. However, for the fulfillment of the relationship (1) in the interpretation of Hammett [12] it is necessary to assume that the first stage, which requires the absorption of 66 kcal, is not limiting, and the second stage, which proceeds with the liberation of heat, is. It is evident that this idea is without basis. Even if it be assumed that the activation energy of the first stage is equal to the heat effect and taking into account that the activation energy of the slower second stage must be, if only a little, greater than the activation energy of the first stage, it can be seen that the activation energy of the entire reaction is, on the whole, close to double the value of the heat effect of the first stage, i. e., − 130 kcal, which is in disagreement with the experimental value $\Delta H^{\#}$ = 13-17 kcal [2b] for gaseous olefins. Using the value 194 kcal for the heat of addition of a proton to gaseous isobutylene, it is readily seen that the formation of solvated $(CH_3)_3C^+$ in solution from the gaseous olefin and an oxonium ion requires the absorption of 17-20 kcal, which agrees with the experimental value for the activation energy of this reaction within the limits of accuracy of the estimation of this value. Thus, in the case of isobutylene, proceeding of the reaction through the carbonium ion is possible. However, the absence of an interconversion of 2-methyl-2-butene and 2-methyl-1-butene under conditions such that dehydration does not occur excludes a mechanism involving a carbonium ion as an intermediate product in equilibrium with the original [13]. Moreover, the closeness of the values of $\Delta H^{\#}$ and $\Delta S^{\#}$ for all these olefins and the existence of the same regularities in kinetics [1, 2] suggests that hydration of these olefins and of isobutylene proceeds by a single mechanism. The heats of formation of carbonium ions by the addition of a proton to the gaseous olefin, obtained from complete cycles, are: for $C_2H_5^+$, 149 kcal; $(CH_3)_2CH^+$, 179 kcal; $(CH_3)_3C^+$, 194 kcal. Thus, if the reaction did proceed through a carbonium ion activated complex, the activation energy for isobutylene and propylene should differ by approximately 15 kcal, but experimentally this difference in heat of activation is 3.2 kcal [14]. It is also improbable that $\Delta H^{\#}$ for ethylene will be greater than the activation for isobutylene by 45 kcal. The smaller difference in the experimental values for the olefins cannot be explained by the difference in the heats of formation of the corresponding carbonium ions.•• We note also that in the case of propylene, between the value for the heat of formation of the carbonium ion in solution from the gaseous olefin and H_3O^+ and the experimental value of $\Delta H^{\#}$ there is a breach which exceeds the error in the determination of the heat of formation of the carbonium ion, and in the case of propylene, reaction through the carbonium ion is impossible. A more probable mechanism for this reaction in aqueous solutions seems to us to be through the transition state pictured in Scheme I. Six electrons move in the field of the six centers of the transition complex, thus providing for a lower activation energy, and the positive charge on the oxonium oxygen also contributes to this. We consider it essential that the transfer of a proton from H_3O^+ to the olefin molecule, forming an alkox-

• The heats of formation of carbonium ions from gaseous ethylene, propylene, isobutylene, and a proton were calculated from thermodynamic data [9-11] for the cycle which includes hydrogenation of the olefin and dehydrogenation of the resulting hydrocarbon through the formation of a radical and ionization of this radical with the formation of the carbonium ion.

•• According to the data of Franklin [10], the difference in the heats of formation of the gaseous ions sec.-$C_3H_7^+$ and tert.-$C_4H_9^+$ is 22 kcal, and in aqueous solution it is 16 kcal. According to the formula of Kondratyev and Sokolov [8], the difference in the heats of solvation of these ions is 4 kcal. Taking into account this figure and the heats of formation of the gaseous ions used here, the difference in $\Delta H^{\#}$ must be ~10 kcal in dilute aqueous solution, and must increase and approach a value of 15 kcal with increasing acid concentration.

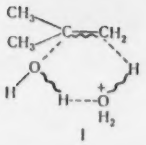

I

onium ion, and regeneration of H_3O^+ are here combined into a single act. It is also possible that in the transition complex, the H_3O^+, the olefin molecule, and the H_2O molecule are disposed in an open chain, which leads to the formation of an alkoxonium ion and water. V. I. Tsvetkova [14] noted that the kinetic regularities observed during hydration in aqueous dioxane solutions [15] and in concentrated acid solutions [14] cannot be satisfactorily explained without considering that a molecule of water is included in the transition complex. Moreover, stagewise mechanisms require additional assumptions which are not in agreement with the experimental data or with theoretical arguments. Thus, for example, from the mechanism of Taft [1] it follows that the equilibrium constant can be expressed as the ratio of the constants of the direct and reverse reactions only at the moment of equilibrium, which is contrary to experiment [14]. Moreover, according to the mechanism of Tsvetkova [14], the limiting stage is the reaction of the carbonium ion or π-complex with a molecule of water, which is difficult to understand in the light of available data on the energetics of this reaction [8]. In concentrated acid solutions, the preliminary formation between the olefin and a molecule of acid (and not a proton) of a π-complex approximating an ion pair in structure is possible. In connection with the discussion of the reaction mechanism in aqueous acid solutions, we note that values of H_0 in separate intervals or within wide limits of concentration can be satisfactorily given by other functional relationships [16-18] besides $H_0 = -\log(a_{H^+} f_B / f_{BH^+})$. In connection with this, the interpretation of kinetic data sometimes becomes ambiguous, as was noted by A. I. Gelbshtein, G. G. Shcheglova and M. I. Temkin [19] during a study of the decomposition of formic acid. S. G. Entelis [20] considers that relation (1) must be observed in the case where the reaction is limited by the reaction of SH^+ with a neutral molecule (for example, the stage $SH^+ + H_2O$) under the condition $a_{H_2O} f_{SH^+} / f_{M_+^\#} = \text{const}$ ($f_{M_+^\#}$ – is the activity coefficient of the transition state $M_+^\#$).

It can be shown that in this case, relation (1) will be satisfied under the condition $a_{H_2O} f_S / f_{M_0^\#} = \text{const}$ or $\log(a_{H_2O} f_S / f_{M_0^\#}) = \alpha + \beta H_0$ ($f_{M_0^\#}$ is the activity coefficient of the complex $M_0^\#$, which differs from the activated complex $M_+^\#$ only in that it does not contain a proton). Similarly, it can be shown that a reaction in which two molecules of water enter into the activated complex obeys the equation $k = k_0 h_0 f_S a_{H_2O}^2 / f_{M_0^\#} \cdot M_0^\#$ in this case corresponds to the stoichiometric composition $S \cdot 2H_2O$. It is readily seen that the nature of the kinetic relation remains independent of whether solvation precedes the transfer of a proton to the complex of the reacting molecules or whether, on the contrary, solvation follows protonization. Depending on the relation among the activity coefficients entering into the equation for the reaction rate constant, either Equation (1) or

$$k_0' = k_0' [H_3O^+], \qquad (2)$$

or, finally, intermediate relationships can be applicable.

On the basis of Equation (1) or (2), in the general case it can be asserted only that the transition complex contains a molecule of substrate and a proton, but it is impossible to make any statement as to the presence of other particles. It is all the more impossible to determine with which of the component parts of the complex the proton is bound.

M. V. Lomonosov Moscow Institute
of Fine Chemical Technology

Received January 28, 1957

LITERATURE CITED

[1] R. W. Taft, J. Am. Chem. Soc., 74, 5372 (1952).

[2] a) R. W. Taft, E. L. Purlee, P. Reisz, C. A. De Fazio, J. Am. Chem. Soc., 77, 1584 (1955); b) J. B. Levy, R. W. Taft, D. Aaron, L. P. Hammett, J. Am. Chem. Soc., 75, 3955 (1955).

[3] K. B. Yatsimirsky, The Thermochemistry of Complex Compounds• , Moscow, 1951.

[4] M. Simonetta, S. Winstein, J. Am Chem. Soc., 76, 18 (1954).

[5] R. S. Mulliken, C. A. Rieke, D. Orloff, H. Orloff, J. Chem. Phys., 17, 1248 (1949).

[6] R. S. Mulliken, J. Am. Chem. Soc., 72, 4493 (1950).

[7] K. P. Mishchenko and A. M. Sukhotin, J. Phys. Chem., 27, 26 (1953).

[8] V. N. Kondratyev and N. D. Sokolov, J. Phys. Chem., 29, 1265 (1955).

[9] T. Kottrell, Strengths of Chemical Bonds,• Moscow, 1956.

[10] J. L. Franklin, Trans. Farad. Soc., 48, 448 (1952).

[11] A. G. Evans, Trans. Farad. Soc., 42, 719 (1946); D. P. Stevenson, Discuss. Farad. Soc., 10, 35 (1951).

[12] L. P. Hammett, Physical Organic Chemistry, N. Y., 1940.

[13] J. B. Levy, R. W. Taft, L. P. Hammett, J. Am. Chem. Soc., 75, 1253 (1953).

[14] V. I. Tsvetkova, Dissertation, Inst. Chem. Phys. Acad. Sci. USSR, 1956.

[15] G. R Lucas, L. P. Hammett, J. Am. Chem. Soc., 64, 1938 (1942).

[16] H. G. Kuivila, J. Phys. Chem., 59, 1028 (1955).

[17] N. C. Deno, R. W. Taft, J. Am. Chem. Soc., 76, 244 (1954); J. C. Brand, J. Chem. Soc., 1950, 997.

[18] N. C. Deno, J. J. Jaruzelski, A. Schriesheim, J. Am. Chem. Soc., 77, 3044 (1955).

[19] A. I. Gelbshtein, G. G. Shcheglova and M. I. Temkin, J. Phys. Chem., 30, 2267 (1956).

[20] S. G. Entelis, Dissertation, Inst. Chem. Phys. Acad. Sci. USSR, 1955.

• In Russian

INVESTIGATION OF THE STRUCTURE OF THE MOLECULAR CHAINS OF POLYISOPRENES BY INFRARED ABSORPTION SPECTRA

K. V. Nelson and I. Ya. Poddubnyi

(Presented by Academician V. A. Kargin, February 2, 1957)

In the overall problem of synthesizing rubbers having given properties, a study of the effect of polymerization conditions on the structure and steric configuration of the basic unit of the molecular chains is essential. In the present work, infrared spectra were used to study the microstructure of a number of polyisoprene rubbers. Polyisoprene produced by catalytic polymerization (SRI), which approaches natural rubber in physico-mechanical properties [1], and emulsion polyisoprene (SEI) produced by free radical polymerization [2] were investigated.

The formation of four different structures of the units of the macromolecule is possible during the polymerization of polyisoprene, the structures differing both with respect to the position of the double bond relative to the basic chain and with respect to the steric configuration of the atoms relative to the double bond: 1,2; 3,4; cis-1,4; and trans-1,4. The quantitative determination of the content in the polymer chain of each of these structures, the combination of which may be called the microstructure of the polymer, was carried out by means of absorption spectra in the infrared region (800 cm^{-1} – 1000 cm^{-1}) as described previously [3].

The following materials were used as standards: natural rubber (841 cm^{-1} band) and gutta percha (845 cm^{-1} band), for determination of the content in the polymer chain of cis-1,4- and trans-1,4-configuration, 1-heptane (909 cm^{-1} band) and 2,3,3-trimethyl-1-butene (887 cm^{-1} band).

The microstructure of SRI rubber was investigated in a number of samples prepared at a particular polymerization temperature. The effect of polymerization temperature (T_p) on microstructure was studied with emulsion polyisoprene SEI; in connection with this, samples of polymer prepared at temperatures of from –47° to +50° were investigated (see Table 1).

From the data in Table 1, it follows, first, that all of the samples of SRI rubber investigated by us were characterized by a high content of cis-1,4-configuration, reaching 75% of the total 1,4-units in the molecular chains. These data show, moreover, that the presence of the few side branches in this polymer is due basically to additions in the 3,4-position (isopropenyl groups); the number of units resulting from 1,2-addition was small in this polymer (1-1.5%).

The results obtained by us in the investigation of the structure of emulsion-polymerized isoprene rubbers synthesized at different temperatures affirms that polymerization temperature has a well-known effect on the microstructure of these polymers. Thus, in rubbers obtained at temperatures of from –47° to 0°, the 1,4-units in the molecular chain were present in the trans-configuration only; a further increase in polymerization temperature led to the appearance of a certain amount of cis-1,4-units which steadily increased with an increase in polymerization temperature and reached 8% at a process temperature of +50°. In addition, over the entire range of polymerization temperatures, the content of 1,2- and 3,4-units in the polymer chains remained practically constant.

On the basis of the data presented in Table 1 on the microstructure of the samples of emulsion-polymerized isoprene rubber obtained at different temperatures, we obtained, by means of the Arrhenius-Eyring equation [4], a general analytical expression which permits calculation of the relative content of the respective units in the microstructure for any polymerization temperature.

In the case under consideration, the Arrhenius-Eyring equation for the rate of formation of the respective components of the microstructure may be written in the form:

$$K_{1,2} = \frac{RT}{Nh} \exp\left[\frac{\Delta S_{1,2}}{R}\right] \exp\left[-\frac{\Delta H_{1,2}}{RT}\right]; \tag{1}$$

$$K_{3,4} = \frac{RT}{Nh} \exp\left[\frac{\Delta S_{3,4}}{R}\right] \exp\left[-\frac{\Delta H_{3,4}}{RT}\right]; \tag{2}$$

$$K_{cis} = \frac{RT}{Nh} \exp\left[\frac{\Delta S_c}{R}\right] \exp\left[-\frac{\Delta H_c}{RT}\right]; \tag{3}$$

$$K_{trans} = \frac{RT}{Nh} \exp\left[\frac{\Delta S_t}{R}\right] \exp\left[-\frac{\Delta H_t}{RT}\right]. \tag{4}$$

Here, ΔH and ΔS_1, are, respectively, the heat and entropy of activation, and h is Planck's constant.

Taking into consideration that $\frac{K_i}{K_j} = \frac{C_i}{C_j}$ (where K_i and K_j are the reaction rate constants and C_i and C_j are the concentrations of the respective configurations), we obtain:

$$\frac{C_{3,4}}{C_{1,2}} = \exp\left[\frac{1}{R}(\Delta S_{3,4} - \Delta S_{1,2}) + \frac{1}{RT}(\Delta H_{1,2} - \Delta H_{3,4})\right]; \tag{5}$$

$$\frac{C_c}{C_{1,2}} = \exp\left[\frac{1}{R}(\Delta S_c - \Delta S_{1,2}) + \frac{1}{RT}(\Delta H_{1,2} - \Delta H_c)\right]; \tag{6}$$

$$\frac{C_t}{C_{1,2}} = \exp\left[\frac{1}{R}(\Delta S_t - \Delta S_{1,2}) + \frac{1}{RT}(\Delta H_{1,2} - \Delta H_t)\right]. \tag{7}$$

Introducing the notation: $\Delta S_i - \Delta S_j = {}^iS_j$, $\Delta H_i - H_j = {}^iH_j$, it is simple to obtain a general expression for the concentrations of any of the components of the microstructure as a function of polymerization temperature:

$$C = 100\left[1 + \sum \exp\left(\frac{{}^iS_i}{R} + \frac{{}^iH_j}{RT}\right)\right]^{-1}. \tag{8}$$

The differences in entropies and heats of activation, determined by us from the experimental data (from a graph of $\ln\frac{C_i}{C_j} = f(T_p)$; Table 1) have the following values:

$$\Delta H_t - \Delta H_c = -5000 \frac{\text{cal}}{\text{mole}}, \quad \Delta S_t - \Delta S_c = -11{,}0 \text{ e. u.} \qquad \left[\frac{\text{cal}}{\text{mole} \cdot \text{deg.}}\right];$$

$$\Delta H_t - \Delta H_{1,2} = -400 \frac{\text{cal}}{\text{mole}}, \quad \Delta S_t - \Delta S_{1,2} = 3{,}6 \text{ e. u.}$$

$$\Delta H_t - \Delta H_{3,4} = -600 \frac{\text{cal}}{\text{mole}}, \quad \Delta S_t - \Delta S_{3,4} = 3{,}6 \text{ e. u.}$$

$$\Delta H_{1,4} - \Delta H_{1,2} = -150 \frac{\text{cal}}{\text{mole}}, \quad \Delta S_{1,4} - \Delta S_{1,2} = 4{,}6 \text{ e. u.}$$

Thus, in the polymerization temperature interval under consideration (from –47 to +50°), the formation of the trans-configuration is energetically less favored than formation of the cis-configuration. As regards growth of the chain in the 1,4-position as compared to 1,2-additions, the values of the entropy and heat of activation favor the formation of a basic chain with internal double bonds C = C.

TABLE 1

Microstructure of SRI and SEI Polyisoprenes of Different Types of Addition

Rubber type	Sample No.	Polymer. Temp. °C	1,2	3,4	Cis-1,4	Trans-1,4	Rubber type	Sample No.	Polymer. Temp. °C	1,2	3,4	Cis-1,4	Trans-1,4
			Per cent							Per cent			
SRI	1	—	1	6	65	28	SEI	—	–47	8	6	0	86
	2	—	1.5	6	64.5	28		—	–35	8	5	0	87
	3	—	2	6	66	26		—	–25	7	4	0	89
	4	—	1	6	70	23		—	+ 5	7	5	1	87
	5	—	1.5	6.5	65	27		—	+30	7	5	5	83
	6	—	2	5.5	66	26.5		—	+40	7	5	6	82
	7	—	1	7	68	24		—	+50	7	5	8	80
	8	—	1	6	70	23							

A very essential characteristic of the structure of the polymer chain from the point of view of its order is the combination type of "head-to-tail" or "head-to-head" 1,4-units. The spectroscopic data on the relative content in the macromolecule of 1,2- and 3,4-components of the microstructure permitted us to clarify this question for the isoprene rubbers investigated by us. In addition, we made the natural assumption that in the 1,4-addition of the monomer units, exposure of the "tails" (between the 3rd and 4th carbon atoms) or of the "heads" (between the 1st and 2nd atoms) of the double bonds occurred with the same probability as in the process of growth accompanied by the formation of side groups. Consequently, from the relative content of 1,2- and 3,4-additions it is possible to judge the order of the molecular chains from the point of view of their construction as "head-to-tail" and "head-to-head" types.

As follows from the experimental results presented in Table 1, the contents of 1,2- and 3,4-units in the emulsion-polymerized isoprene rubbers were approximately equal, and in the SRI rubbers they were 1% and 6%, respectively. This leads to the conclusion that while the molecular chains of the emulsion polyisoprenes consist of disordered, alternating trans-1,4-units added "head-to-tail" and "head-to-head" with equal probability, the macromolecules of SRI rubber are primarily ordered chains consisting mainly of cis-1,4-units added "head-to-tail". The latter is responsible for the ability of SRI isoprene rubbers to crystallize during elongation.

Received January 30, 1957

LITERATURE CITED

[1] A. A. Korotkov, K. B. Piotrovsky and D. P. Feringer, Proc. Acad. Sci. USSR, 110, 89 (1956).

[2] G. P. Belonovskaya, B. A. Dolgoplosk and E. I. Tinyakova, Thesis Reports of the 9th Conference on High Molecular Weight Compounds*, January, 1957, Izd. AN SSSR, 1956, p. 18.

[3] K. V. Nelson, Bull. Acad. Sci. USSR, Ser. Phys., No. 6, 741 (1954).

[4] S. Glasstone, K. Laidler and H. Eyring, Theory of Absolute Reaction Rates [The Theory of Rate Processes – Kinetics of Chemical Reactions, Viscosity, Diffusion, and Electrochemical Phenomena], Foreign Lit. Press, 1948. (Translation)

* In Russian.

LIQUID DIFFUSION ELECTRODES

R. M. Perskaya and I. A. Zaidenman

(Presented by Academician A. N. Frumkin, February 11, 1957)

The use of liquid diffusion electrodes as chemical sources of current and for carrying out continuous electrolytic processes is promising [1-3]. With the aim of clarifying the basic rules by which such electrodes operate, we undertook a theoretical and experimental investigation of some of the questions of their macrokinetics, which are determined by the distribution of current density in the pores. Unlike the problems previously considered [4-7], in all practical cases the problem of current distribution in a liquid diffusion electrode requires, first, calculation of the ultimate thickness of the electrode and, second, calculation of the change in concentration of reacting substances across the thickness of the electrode. In the present communication we shall consider only flat, metallic diffusion electrodes with uniform porosity (the electrical resistance of the metal is assumed to be zero in comparison with the resistance of the electrolyte in the pores).

The basic equation defining current distribution for such electrodes has the form:

$$\frac{d^2\varphi}{dx^2} = pR_e i\,(\varphi, c), \tag{1}$$

where φ is the polarization of the electrode at points a distance x from its boundaries (here and in the remainder of the article, x is measured in the direction of electrolyte flow from the rear to the polarized side of the electrode); p is the perimeter of the pores, and is constant at any cross-section $x = \text{const.}$; R_e is the linear resistance of the electrolyte in the pores, i. e., the resistance per cm of electrode thickness; c is the concentration of active material at the point x.

In practically important cases of liquid oxidation-reduction systems in a diffusion electrode, the polarization characteristic of the electrode is determined only by the concentration changes along the thickness of the electrode, ξ, and the activation polarization, η. Thus, the current density at the point x can be expressed in the form

$$i = j_o^0 (c_r^0)^{1-\alpha} (c_o^0)^{\alpha} \left[\frac{c_r^x}{c_r^0} \exp\left(\frac{\alpha\varphi nF}{RT}\right) - \frac{c_o^x}{c_o^0} \exp\left(\frac{-(1-\alpha)\varphi nF}{RT}\right)\right], \tag{2}$$

where, $j_o^0 (C_r^0)^{1-\alpha} (C_o^0)^{\alpha} = j_o$ is the current exchange for a given electrode reaction at the point $x = 0$; $\varphi = \xi + \eta$ is the polarization of the electrode at the point x.

Expressing the concentrations of the reducing agent and oxidizing agent at the point x (C_r^x and C_o^x) in terms of the concentrations in the original solution: $C_r^x = C_r^0 - I_x C_r^0 / I_{da}$ and $C_o^x = C_o^0 + I_x C_o^0 / I_{dc}$, where the limiting anode (I_{da}) and cathode (I_{dc}) currents depend on the rate of flow ("input") Q, the concentration C^0, and the electrochemical equivalent (E) of the reacting substances: $I_{da} = C_r^0 Q / E$ and

$I_{dc} = C_0^0 Q/E$, and, from (2) and taking into account that, according to Ohm's law, for the electrolyte in the pores $I_x = p\int_0^x i\,dx = \frac{1}{R_e}\frac{d\varphi}{dx}$, we obtain the basic equation for current distribution in a flat liquid diffusion electrode:

$$\frac{d^2\varphi}{dx^2} = pR_e\, i_0\left[\left(1 - \frac{1}{R_e I_{da}}\frac{d\varphi}{dx}\right)\exp\left(\frac{\alpha\varphi nF}{RT}\right) - \left(1 + \frac{1}{R_e I_{dc}}\frac{d\varphi}{dx}\right)\exp\left(\frac{-(1-\alpha)\varphi nF}{RT}\right)\right]. \quad (3)$$

We may assume the following limiting conditions for an electrode of thickness L

$$\left.\frac{d\varphi}{dx}\right|_{x=0} = 0; \quad \left.\frac{d\varphi}{dx}\right|_{x=L} = R_e I, \quad (4)$$

where, $I = I_{x=L}$ is the total current flowing through the electrode.

In place of (4), it is sometimes more convenient to assume the conditions

$$\varphi|_{x=0} = \varphi_0; \quad \varphi|_{x=L} = P, \quad (5)$$

where the values of the polarization on both electrode surfaces, φ_0 and P are readily subject to experimental determination.

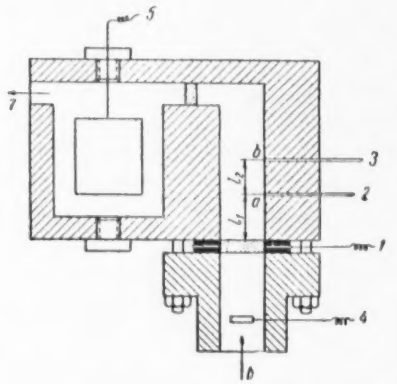

Fig. 1. Diagram of the measuring cell. 1) diffusion electrode; 2 and 3) capillaries leading to an Hg/Hg_2SO_4 electrode; 4) Pt reference electrode; 5) auxilliary electrode for polarization; 6) electrolyte inlet; 7) electrolyte exit.

At low values of I, when it may be assumed that $\exp(\alpha\varphi nF/RT) = 1 + \alpha\varphi nF/RT$ and $\exp[-(1-\alpha)\varphi nF/RT] = 1-(1-\alpha)\varphi nF/RT$, solution of Equation (3) for limiting conditions (4) makes it possible to calculate the initial polarization resistance of the electrode

$$R_D = \lim_{I\to 0}\left(\frac{d\varphi}{dI}\right)_{x=L} = \lim_{I\to 0}\left(\frac{dP}{dI}\right).$$

We obtain

$$R_D = \frac{RT}{2nF}\left(\frac{1}{I_{da}} + \frac{1}{I_{dc}}\right) + \sqrt{\left(\frac{RT}{2nF}\right)^2\left(\frac{1}{I_{da}} + \frac{1}{I_{dc}}\right)^2 + \frac{R_e RT}{p i_0 nF}} \times$$

$$\times \cot\left(L\sqrt{\frac{p^2 i_0^2}{4}\left(\frac{1}{I_{da}} + \frac{1}{I_{dc}}\right)^2 + \frac{pR_e\, i_0 nF}{RT}}\right). \quad (6)$$

As $Q \to \infty$, I_{da} and $I_{dc} \to \infty$, and the factor determining the concentration polarization across the electrode

$\frac{RT}{nF}\left(\frac{1}{I_{da}}+\frac{1}{I_{dc}}\right)\to 0$, then

$$R_D \to \frac{R_e \cot(aL)}{a}, \qquad (7)$$

where, $a = \sqrt{pR_e i_0 nF/RT}$, i. e., R_D is determined only by the activation polarization.

In order to confirm the basic rules which follow from Equations (3) and (6), the dependence of voltage-amperage characteristics on the input and concentration of active substances was investigated for the oxidation-reduction systems Fe^{2+}/Fe^{3+} and Ce^{3+}/Ce^{4+} in 1 N H_2SO_4 at 25°.

The diffusion electrode – a porous disc of 1 mm thickness – was prepared from platinum powder by a metalloceramic method. The measuring cell was constructed from organic glass (Fig. 1). Polarization measurements were carried out by the compensation method with an accuracy of ± 0.1 mv.

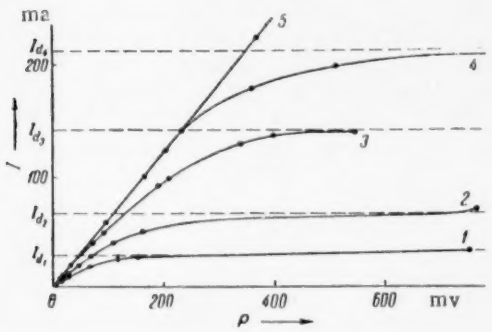

Fig. 2. Curves of P = f (I) for various values of Q at $c_r^0 \approx c_o^0 = 0.005$ N(Fe^{2+}/Fe^{3+} in 1N H_2SO_4). 1) Q = 5; 2) Q = 8.8; 3) Q = 20; 4) Q = 30; 5) Q = = 60 ml/min; I_d – theoretical value of the limiting current for the corresponding inputs.

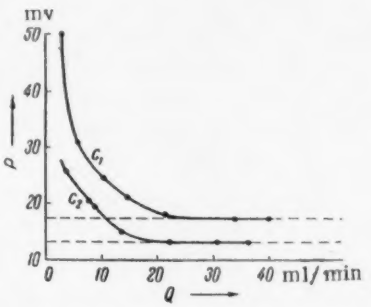

Fig. 3. Variation in P with Q at I = const for two different concentrations ($C_2 > C_1$). System Fe^{2+}/Fe^{3+} in 1 N H_2SO_4.

The polarization was measured from both sides of the electrode – in the electrolyte leaving the electrode ("frontal polarization", P) and in the electrolyte coming to the electrode ("rear polarization", φ_0). The value of P was determined by means of two reference electrodes (Hg/Hg_2SO_4 in 1 N H_2SO_4), the capillaries of which were introduced into the cell at points a and b (Fig. 1).

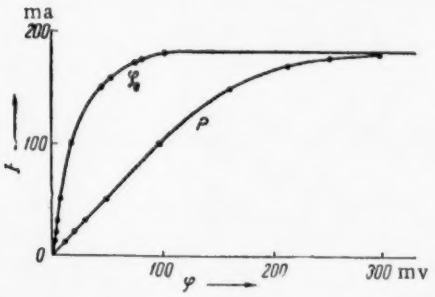

Fig. 4. Variation in P and φ_0 with I. Pt electrode (1 sq. cm.) in a solution of Fe^{2+}/Fe^{3+} (0.005 N in 1 N H_2SO_4); Q = 2.3 ml/min.

The distances l_1 and l_2 were accurately measured, thus making it possible to calculate a correction for ir drop outside the diffusion electrode: $\Delta\varphi_{ir} = [(\varphi_2 - \varphi_1) - (\varphi_2^0 - \varphi_1^0)]\, I_1 \varrho / l_2$, where φ_1, φ_2 are the potentials of the polarized diffusion electrode relative to the first and second reference electrodes, respectively; φ_1^0, φ_2^0 are the zero-current potentials of the diffusion electrode relative to these same reference electrodes. An equilibrium oxidation-reduction electrode – a Pt plate in the original electrolyte solution – was used as a reference electrode for the measurement of φ_0.

As a result of the measurements, it was established:

1. Oxidation-reduction reactions at a diffusion electrode are accompanied by a well-defined limiting current (Fig. 2).

2. The value of the limiting current, I_d, corresponds to complete (100%) reduction of the oxidized form or oxidation of the reduced form; i. e., it is directly proportional to the input and concentration of the active substance: $I_d = FcQ$, where F is Faraday's constant in appropriate units.

3. The portions of the polarization curves in the current region $I < 0.5\, I_d$ are linear, the linearity being retained for polarization values considerably exceeding $2RT/F = 51.2$ mv at 25°.

4. The slope of the linear part of the polarization curve, $R_D = P/I$, depends on the input and concentration of active substance (Fig. 2 and 3). At constant concentration and with increasing Q, the slope of the curves tends toward a limit which is reached at a definite – "limiting" – input, Q_p. The value of Q_p becomes less the greater the concentration of active substance.

5. The curve for rear polarization, $\varphi_0 = f(I)$, is of the same type as the curve for frontal polarization (Fig. 4), but $\varphi_0 < P$. With a decrease in $\underline{c}$ and Q, the difference between φ_0 and P decreases, and the frontal current density, i_L, which is easily calculated from $\eta = \varphi - \xi$, increases; i. e., redistribution of the current density inside the electrode takes place. This can be explained by the formation (as a result of the occurrence of electrode reactions inside the pores and the emergence of a concentration gradient) of a short-circuited concentration element at which the direction of the discharge current in the pores coincides with the direction of the polarization current. With a decrease in $\underline{c}$ and Q, at the front surface of the liquid diffusion electrode ($x = L$) is subtracted from the current density of the external polarization, and at the back surface of the electrode ($x = 0$) is added, all of the increasing current density of the self-discharge of this concentration element. In addition, obviously, the overall true current density at all times satisfies at all points the basic equation for current distribution (3).

6. At high values of $\underline{c}$ and Q, the value of the limiting current becomes less than theoretical. We will not consider this region in the present communication.

The experimental data obtained on the relationship between the voltage-amperage characteristics of the electrodes and the inputs and concentrations are in qualitative and quantitative agreement with the conclusions which follow from Equations (6) and (7).

From the above it follows that measurements of $(R_D)_{lim}$ for solutions of different substances at the same electrode permit determination of the relative values of the exchange currents. Owing to the linearity of large parts of the voltage-amperage characteristics, it is sufficient to measure one point of $P = f(I)$ for a sufficiently high input.

In conclusion, we take this opportunity to express our appreciation to A. N. Frumkin and N. S. Lidorenko for aid and advice during the completion of this work.

All-Union State Sci. Res.
Elemento-Electrocarbon Institute

Received February 5, 1957

LITERATURE CITED

[1] G. W. Heise, Trans. Electrochem. Soc., 75, 147 (1939).

[2] A. Schmid, Final Report BJOS, Item 31 (1945).

[3] I. E. Bauslit, G. Z. Kiryakov and V. V. Stender, Bull. Acad. Sci. KazSSR, Ser. Chem., 20, No.2 (1948).

[4] V. S. Daniel-Bek, J. Phys. Chem.22, 697 (1948).

[5] A. N. Frumkin, J. Phys. Chem., 23, 1477 (1949).

[6] O. S. Ksenzhek and V. V. Stender, Proc. Acad. Sci. USSR, 107, No. 2 (1956).

[7] J. J. Coleman, Trans. Electrochem. Soc., 90, 545 (1946).

[8] K. Vetter, Zs. phys. Chem., 194, 284 (1950).

INVESTIGATION OF ISOTACTIC POLYPROPYLENE BY MEANS OF INFRARED SPECTRA

E. I. Pokrovsky and M. V. Volkenshtein

(Presented by Academician A. V. Topchiev, February 13, 1957)

Samples of isotactic polypropylene, prepared by different methods, were studied in the form of films 0.2 mm thick. The films were prepared by melting the polymer and pressing the molten material between two plates of rock salt. The infrared absorption spectra were measured on an IKS-11 spectrometer with NaCl and LiF prisms in the region 700-3000 cm^{-1}. The spectra were measured point-by-point, and were also recorded by means of an EPP-09 recorder. Electrical heating was used for measurements at different temperatures (in the range 20-200°).

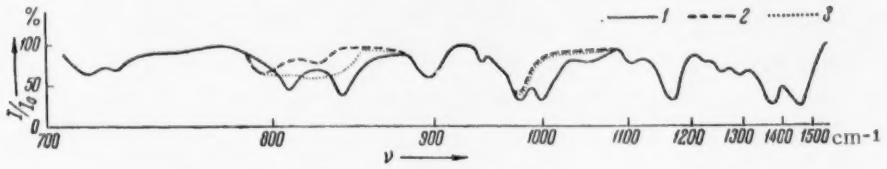

Fig. 1. Infrared absorption spectra of polypropylene: 1) isotactic polypropylene at 20°; 2) isotactic polypropylene at 170°; 3) fraction extracted with ether.

The following bands were found in the absorption spectra of all samples of isotactic polypropylene: 720, 730, 790, 810, 839, 894, 935, 969, 992, ~1050, 1108, 1170, 1376, 1460, ~2850, 2875, 2924, and 2957 cm^{-1} (Fig. 1). In the region 830-1000 cm^{-1} the spectra agree with those of Natta et al [1] (who gave the spectrum only in the region indicated) with the exception of a very weak band at 935 cm^{-1}, which we did not find in all samples. The presence of weak bands at 894 cm^{-1} and 992 cm^{-1} is characteristic of crystalline isotactic polypropylene; these bands were very weak for the fraction extracted with ether (see Fig. 1). We investigated the crystallinity of the isotactic polypropylene by the method described in references [2-4]. On heating the polymer to a temperature of 140-150°, there was a change in the spectrum, a weakening of the bands at 810, 839, 894, and 992 cm^{-1}. These bands practically disappear at a temperature of ~170°, where melting of the polymer is concluded. Natta gives a T_m of 160-170° for isotactic polypropylene [5]. It is evident that these bands can be considered as "crystallinity bands"; they are characteristic of the most stable rotatable isomer in the crystal. A spectrum of the molten polymer is also presented in Fig. 1, and a curve showing the dependency of transmission at the maximum of the 992-cm^{-1} band on temperature is shown in Fig. 2. This curve is S-shaped, which is normal for molten crystalline polymers [2-4]. It is seen that the melting point of the polymer can be determined from this curve.

The degree of crystallinity was determined by an investigation of the temperature dependence of the intensity of the band at 790 cm^{-1}. The intensity of this band increases strongly during melting of the polymer. On the other hand, this band was present in the spectrum of the fraction of polypropylene extracted with ether.

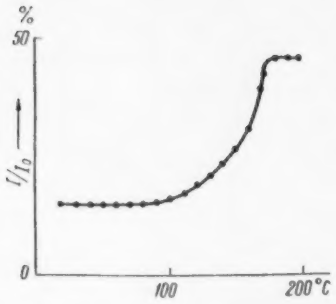

Fig. 2. Temperature dependence of the transmission of the 992 cm^{-1} band of isotactic polypropylene.

The spectrum of this fraction practically coincided with the spectrum of the molten isotactic polymer with the exception of minor differences in the region of 800-850 cm^{-1} (see Fig. 1). The band at 790 cm^{-1} can be assigned to amorphous polymer. The content of amorphous polymer was determined by a comparison of the optical density at the maximum of the 790 cm^{-1} band at room temperature with the optical density at a temperature above T_m. The degree of crystallinity was found by difference [2]. For the three samples investigated, the values of the degree of crystallinity were ~75, ~90, and ~100%. It should be noted that these determinations make no pretense of high quantitative accuracy, since they were carried out by means of differential intensities. However, it can be said that the degree of crystallinity of the samples investigated were very high.

The authors express their appreciation to B. A. Krentsel, N. I. Nikolaev and L. M. Romanov for presenting to us samples of isotactic polypropylene, prepared by them, for our investigation.

Institute of Highmolecular Compounds
Academy of Sciences USSR

Received February 6, 1957

LITERATURE CITED

[1] G. Natta, P. Pino et al., La Chimica e l'industria, No. 2, 124 (1956).

[2] V. N. Nikitin and E. I. Pokrovsky, Proc. Acad. Sci. USSR, 95, No. 1, 109 (1954).

[3] V. N. Nikitin and E. I. Pokrovsky, Bull. Acad. Sci. USSR, Ser. Phys., No. 6, 735 (1954).

[4] E. I. Pokrovsky and I. P. Kotova, J. Tech. Phys. 26, No. 7, 1456 (1956).

[5] G. Natta, Angew. Chem., 68, No. 12, 393 (1956).

DEPENDENCE OF THE CATALYTIC ACTIVITY OF SKELETAL NICKEL ON CONDITIONS OF ACTIVATION OF THE HYDROGEN

Academician Acad. Sci. KazSSR D. V. Sokolsky and S. T. Bezverkhova

The catalytic properties of skeletal nickel* are dependent on sorbed hydrogen. A change in the amount, as well as in the state, of this hydrogen causes a change in the activity of the contact mass [1].

The aim of the present investigation was to investigate the effect of preliminary dehydrogenation of skeletal nickel catalyst on the rate of hydrogenation of dimethylethynylcarbinol in various media (0.1 N NaOH, water, and 96% ethyl alcohol) and at various temperatures (20, 40, and 60°).

The catalyst (1.55 g) was prepared by leaching a 31% nickel-aluminum alloy, carefully washing, and placing in a bomb with 30 ml of the working solution where it was saturated with hydrogen for an hour, with agitation, until a standard state was reached. Three experiments were successively carried out on the same sample of catalyst:

TABLE 1

The Effect of Preliminary Dehydrogenation of Skeletal Nickel Catalyst on Its Activity in the Hydrogenation of Dimethylethynylcarbinol (1.55 g of catalyst, 0.2 ml (0.1722 g) of Dimethylethynylcarbinol)

Temp. °C	ml hydrogen removed	H withdrawn during saturation, ml	$\Delta v_0/\Delta t$** ml/min.	$\Delta v_0'/\Delta t$** ml/min.	Change in rate, ml	% Change in rate
0,1N NaOH						
20	23	23		9.6		
20	46	46	26.0	9.6	16.4	63
20	85	80		9.3		
40	23	23		21.0		
40	46	46	32.0	20.0	11.0	34
40	94	79		22.0		
60	23	22		34.0		
60	46	34	36.0	34.0	2.0	5.5
60	101	81		36.0		
Water						
20	23	23		21.0		
20	46	44	31.5	20.0	10.5	33
20	72	66		21.0		
Water						
40	23	18		27.5		
40	46	40	35.0	27.5	7.5	21
40	85	77		27.5		
60	23	23		—		
60	46	26	53.0	50.0	3.0	6
60	92	77		50.0		
96% Ethyl alcohol						
20	23	17.6		72.7		
20	46	40.0	72.0	72.0		
20	64	54.0		71.6		

* [Raney nickel – Trans. note.]

** $\Delta v_0/\Delta t$ and $\Delta v_0'/\Delta t$ are the maximum reaction rates for, respectively, the fresh and dehydrogenated catalyst.

1. The activity of the freshly prepared catalyst was determined by hydrogenating 0.2 ml of dimethylethynylcarbinol. In addition, the amount of reacting hydrogen was measured, and the potential of the catalyst relative to a reversible hydrogen electrode was simultaneously recorded.

2. At the conclusion of the reaction, the hydrogen was purged from the gas phase of the bomb with a stream of nitrogen without agitation. The calculated amount of dimethylethynylcarbinol to remove from the catalyst in a period of 30 minutes a specific, predetermined amount of sorbed hydrogen was introduced into the bomb [2]. Then, after changing the working solution and washing, the catalyst was saturated with hydrogen from the gas phase until the adsorption of gas ceased and the potential of the reversible hydrogen electrode was reached.

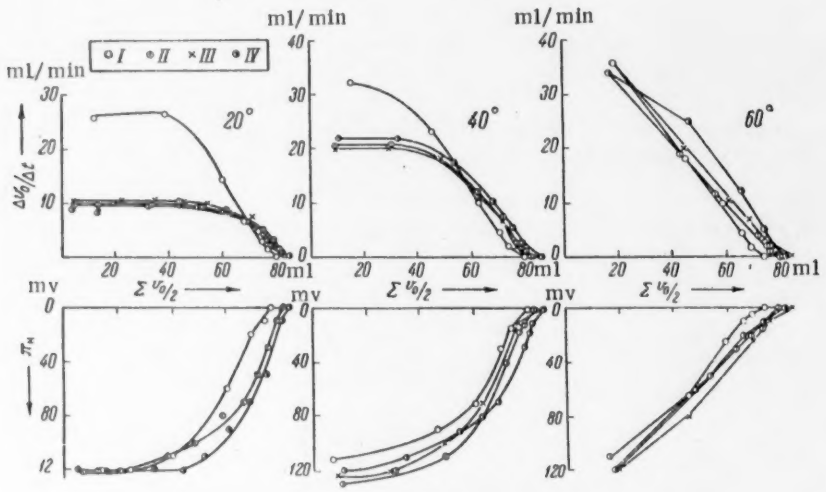

Fig. 1. The effect of preliminary dehydrogenation of skeletal nickel on its activity in the hydrogenation of dimethylethynylcarbinol in alkaline medium: I) hydrogenation over freshly prepared catalyst; II) hydrogenation over the catalyst after the removal of 23 ml of sorbed hydrogen; III) hydrogenation after removal from the nickel of 46 ml of hydrogen; IV) hydrogenation after removal from the catalyst of all of the hydrogen reactive with respect to dimethylethynylcarbinol.

3. The change in the catalyst activity due to the dehydrogenation was determined by hydrogenating 0.2 ml of dimethylethynylcarbinol over hydrogen-saturated catalyst.

The catalyst samples for each medium and each temperature were subjected to successively increasing dehydrogenation comprising 23 ml of hydrogen for Catalyst I and 46 ml of hydrogen for Catalyst II. From Catalyst III was removed all of the hydrogen reactive under the given conditions, the amount of which was determined on the basis of kinetic curves for the hydrogenation of dimethylethynylcarbinol in an atmosphere of nitrogen using the sorbed hydrogen [2].

The results of the experiments on the hydrogenation of dimethylethynylcarbinol over dehydrogenated skeletal nickel at temperatures of 20, 40, and 60° are presented in Table 1 and, for alkaline medium, in Fig. 1. The kinetic curves in the upper half of the graphs represent the rate of hydrogenation of 0.2 ml of the acetylenyl alcohol; the lower curves show the change in the potential of the catalyst during the course of the reaction. Similar curves were obtained in the experiments with aqueous and alcoholic media.

From Fig. 1 and Table 1 it is seen that, depending on the medium and temperature, the preliminary removal from the surface of the catalyst of part or all of the sorbed hydrogen variously affects the catalytic activity of the nickel. An especially great change in the reaction rate as a result of dehydrogenation occurred during the hydrogenation in the alkaline medium at low temperatures. Thus, at 20°, the removal of 23 ml of

hydrogen from the surface of the catalyst caused a decrease in activity of 63%; on increasing the temperature to 40°, the decrease in reaction rate resulting from the removal of 23 ml of hydrogen was 34%; while at 60° under the same conditions, partial dehydrogenation had almost no effect on the activity of the contact mass.

In aqueous medium, the skeletal nickel was less sensitive to dehydrogenation. At 20°, the hydrogenation rate of 0.2 ml of dimethylethynylcarbinol after the removal of 23 ml of hydrogen from the surface decreased 33%, at 40° – 21%, and at 60° – 6%. It is interesting to note that a further increase in the degree of dehydrogenation in alkaline and aqueous medium caused no further change in the activity of the catalyst.

In alcoholic medium, removal from the surface of all of the hydrogen reactive with respect to the dimethylethynylcarbinol had absolutely no effect on the rate of the hydrogenation process.

These results can be explained by a different rate of activation of hydrogen on the dehydrogenated catalyst depending on the medium and temperature. In alkaline medium, where the hydrogen is very tightly bound to the surface, its renewal proceeds with great difficulty and at a low rate, which finds expression in a decrease in reaction rate by 63% in spite of the fact that during saturation of the catalyst from the gas phase the amount of hydrogen removed is completely absorbed. In aqueous medium, activation of the hydrogen proceeds more quickly and easily; therefore, the dehydrogenation process affects the rate to a lesser degree. In alcoholic medium, where the bond of the hydrogen with the catalyst surface is very insignificant, easy renewal of the activated hydrogen provides a stable working state of the skeletal nickel.

Since an increase in experiment temperature has a favorable effect on activation of the hydrogen, dehydrogenation at 40 and 60° causes essentially no lowering of the reaction rate.

S. M. Kirov Kazak
State University, Alma-Ata

Received February 18, 1957

LITERATURE CITED

[1] L. Kh. Freidlin and N. I. Ziminova, Bull. Acad. Sci. USSR, Div. Chem. Sci., 1951, 145.

[2] D. V. Sokolsky and S. T. Bezverkhova, Proc. Acad. Sci. USSR, 94, 493 (1954).

ELECTROLYTIC OXIDATION OF β-PICOLINE

V. G. Khomyakov, S. S. Kruglikov

and Associate Member Acad. Sci. USSR N. A. Izgaryshev

It has been shown in a number of papers that picolines are readily oxidized electrochemically with the formation of the corresponding aldehydes [1, 2] and pyridine carboxylic acids [1-4], as well as oxidation products of the pyridine ring [2]. However, there are no data in the literature on the effect of electrolyte composition and electrolysis conditions on the yield of the individual products. The present communication reports the results of an investigation of the process of the electrochemical oxidation of β-picoline.

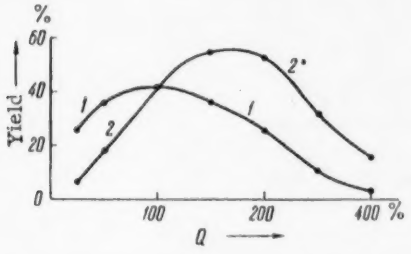

Fig. 1. Effect of the amount of electricity passed through the electrolyte on the current (1) and material (2) yields of nicotinic acid

The original β-picoline was recovered from an aqueous solution of a picoline fraction (b. p. 138-144°) as the difficultly soluble complex salt $CuSO_4 \cdot 5H_2O \cdot C_6H_7N$ [5], which was subsequently decomposed with sodium hydroxide. Further purification of the β-picoline by three-fold chilling with crystallization gave a product of ~99% purity.

Preliminary experiments established that β-picoline can be oxidized electrochemically only in acid medium at platinum and lead anodes which have first been covered with a layer of the dioxide. The oxidation of β-picoline proceeded with considerably higher current efficiency at the lead anode than at the platinum anode; therefore, further experiments were carried out only with a lead anode in an electrolytic cell with a porous ceramic diaphragm. β-Picoline in sulfuric acid solution was introduced into the anode compartment, which had a volume of ~50 cc. The lead anode was placed inside the compartment formed by the diaphragm and containing a dilute solution of sulfuric acid. The surface of the anode was 2 sq. dm. At the conclusion of an electrolysis, the sludge was filtered from the anolyte, neutralized with soda, then acidified with sulfuric acid to a pH of 4-4.5, and heated on a boiling water bath. Copper sulfate or acetate was added to the hot solution, and heating on the bath was continued for several hours. The precipitated copper nicotinate was filtered and dried.

The effect of the amount of electricity passed through the electrolyte, current density, temperature, the addition of polyvalent metals (Mn and Cr), and the concentration of β-picoline and sulfuric acid on current and material yields of nicotinic acid was investigated. In separate experiments, the overall current consumption in the oxidation of organic materials was determined by a comparison of the volumes of oxygen liberated during equal time intervals in a gas coulometer and in the electrolytic cell containing a sulfuric acid solution of β-picoline. Comparison of the results of these experiments with the yields of nicotinic acid obtained under the same conditions makes it possible to determine the rate of oxidation side reactions proceeding at the anode.

In Fig. 1 is shown the effect of the amount of electricity passed through the electrolyte * on the current and material yields on nicotinic acid. The experiments were carried out under the following conditions:

* Q = 100% corresponds to 6 F per mole of β-picoline.

temperature, 40°; anode current density, 10 amp./sq. dm.; anolyte, 1 M/liter solution of β-picoline in 7 N sulfuric acid. As may be seen from the curves, the nicotinic acid formed as a result of the oxidation of β-picoline is rather easily oxidized further. However, the oxidation of β-picoline proceeds at a considerably higher rate. This was also confirmed by specially conducted experiments on the electrolytic oxidation of nicotinic acid. The increase in current yield of nicotinic acid, observed at the beginning of the electrolysis, indicates the formation of unstable intermediate products in the oxidation of β-picoline to nicotinic acid, for example, 3-pyridinecarboxaldehyde.

TABLE 1

Yield of Nicotinic Acid (in per cent)

Q, %	Yield	Anolyte temperature, °C				
		20	30	40	60	80
100	Current and material	39		41	38	36
150	Current	30	35	37	28	25
	Material	45	53	54	42	37
200	Current	24	27	27	23	17
	Material	48	54	54	47	35

TABLE 2

Yield of Nicotinic Acid (in per cent) (concentration of β-picoline, 1 M/liter; temperature, 40°; current density, 5 amp./sq. dm.)

Q, %	Yield	Conc. sulfuric acid, N				
		3	7	11.5	17	25
100	Current and material	36	41	48	51	34
150	Current	31	37	42	43	22
	Material	57	54	63	65	33
200	Current	25	27	27	29	17
	Material	51	54	55	59	34

TABLE 3

Yield of Nicotinic Acid (in per cent) (Temperature, 40°; current density, 5 amp./sq. dm.)

Q, %	Yield	Concentration of β-picoline, M/l		
		1	1.7	3.5
		Concentration of sulfuric acid, N		
		17	15.5	13
100	Current and material	51	55	49
150	Current	43	43	38
	Material	65	65	57
200	Current	29	29	22
	Material	59	59	44

A change in the anode current density in the range of 1 to 10 amp./sq. dm. had almost no effect on the yield of nicotinic acid. Only at low values of Q (50-100%) was the yield somewhat decreased by an increase in current density. The introduction of small amounts of Mn^{++} and Cr^{+++} into the anolyte also had no appreciable effect.

The effect of temperature (Table 1) was studied in an electrolyte of the composition indicated above at a current density of 5 amp./sq. dm. The decrease in product yield with an increase in temperature is apparently connected with an increase in the specific effect of side reactions at high temperature, since the total current consumption in the overall oxidation process was almost unchanged by an increase in temperature (92% at 20° and 97% at 80°). A similar effect was also observed during the investigation of the effect of electrolyte acidity (Table 2); here, a marked change in nicotinic acid yield was observed with an increase in acidity at a constant overall rate of oxidation of organic material.

The maximum yield of nicotinic acid could be obtained over a rather broad range of anolyte acidity, from 11 to 17 N. An increase in anolyte acidity during electrolysis due to the passage of electricity was proportional to the amount of electricity passed; therefore, in experiments in which the concentration of β-picoline was varied, the initial sulfuric acid concentration was chosen so that the average acidity during the electrolysis was approximately equal in all experiments and did not exceed the limiting value corresponding to maximum yield of nicotinic acid (Table 3).

It should be noted that the material yield of nicotinic acid was calculated on the initial weight of the β-picoline; i. e., in the majority of cases it was somewhat too low, since at Q = 100 or 150%, the anolyte after

the electrolysis still contained a certain amount of unoxidized β-picoline. The latter could be recovered in a process carried out on a larger scale.

D. I. Mendeleev Moscow
Chemical-Technicological Institute

Received February 21, 1957

LITERATURE CITED

[1] L. N. Ferguson, A. J. Levant, Nature, 167, 817 (1951).

[2] M. Yokoyama, Bull. Chem. Soc. Japan, 7, 69 (1932).

[3] M. Kulka, J. Am. Chem. Soc., 68, 2472 (1946).

[4] A. Ito, K. Kawada, Ann. Rept. Takamine Lab., 5, 14 (1953); Chem. Abstr, 49, 1451 (1955).

[5] B. F. Herr, U. S. Pat. 2,489,884, November 29, 1949; Chem. Abstr., 44, 2734c (1950).

KINETICS OF THE DECOMPOSITION OF HYDROGEN PEROXIDE UNDER THE INFLUENCE OF GAMMA-IRRADIATION

V. Ya. Chernykh, S. Ya. Pshezhetsky and G. S. Tyurikov

(Presented by Academician V. A. Kargin, February 16, 1957)

The kinetics of the decomposition of hydrogen peroxide in aqueous solutions under the influence of ionizing irradiation have been investigated in a number of works [1]. However, the results obtained in these works are contradictory in many respects. This applies to the dependence of reaction rate on H_2O_2 concentration and on the intensity of the irradiation, and also applies to the yield of the reaction based on the absorbed energy of the irradiation. The disagreement among the results of the various works is, in many respects, attributable to the fact that the measurements were carried out in different and narrow ranges of H_2O_2 concentrations, chiefly in dilute solutions.

It was of interest to determine the extent to which the actual kinetic regularities depend on the concentration region in which measurements are carried out; in particular, it was essential to investigate the kinetics of this reaction in concentrated solutions.

In order to clarify the specificity of the radiation reaction, it was of interest to compare its kinetics with those of the thermal reaction and the photoreaction measured in the same concentration region.

We investigated the kinetics of the decomposition of H_2O_2 in aqueous solutions over the broad concentration range of from 2 to 92 mole % under the influence of gamma irradiation, and we also investigated certain kinetic regularities of the thermal reaction and photoreaction in the same concentration region.

Co^{60} with an activity of 80 curies served as the source of the gamma radiation; the source of u. v. radiation was a PRK-2 mercury lamp. The initial solution was a 92.23 mole % solution of hydrogen peroxide, which was obtained by three-fold distillation; its specific electrical conductivity was $7.3 \cdot 10^{-6}$ $ohm^{-1} \cdot cm^{-1}$.

The rate of the decomposition of the hydrogen peroxide was measured volumetrically by the rate of liberation of oxygen from the solution. The rate of the radiation or photochemical reaction was determined by the difference between the measured rate and the rate of the thermal reaction.

Measurement of the radiation energy absorbed by the solution was carried out with the aid of a dosimetric reaction – the oxidation of divalent to trivalent iron in 0.8 N H_2SO_4 solutions. In the calculations, it was assumed that 15.5 equivalents of divalent iron were oxidized for each 100 ev of absorbed energy.

Variation in the intensity of radiation was accomplished by changing the distance of the apparatus from the radiation source.

Kinetics of the reaction initiated by gamma-radiation. The variation in reaction rate with solution concentration was measured in the interval of 1.78 to 92.23 mole % H_2O_2.

The intensity of the γ-radiation was varied from $0.26 \cdot 10^{18}$ to $1.84 \cdot 10^{18}$ ev /liter/sec; the temperature was varied from –30 to 50°. The variation in reaction rate with H_2O_2 concentration is shown in Fig. 1, from which it is seen that the reaction rate, as a function of H_2O_2 concentration, goes through a maximum at all temperatures.

The measurements of the dependence of reaction rate on radiation intensity showed that the reaction rate is proportional to the square root of the radiation intensity at all concentrations investigated from 1.78 to 92.23 mole % H_2O_2.

The variation in reaction rate with temperature was investigated at 50, 30, 10, 1, –4, –11, and –21°. The decomposition of a 92.33% solution of H_2O_2 at –30° was also investigated.

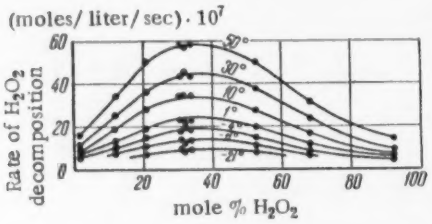

Fig. 1. Variation in the rate of the radiation reaction with solution composition and temperature. Radiation energy absorbed, 1.84 · $\cdot 10^{18}$ ev /liter/sec.

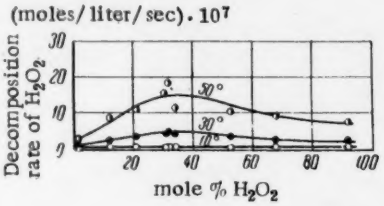

Fig. 2. Variation in the rate of the thermal decomposition of H_2O_2 on solution concentration and temperature.

$\text{Log}W(\frac{1}{T})$ was linear for all solutions. However, the straight line had a break at ~10°. In the temperature region from –21° to 10°, the average value of the activation energy was 6.5 ± 1.0 kcal./mole. Above 10°, the average value of the activation energy was 2.8 ± 1.0 kcal./mole.

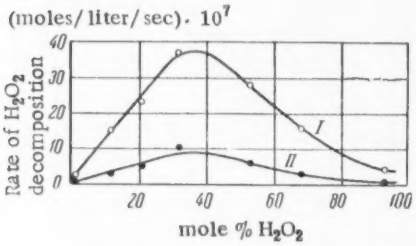

Fig. 3. Variation in the rate of the u. v.-initiated decomposition of H_2O_2 with concentration at a temperature of 30°. I) photochemical reaction, II) thermal reaction in the same vessel.

As experiments showed, agitation of the solution at temperatures above 10° increased the rate of liberation of oxygen. Below 10°, agitation had no effect. This shows that above 10° diffusion is superimposed on reaction rate, which is the reason for the apparent decrease in activation energy.

Yields from the reaction based on energy absorbed depend on concentration and temperature, and lie in the range of from 21 (at –4°) to 230 (at 50°) molecules of peroxide per 100 ev of absorbed gamma-radiation. Thus, the yields are characteristic of a chain process.

Kinetics of the thermal reaction. Measurement of the rate of the thermal reaction was carried out in the same concentration range at 10, 30, and 50°. Below 10°, the reaction rate was low and difficult to measure. The results of the measurements are presented in Fig. 2. As may be seen from the figure, the variation in reaction rate with H_2O_2 concentration is of the same nature. In absolute value, the rate of the thermal decomposition at 30-50° is approximately an order of magnitude lower than the rate of the radiation decomposition.

The average value of the activation energy of the thermal reaction was 12.6 ± 1.5 kcal./mole. The activation energy at very low and very high concentrations was somewhat lower than this value.

Kinetics of the decomposition of hydrogen peroxide under the influence of ultraviolet radiation. The concentration dependence of the rate of the reaction under the influence of ultraviolet light was investigated in the same concentration range. The variation in reaction rate with H_2O_2 concentration was measured at 30°. The results of these measurements are presented in Fig. 3. The $\text{log}W(\frac{1}{T})$ curve has a break at approximately 10°.

In the range 1-10°, the activation energy is 7.3 kcal./mole, and in the range of 10-50° it is 4.0 ± 1.0 kcal./mole.

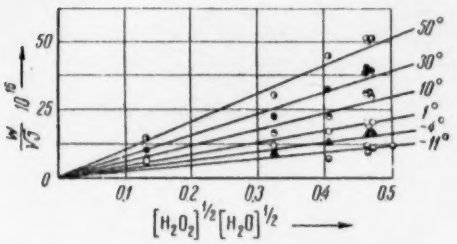

Fig. 4. Graph for the determination of K by means of Equation (2).

Agitation of the solution led to elimination of the break in the $\log W(\frac{1}{T})$ curve. In addition, the activation energy was 8.9 kcal./mole in the 1-10° range and 7.9 ± ± 1.5 kcal./mole in the 10-50° range; i. e., the values for the two temperature intervals were practically the same. This value is close to the activation energy for the reaction proceeding under the influence of gamma-irradiation.

Kinetic equation and probable reaction mechanism. The uniform nature of the dependence of reaction rate on concentration during the radiation, light, and thermally initiated reactions, as well as the closeness of the activation energies for radiation decomposition and photodecomposition, indicates that the basic mechanism of the reactions does not depend on the nature of the initiation. This is because the decomposition of hydrogen peroxide is a chain process.

Comparison shows that the dependence of the rate of the decomposition reaction on H_2O_2 concentration is similar to the dependence of the specific electrical conductivity of the solutions on concentration [2]. The similar course of these relationships indicates that ions play a large part in the process of decomposition of hydrogen peroxide. This is confirmed by a series of investigations establishing the participation of ions in the processes of photochemical and thermal decomposition of hydrogen peroxide in aqueous solutions.

The elemental stages in the process having the most significance are apparently the following:

	Reaction rate constant
(1) $H_2O_2 \rightarrow 2\,OH$	K_1
(2) $OH + H_2O_2 \rightarrow H_2O + HO_2$	K_2
(3) $H_2O_2 + HO_2 \rightarrow H_2O + O_2 + OH$	$K_2 - K_3$
(3') $HO_2 + H_2O \rightarrow H_3O^+ + O_2$	$K_3 - K_3'$
(4) $H_2O_2 + \overline{O_2} + \rightarrow HO^- + OH + O_2$	K_4
(5) $HO + HO_2 \rightarrow H_2O + O_2$	K_5

Since the radical HO_2 is unreactive, decomposition of hydrogen peroxide according to Equation (3') must take place slowly. In aqueous solutions, dissociation of HO_2 proceeds according to Reaction (3). Further, a charge transfer process must take place:

$$H_2O_2 + \overline{O_2} \rightarrow H_2O_2^- + O_2,$$

which leads to the dissociation of hydrogen peroxide:

$$H_2O_2^- \rightarrow OH^- + OH.$$

Reaction (3) and both of these processes must proceed rapidly, since the transfer of a proton or of an electron must take place without a substantial energy barrier. This reaction was considered by Weiss [3] and applied by him to the decomposition of peroxide in the presence of the Fe^{++} ion, by Kornfeld [4] for the photodecomposition of H_2O_2, and was substantiated by Kondratyev [5].

In dilute solutions, origination of active centers must also occur as a result of radiolysis of the water.

Considering the bimolecular nature of Reaction (3), it can be assumed that its rate is defined by a second order equation:

$$W_3 = K_3 [HO_2] [H_2O]. \tag{1}$$

On the basis of the reaction mechanism described above and applying the method of steady state concentration of intermediate products, we obtain the following approximate equation for the reaction rate:

$$W = -\frac{d[H_2O_2]}{dt} \simeq K \sqrt{J} \sqrt{[H_2O_2][H_2O]}, \tag{2}$$

where

$$K = 2\sqrt{\frac{K_1 K_2 K_3}{K_5}}.$$

As indicated, the reaction rate is proportional to $\sqrt{J}$, as is required by Equation (2).

The data presented in the graph of Fig. 4 are illustrative of the applicability of Equation (2) to the radiation reaction. Agreement with the experiments is also satisfactory for photodecomposition and thermal decomposition in all concentration regions and for all temperatures at which the measurements were carried out.

It can be assumed that in a number of cases the equations obtained in other works for the rate of the radiation decomposition of H_2O_2 are approximations of the true kinetic law applying to the reaction in the different narrow concentration intervals – dilute solutions of H_2O_2.

L. Ya. Karpov Physicochemical Institute

Received February 4, 1957

LITERATURE CITED

[1] a) F. S. Dainton, J. Rombottom, Trans. Farad. Soc., 49, 1160 (1953); b) J. Hart, M. S. Matheson, Disc. Farad. Soc., 12, 169 (1952); c) J. Weiss, Disc. Farad. Soc., 12, 161 (1952); d) V. I. Veselovsky and G. S. Tyurikov, Coll. Works on Radiation Chemistry*, Izd. AN SSSR, 1955, p. 61.

[2] W. C. Schumb, Ind. and Eng. Chem., 41, 992 (1949).

[3] J. Weiss, Trnas. Farad. Soc., 31, 1547 (1935).

[4] Ms. G. Kornfeld, Zs. Phys. Chem., 29, 205 (1935).

[5] V. N. Kondratyev, Coll. Problems of Kinetics and Catalysis, 4, 63 (1940).

* In Russian.

* In Russian.

CERTAIN FEATURES OF THE KINETICS OF THE ADDITION OF HYDROGEN IODIDE TO UNSATURATED COMPOUNDS

Academician Acad. Sci. UkrSSR E. A. Shilov and D. F. Mironova

We have established that iodine accelerates the addition of HI to cyclohexene and allyl chloride if the reaction is carried out in benzene solution. Measurements showed that the rate of both reactions is expressed by the equation

$$-\frac{d[HI]}{dt} = k_3 M [HI][I_2]$$

where M is the concentration of the unsaturated compound.

The rate of the reaction of HI with cyclohexene does not depend on temperature, at least not in the range of 4 to 30°. This is revealed by Fig. 1, where data from several kinetic experiments at different temperatures are presented. It can be seen that, within the limits of experimental error, the changes in the titre of HI in the mixture for all temperatures fall on the same curve, for which k_3 is 6.7 $l^2 \cdot mole^{-2} \cdot sec^{-1}$. Thus, the temperature coefficient for the rate of the reaction between cyclohexene and HI in benzene solution is zero. The overall activation energy is also zero, and the pre-exponential factor $\alpha = k_3 = 6.7$ – a very rare case for reactions in solution.

If the reaction of cyclohexene with HI is carried out in glacial acetic acid, iodine ceases to act as a catalyst and, on the contrary, retards the reaction if it is present in a concentration commensurate with the concentration of HI. The temperature coefficient of the rate acquires the normal value of ~2.4 per 10° (Fig. 2). The rate of the reaction of HI with cyclohexene in acetic acid is expressed by the equation

$$-\frac{d[HI]}{dt} = k_3' M [HI]^2,$$

where k_3' = 0.096 at 20° and 0.23 at 30° (in the same units), E = 14.7 kcal. The addition of LiI appreciably retards the reaction; apparently, the LiI replaces a molecule of HI in the transition complex of the addition reaction.

In benzene and in the presence of iodine, HI adds to allyl chloride much more slowly than to cyclohexene: $k_3 = 0.0088$ $l^2 \cdot mole^{-2} \cdot sec^{-1}$. The addition does not go at all in acetic acid. The rate of addition of HI to allyl chloride in benzene solution increases by a factor of 2.2 in the temperature interval 12-30°.

1,2-Dimethyl-1-cyclohexene reacts with HI so fast that it is impossible to obtain accurate values for the rate constant even at a temperature of about 0°. However, there is no doubt of the catalytic action of iodine.

From the data presented, it follows that the kinetics of HI addition in these three reactions are determined by the action of an electrophilic agent. As a matter of fact, groups with an electron donor effect (CH_3) accelerate, and those with an electron acceptor effect (CH_2Cl) retard the addition reaction. However, we observe that the reaction is accelerated on changing from cyclohexene to dimethyl acetylenedicarboxylate – a compound which tends to react with nucleophilic rather than with electrophilic reagents.

In the absence of iodine, the addition of HI to acetylenedicarboxylate in benzene follows a second order equation:

$$-\frac{d[HI]}{dt} = k_2 M\,[HI].$$

The constant in this equation is independent of temperature in the range 3 to 30°. This is seen in Fig. 3, where the same Curve 1 represents values measured at 3, 13, and 30°; k_2 for this reaction is equal to 0.24 liter · mole^{-1} · sec^{-1}. Iodine retards the addition of HI to the acetylenedicarboxylate, as shown by Curve 2 in Fig. 3 which corresponds to experiments with the addition of iodine in the amount of 0.0058 mole/liter.

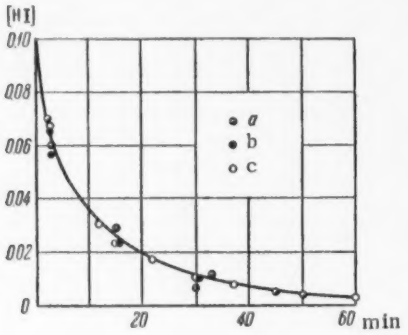

Fig. 1. Cyclohexene and HI in benzene $[C_6H_{10}]_0$ = 0.13 M; a) 4°, b) 14°, c) 30°.

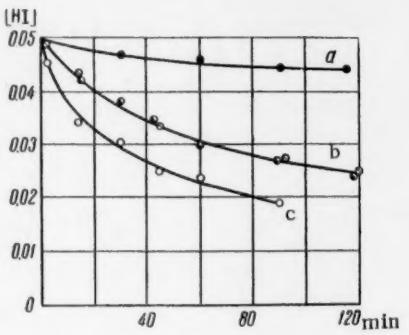

Fig. 2. Cyclohexene and HI in glacial acetic acid. $[C_6H_{10}]_0$ = 0.05 M; a) 20°, $[I_2]$ = 0.052 M; b) 20°, $[I_2]$ = 0.0009 M; c) 30°, $[I_2]$ = 0.0008 M

Curves 3, 4, and 5 in Fig. 3 reveal that the addition of HI to the acetylenedicarboxylate is retarded on going from benzene solution to solution in petroleum ether and is accelerated on going to more protophilic solvents – mixtures of benzene with dioxane or with acetic acid.

Apparently, HI acts in the first stage of this reaction, not as an electrophilic, but as a nucleophilic agent [1]. Consequently, in the transition from cyclohexene to the acetylenedicarboxylate not only the rate constant, but also the mechanism of HI addition is changed.

The very low temperature coefficient of the rate of the addition of HI to cyclohexene and to the acetylenedicarboxylate in benzene solution is apparently explained by the intermediate formation of an active complex, the concentration of which decreases with an increase in temperature, thereby compensating for the thermal acceleration of the reaction. Of the various complexes possible in our systems, the most probable for such a role is the π-complex $C_6H_6 \cdots \rightarrow HI$. If its energy of formation (ΔH) is close to the value of the energy (E_a) of its transition into a critical complex, the observed activation energy $E = \Delta H - E_a$ will be close to zero.

This relates to the addition of HI to cyclohexene and to acetylenedicarboxylate. For allyl chloride, the energy of formation of the transition complex so greatly exceeds the free energy of formation of the complex $C_6H_6 \cdots \rightarrow HI$ that the temperature of the reaction rate differs little from normal.

The catalytic action of iodine in the reactions of HI with cyclohexene and with allyl chloride is connected, we think, with its electrophylic properties. The reaction probably proceeds through a trimolecular transition complex of the composition

in the formation of which the complex $C_6H_6 \cdots \rightarrow HI$ plays the role of a nucleophilic agent. With the splitting out of HI, 1,2-diiodocyclohexane is formed, which is immediately reduced to the monoiodo-derivative. The stage of the reduction of the diiodide proceeds so rapidly that it does not limit the overall reaction rate and is not reflected in the kinetic equation.

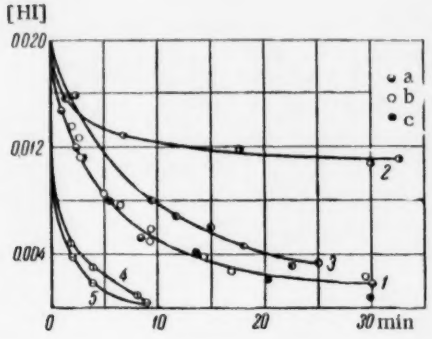

Fig. 3. Dimethyl acetylenedicarboxylate and HI $[C_6H_6O_4]_0 = 0.02$ M; 1) in benzene, $[I_2] = 0.0001$ M [a) 3°, b) 13°, c) 30°]; 2) in benzene, $[I_2] = 0.0058$, 13°; 3) in petroleum ether, 14°; 4) in a mixture of C_6H_6 and CH_3CO_2H (1:1), 14°; 5) in a mixture of C_6H_6 and dioxane (1:1), 13°.

Thus, we assume the formation of 1,2-diiodocyclohexane as an intermediate stage in the hydriodination of cyclohexene and allyl chloride. For confirmation of this hypothesis, it is necessary to know the rate of the formation of the diiodide and the rate of its reduction. However, it turns out that in the absence of HI, iodine adds slowly to cyclohexene, and in the presence of hydrogen iodide, the addition of iodine cannot be observed, because HI is added instead of iodine. If the adduct of iodine and cyclohexene is contained in the solution, it liberates iodine extremely rapidly after the addition of HI to the solution. However, the rate of formation of diiodocyclohexane in the presence of HI remains unknown, and, consequently, exhaustive proof of our assumption cannot be given.

EXPERIMENTAL

The cyclohexene, prepared from cyclohexanol, had a b. p. of 82°. The 1,2-dimethyl-1-cyclohexene was prepared from 1,2-dimethyl-1-cyclohexanol by distillation with iodine [2]; b.p. 135-136°. The dimethyl acetylenedicarboxylate was prepared as in previous work [3]. The allyl chloride (from allyl alcohol and HCl) boiled at 44-45°. The solvents were carefully dried and distilled. Gaseous HI was purified from iodine by means of a solution of CaI_2, from water with phosphorous pentoxide, and from PH_4I by cooling to −25°.

Solutions of HI in organic liquids were protected from light, and were used in the kinetic experiments in an atmosphere of carbon dioxide for protection from oxidation by air, which especially easily enters acetic acid solutions.

The kinetic experiments were carried out in special vessels connected with a pipet for dosing [4]. For the hydrogen iodide determinations, samples with a volume of 1 ml were mixed in a dropping funnel with several milliliters of CCl_4 and were shaken with water. The HI in the aqueous layer was determined by Volhard titration. The iodine in the CCl_4 layer was titrated with thiosulfate.

In each separate experiment, the values of the constant were constant within the limits of error of the measurements. As examples are cited the data of two experiments. Concentrations are given in moles per liter. HI concentrations were taken from curves.

Cyclohexene and HI in benzene

$[C_6H_{10}]_0 = 0.123$, $[I_2] = 0.00515$ M, 17°

t, min.	[HI]	k_2, $l \cdot mole^{-1} \cdot sec^{-1}$
0	0.097	-
5	0.042	0.0314
7	0.032	0.0301
10	0.0245	0.0297
15	0.016	0.0301
20	0.011	0.0313
25	0.008	0.031
		0.0307

Acetylenedicarboxylate and HI in benzene

$[C_6H_6O_4]_0 = 0.0316$ M, 13°

t, min.	[HI]	k_2, $l \cdot mole^{-1} \cdot sec^{-1}$
0	0.0300	-
5	0.0144	0.111
10	0.0092	0.113
15	0.0086	0.115
20	0.0059	0.113
		0.113

$$k_3 = \frac{k_2}{[I_2]} = 6.0\ l^2 \cdot mole^{-2} \cdot sec^{-1}$$

TABLE 1

Cyclohexene and HI in Benzene

T, °C	$[HI]_0$	$[C_6H_{10}]_0$	$[I_2]$	$k_2 \cdot 10^4$, $l \cdot mole^{-1} \cdot sec^{-1}$	$k_3 = \frac{k_2}{[I_2]}$, $l^2 \cdot mole^{-2} \cdot sec^{-1}$
30	0.120	0.380	0.0004	24.6	
30	0.120	0.649	0.0004	23.6	
17	0.097	0.123	0.0014	89	6.3
17	0.097	0.123	0.00255	158	6.2
17	0.097	0.123	0.00515	307	6.0
4.4.30	0.096	0.131	0.0026	185	6.7
14	0.091	0.131	0.0025	170	6.8
4.30	0.094	0.131	0.00105	50	5.0
					6.2

TABLE 2

Allyl Chloride and HI in benzene

T, °C	$[HI]_0$	$[C_3H_5Cl]_0$	$[I_2]$	$k_2 \cdot 10^4$, $l \cdot mole^{-1} \cdot sec^{-1}$	$k_3 \cdot 10^3$ $l^2 \cdot mole^{-2} \cdot sec^{-1}$
30	0.102	0.408	0.012	0.93	7.9
30	0.098	0.408	0.024	2.03	8.5
30	0.105	0.408	0.049	4.0	8.2
30	0.118	0.408	0.125	11.7	9.4
30	0.17	0.408	0.025	2.26	9.0
30	0.098	0.408	0.049	4.37	8.9
30	0.10	0.10	0.058	6.1	9.9
					8.8
12	0.10	0.10	0.078	2.4	3.0

Some of the average values of the constants k_2 and k_3 are summarized in Tables 1 and 2. It should be noted that the discrepancies among the values of the constants from the various experiments are rather significant, which is explained by the inaccuracy in the analytical determinations of elemental iodine in the samples.

Institute of Organic Chemistry
Academy of Sciences UkrSSR
Kiev Sanitary-Chemical Institute

Received February 22, 1957

LITERATURE CITED

[1] E. A. Shilov, Coll. Questions of Chemical Kinetics, Catalysis, and Reactivity. Izd. AN SSSR, 1955, p. 750.*

[2] T. K. Signaigo, P. L. Cramer, J. Am. Chem. Soc., 55, 3330 (1933).

[3] I. V. Smirnov-Zamkov and E. A. Shilov, Proc. Acad. Sci. USSR, 67, 671 (1949).

[4] I. V. Smirnov-Zamkov and G. A. Piskovitina, Ukr. Chem. J., 23, 209 (1957).

* In Russian.

CERTAIN FEATURES OF THE CATHODIC REDUCTION OF CHROMIC ACID AT A CARBON ELECTRODE

G. V. Shteinberg and V. S. Bagotsky

(Presented by Academician A. N. Frumkin, February 11, 1957)

During cathodic polarization of carbon or other inert electrodes in solutions of chromic acid, the phenomenon of a sudden retardation of the reduction of the chromic acid anion occurs, $Cr_2O_7^{--} + 14\ H^+ + 6e \rightarrow$ $\rightarrow 2Cr^{+++} + 7H_2O$, accompanied by a staggered shift of the electrode potential in a negative direction.

Cathodic polarization at high current densities leads to a sharp shift in potential of approximately 1 volt in a negative direction, after which the liberation of hydrogen begins ("complete passivation" of the electrode). In addition to this phenomenon, in certain cases at low current densities there is observed a potential shift of several tenths of a volt, but the hydrogen liberation potential is not reached. This phenomenon will be called "partial passivation" of the electrode in the future. Complete and partial passivation are observed both with a constant increase in current density when obtaining polarization curves and during protracted polarization of the electrode at constant current density.

Complete passivation of inert electrodes in solutions of chromic acid has been the subject of investigation by many authors. Müller [1] introduced the widespread concept of the formation on the surface of the electrode, during the course of the electrolysis, of a diaphragm of difficultly soluble compounds of tri- and hexavalent chromium (the so-called chromichromate film) which does not pass chromic acid ions to the cathode and which leads thereby to retardation or cessation of the given electrochemical reaction. Partial passivation has been studied to a considerably less extent. Individual observations on inert metallic electrodes, relating to the region of partial passivation (i. e., to a potential more positive than that at which hydrogen is liberated) were interpreted by Libreich [2] also on the basis of the assumption of the formation on the electrode of a film of difficultly soluble compounds of trivalent chromium. Partial passivation of a carbon electrode in chromic acid solutions has not been studied in detail, although this phenomenon has great significance for chemical sources of current (Grenet type cells), since it leads to the step-wise form of the discharge curve [3].

In the present work, the effect of a number of factors (solution composition, stirring, and cathode treatment) on partial passivation of a carbon electrode was investigated. Curves relating potential to time were determined at various current densities with a rotating electrode of "spectroscopic" uncalcined carbon. In Fig. 1 is shown the effect of bichromate ion concentration, in Fig. 2 is shown the effect of hydrogen ion concentration, and in Fig. 3 is shown the effect of the concentration of salts on the partial passivation of the carbon electrode. It is seen from the figures that the potentials of the upper and lower levels of the curves, which correspond to the active and partially passivated states of the electrode, and also the duration of the active state depend on the composition of the solution; the effects of the same component on the potential of the active electrode and on that of the partially passivated electrode differ. The effect of the addition to the solution of a large concentration of an indifferent salt was especially conspicuous; this addition sharply decreased the potential of the partially passivated electrode in a negative direction, and had almost no effect on the potential of the active electrode.

The introduction into the solution of the product of the reduction of chromic acid – trivalent chromium – in a concentration several times exceeding its steady state concentration at the surface of the rotating electrode had practically no effect on partial passivity. This result was obtained regardless of whether the trivalent

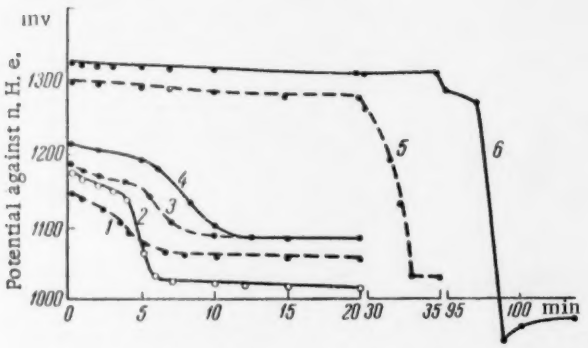

Fig. 1. Effect of bichromate ion concentration: 1) Cr_2O_3 0.5 mole/liter, H_2SO_4 0.5 mole/liter, $[H^+]$ = 1.5 g-equiv/liter; 2) CrO_3 1.5 mole/liter, no H_2SO_4, $[H^+]$ = 1.5 g-equiv/liter; 3) CrO_3 1.0 mole/liter, H_2SO_4 0.5 mole/liter, $[H^+]$ = 2 g-equiv/liter; 4) CrO_3 3.0 mole/liter, no H_2SO_4, $[H^+]$ = 2-gequiv/liter; 5) CrO_3 3.0 mole/liter, H_2SO_4 0.5 mole/liter, $[H^+]$ = 8 g-equiv/liter; 6) CrO_3 7.0 mole/liter, H_2SO_4 0.5 mole/liter, $[H^+]$ = = 8 g-equiv/liter; i = 20 ma/sq.cm., t = 25°, w = 550 rpm.

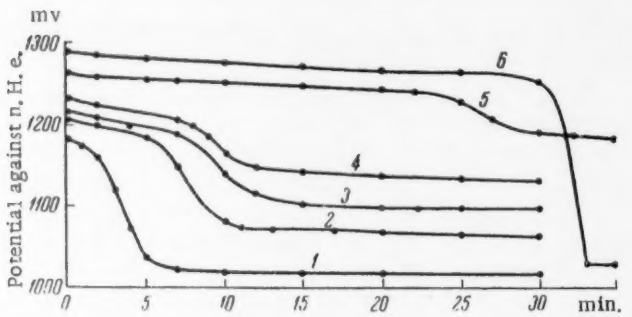

Fig. 2. Effect of H^+-ion concentration: 1) 1 g-equiv/liter, 2) 2 g-equiv/liter, 3) 3 g-equiv/liter, 4) 4 g-equiv/liter, 5) 6 g-equiv/liter, 6) 8 g-equiv/liter; $[CrO_3]$ constant at 3 mole/liter; i = 20 ma/sq. cm., t = 25°, w = 550 rpm.

chromium was added in the form of a salt (chromium sulfate) or in the form of a previously electrolytically reduced solution of chromic acid (in the latter case, along with the formation of trivalent chromium, there is also a change in the acidity of the solutions similar to that which occurs in the layer of solution next to the electrode during polarization of the electrode). In solutions to which were added very small concentrations of chromium sulfate there was observed a sharp shift in the potential of the partially passivated electrode; apparently, however, this effect is not connected with the presence of trivalent chromium, but with an increase in the overall concentration of the electrolyte, since the same shift of the curve also occurred with the addition to the solution of an equivalent concentration of sodium sulfate or perchlorate (Fig. 3). A sharp shift in the potential of the partially passivated electrode was also observed in solutions with a high concentration of sulfuric or chromic acid (Fig. 1, Curves 5 and 6, Fig. 2, Curve 6). A change in the rotational speed of the electrode, which also led to a change in the steady state concentration of the reaction components (particularly of trivalent chromium) in the layer of solution next to the electrode, had practically no effect on the potentials of the upper and lower parts of the polarization curve nor on the duration of the active state of the electrode.

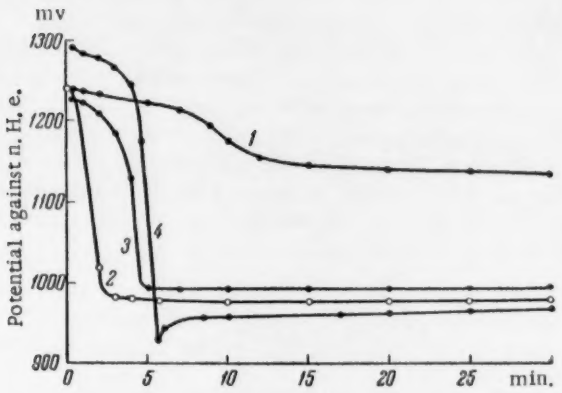

Fig. 3. Effect of salt concentration: 1) CrO_3 3 mole/liter, H_2SO_4 0.5 mole/liter; 2) same as 1 plus 4.5 g-equiv/liter of $Cr_2(SO_4)_3$; 3) same as 1 plus 4.0 g-equiv/liter of Na_2SO_4; 4) same as 1 plus 4.0 g-equiv/liter of $NaClO_4$; i = 20 ma/sq. cm., t = 25°, w = 550 rpm.

These phenomena should be considered as a retardation of the electrochemical reaction, and not as a change in its nature, since at the potential of either the upper or the lower level of the curve the only steady state electrode reaction under these conditions is, for thermodynamic reasons, the reduction of hexavalent chromium to trivalent.

The experimental data obtained in the present work refute the assumption that the reason for the retardation of the reaction is the formation at the cathode of a film of difficultly soluble compounds of trivalent chromium. This follows from the independence of the phenomenon of partial passivity from the addition of trivalent chromium to the solution and from the rate of stirring.

It appears probable that the phenomenon of partial passivity is connected with a change in the state of the oxide layers on the surface of the electrode, which occurs simultaneously with the reduction of the chromic acid. In particular, this follows from the experimental data which show that all factors which shift the potential of the active electrode in a positive direction simultaneously lead to a decrease in the duration of the active state of the electrode. Also in support of this idea are experiments studying the effect of preliminary treatment of the electrode. Preliminary cathodic polarization of the electrode in chromic acid solution led to the disappearance of the active portion of the curve or, at least, to sharp curtailment of it on a second polarization after a brief current interruption. With a long interruption the electrode "rests", and a second polarization gives the normal form of the curve with "active" and "semi-passivated" portions. Depassivation of the electrode is not accelerated by changing the electrolytic solution during the interruption. However, the electrode very rapidly (after 1-1.5 minutes) regains its normal active state on weak anodic polarization. An electrode subjected to preliminary strong anodic polarization in either chromic acid solution or, for example, sulfuric acid solution behaves differently. In this case, on subsequent cathodic polarization of the electrode in chromic acid solution the upper portion of the curve completely disappears, and the electrode works only in the partially passivated state. The change in the state of the electrode is irreversible – the electrode does not "rest" and is not restored to the active state.

In the consideration of the data presented above on the effect of a high concentration of dissolved substances, it is necessary to take into consideration that aggregation of the chromic acid ions into the polychromate ions $Cr_3O_{10}^{--}$ and $Cr_4O_{13}^{--}$ is possible at high ionic concentrations. The change in the reduction potential of chromic acid under such conditions is, therefore, naturally explained by a change in the nature of the particles containing the hexavalent chromium. It is interesting to note that such an effect of the nature of the particles on the rate of reduction is not observed with the electrode in the active state.

The data presented above are in support of the idea that certain forms of surface oxides correspond to the active state of the electrode, these oxides gradually disappearing during cathodic polarization and forming again during mild anodic polarization of the carbon. These oxides either participate themselves in the process, or contribute to the emergence of active zones on the surface of the electrode on which the process of reduction of $Cr_2O_7^{--}$ proceeds more easily than on the remaining surface. Acceleration of the reduction process on these zones is possibly connected with the formation at these zones of intermediate surface compounds, while on the inactive surface the reduction of chromic acid ions proceeds directly. With sufficient energy of adsorption of the intermediate compounds, a considerable portion of the active zones can be filled regardless of the form in which the hexavalent chromium occurs in the solution. In this way, in particular, it would be possible to explain why the nature of the chromic acid ions affects the reduction potential only on the partially passivated electrode, on which intermediate surface compounds are not formed.

Thus, the phenomenon of partial passivation of a carbon electrode can be considered as a change in the electrochemical mechanism of the reduction of ions containing hexavalent chromium to trivalent chromium, occurring as a result of a change in the state of the oxide layers on the surface of the electrode.

Qualitatively similar phenomena are observed with inert platinum and gold electrodes.

We express our appreciation to Academician A. N. Frumkin for valuable counsel during discussion of the results of this work.

All-Union
Scientific Research
Electrocarbon Element Institute

Received February 5, 1957

LITERATURE CITED

[1] E. Müller, Zs. Elektrochem., 32, 400 (1926).

[2] E. Libreich, Zs. Elektrochem., 27, 94, 453 (1921); 40, 73 (1934).

[3] H. A. Barbiand, McNulty, Trans. Electrochem. Soc., 91, 387 (1947).

THE PHOTOIONIZATION OF THE VAPORS OF CERTAIN ORGANIC COMPOUNDS

F. I. Vilesov and Academician A. N. Terenin

In connection with the investigations which are being carried out in our own and in associated laboratories on the electronics of the aromatic compounds in general [1] and of the surface active adsorbents in particular [2], it became necessary to obtain values of the energy of electron detachment for the molecules of these compounds in the gaseous condition. The present work was carried out in 1956; preliminary results were obtained in 1955.

The following photoelectric techniques have been employed by us in measuring the ionization potentials of organic vapors: 1) the condenser method, 2) the ionization chamber method, with gas amplification and 3) the Geiger counter method.

Thanks to the work of Wetanabe and his collaborators [3], the condenser method has been widely applied in recent years. The ionization chamber in this method has the form of a vessel equipped with two plane electrodes to which a small difference of potential (10-20 V) is applied. Light in passing between these electrodes brings about the photoionization of the investigated vapors. The ionization currents are of the order of magnitude of $10^{-12} - 10^{-4}$ amp, and are measured with an electrometer amplifier.

The second method, and the one which was initially applied by us for measuring the ionization potentials of organic vapors, uses an ionization chamber which is in the form of a gas filled cell. Hydrogen, or argon, serves as the working gas. Under electrode potentials of 300-500 V and gas pressures up to 100 mm of Hg, this ionization cell gives an amplification of the order of 100-500. Thus the sensitivity here is two orders greater than it is in the condenser method.

The construction of this cell was such that it was possible to simultaneously measure the transmission spectra of the investigated vapors, use being made of a photomultiplier which was equipped with a fluorescent screen of sodium salicylate.

The Geiger counter method for studying photoionization was first employed in 1951 [4], but failed to find subsequent applications because the results of the initial investigations agreed poorly with those obtained through the condenser method in which secondary processes are reduced to a minimum. We constructed a cylindrical counter with an end window, the cathode being a glass cylinder, 6 cm in diameter, which was covered with a semiconducting film. In the self-quenching regime a mixture of argon with benzene, or methane, served as the working gas; in the nonself-quenching regime, hydrogen, or argon. This is the most sensitive of the methods since it permits the registration of each act of ionization.

A high voltage hydrogen tube served as the source of illumination; light from this tube passed into the ionization chamber through a vacuum monochromator with a concave diffraction grating of 600 lines/mm and 1 m focus, which operated at normal incidence. Registration of the spectra of photoionization and transmission was carried out on a recorder of the EPP-09 type.

For benzene, toluene and n-xylene, photoionization was measured by all of the above mentioned methods. It was established that all three gave values of the ionization potential which agreed within the limits of experimental error with the most trustworthy data of other authors which are at present available on spectral absorption lines.

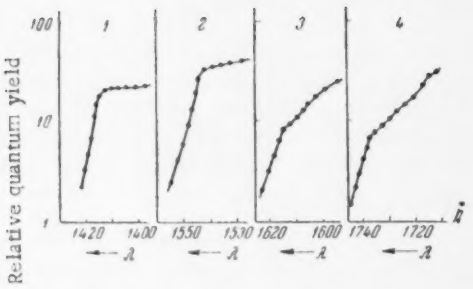

Fig. 1. Photoionization curves: 1) toluene; 2) tetramethyl benzene; 3) analine; 4) dimethyl analine.

For measuring the photoionization potentials of difficultly volatile substances (quinone, phenylhydrazine, phenol, etc.) with vapor pressures of the order of $10^{-2} - 10^{-3}$ mm of Hg at 18°, the method of the Geiger counter was employed, this permitting the observation of photoionization currents down to 10^{-19} amp.

In Fig. 1 there are presented certain curves showing the dependence of the photoionization current on the wave length of the acting radiation. On the axis of ordinates there is plotted the natural logarithm of the ratio of the photoionization current to the number of absorbed quanta, expressed in relative units. The ionization potentials were determined from the breaks on these curves, these breaks corresponding to the O-O transition from the normal state of the molecule into the normal state of the singly charged ion. Ionization by a smaller number of light quanta is brought about by transitions from the vibrational levels of the normal state of the molecule.

TABLE 1

Photoionization of the vapors of certain organic compounds

Compound	Photoionization potentials		Precision	Compound	Photoionization potentials		Precision
	Å	ev			Å	ev	
C_6H_6	1340	9.24	±0.02	$C_6H_5—CH_2—NH_2$	1434	8.64	±0.02
$C_6H_5CH_3$	1407	8.81	±0.02	$C_6H_5—OH$	1457	8.52	±0.02
o-$C_6H_4(CH_3)_2$	1447	8.56	±0.02	Haphthlene	1523	8.14	±0.02
m-$C_6H_4(CH_3)_2$	1444	8.59	±0.02	$C_6H_5—HCO$	1292	9.60	±0.02
n-$C_6H_4(CH_3)_2$	1469	8.44	±0.02	Quinone	1281	9.67	±0.02
$C_6H_3(CH_3)_3$	1474	8.41	±0.02	$NH_2—NH_2$	1297	9.56	±0.02
$C_6H_2(CH_3)_4$	1540	8.05	±0.02	(H_2CO) monomer	1137	10.90	±0 03
$C_6H(CH_3)_5$	1565	7.92	±0.02	$(H_2CO)_2$dimer	1179	10.51	±0.03
$C_6H_5—NH_2$	1612	7.69	±0.02	$(CH_3)_2C=O$	1280	9.71	±0.03
$C_6H_5—NH—NH_2$	1623	7.64	±0.02	$CH_3HC=O$	1215	10.20	±0.03
m-toluidine	1652	7.50	±0.02	$CH_3C_2H_5C=O$	1300	9.55	±0.03
$C_6H_5—NH—CH_3$	1689	7.34	±0.02	$CH_3C_3H_7C=O$	1308	9.47	±0.03
$C_6H_5—N(CH_3)_2$	1734	7.14	±0.03	$(C_2H_5)_2O$	1287	9.65	±0.03
				$CH_3C_4H_9OC=O$	1296	9.56	±0.03

It is clear from Fig. 1 that the quantum yield for photoionization in the aromatic amines at wave lengths close to the ionization threshold is considerably less than that for the other compounds. According to the Franck-Condon principle, this must indicate that the internuclear distances in the molecules, and in the corresponding ions, are of considerably different magnitude.

In Table 1 above there are shown the values found by us for the first photoionization potentials.

In Fig. 2 there is shown the relation between the ionization potentials of the derivatives of benzene (Curve 1) and analine (Curve 2) and the number of hydrogen atoms which have been replaced by $-CH_3$ groups. The gradual decrease of the ionization potentials accompanying the increase of the number of replaced hydrogen atoms is related to the increase in the density of the electron cloud in the benzene ring.

The A. A. Zhdanov State
University, Leningrad

Received July 26, 1957

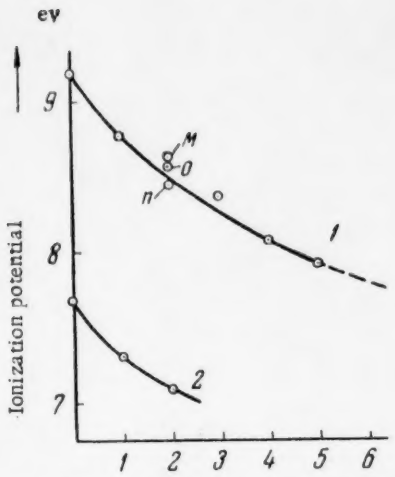

Fig. 2. The change in the ionization potential and its dependence on the number of substituted hydrogen atoms in benzene (1) and in analine (2).

LITERATURE CITED

[1] A. N. Terenin, Radio Practice and Electronics, 1, No. 8, 1127 (1956).

[2] A. I. Sidorova and A. N. Terenin, Bull. Acad. Sci. USSR, Div. Chem. Sci., No. 2 (1950); A. I. Sidorova, Proc. Acad. Sci. USSR, 77, 327 (1950); A. I. Sidorova, J. Phys. Chem., 28, 525 (1954); E. I. Kotov, Optics and Spectroscopy 1, No. 4, 500 (1956).

[3] K. Wetanabe, Phys. Rev., 91, 1769 (1953); J. Chem. Phys., 21, 1026 (1953); 22, 1564 (1954); E. C. Y. Inn, Phys. Rev., 91, 1195 (1953); Spectrochimica Acta, 7, 65 (1955).

THE RELATIVE ROLES OF THE ELECTRICAL AND DIFFUSIONAL PROCESSES IN THE PHENOMENA OF THE ADHESION OF TWO POLYMERS

L. P. Morozova and N. A. Krotova

(Presented by Academician P. A. Rebinder December 18, 1956)

In previous papers [1] an electrical theory of adhesion has been developed by one of us. Various authors have, on the other hand, repeatedly expressed opinions as to the role of diffusional processes in the formation of the adhesive and the autoadhesive bonds [2].

In view of the interest attaching to this question, the experimental study of the formation of the adhesive bond, particularly in the case of the union of two high molecular substances, acquires a special significance, the aim being here to elucidate the relative roles of the electrical and diffusional processes in the phenomena of adhesion.

TABLE 1

The Work, A_0, of Detachment of a Polymer Film From Various Surfaces and the Velocity of the Electrons Which Are Emitted in the Detachment Process at $P = 10^{-4}$ mm of Hg•

Polymer	Base	Velocity of electrons, ev;	A_0, exp., erg/cm^2	A, calculated from the electron velocity, erg/cm^2
Perchlorvinyl	Brass	$2.45 \cdot 10^3$	$2.45 \cdot 10^4$	$1.04 \cdot 10^4$
	Glass	$6.25 \cdot 10^3$	$3.16 \cdot 10^4$	$2.52 \cdot 10^4$
	Gelatin	$1 \cdot 10^4$	$3.16 \cdot 10^5$	$2.82 \cdot 10^5$
	SKD rubber (kaolin filler)	$2.5 \cdot 10^4$	$1.59 \cdot 10^6$	$5.63 \cdot 10^5$
Polyisobutylene	Gelatin	$1 \cdot 10^4$	$3.56 \cdot 10^5$	$3.17 \cdot 10^5$

• The experiments were carried out in vacuum; the curve was obtained in the region of high velocities.

For solving the question as to the character of the adhesive bond, the form of the adhesiogram is very significant. The influence of the detachment rate is poorly expressed in the case where the adhesive bond is conditioned by diffusional phenomena. On the other hand, if the adhesive bond is of electrical nature the adesiogram usually discloses three clearly defined sections [3].

With the aid of a rolling adhesiometer we have developed adhesiograms for a number of polymers (BF type glues; polyurethans, polyamides, polymers of the vinyl series, rubber and gutta-percha, cellulose esters, etc.). Adhesiograms for various combinations of these polymers with glass, metals and rubbers based on Na-butadiene and acrylonitrile usually show three sharply delineated sections. In certain cases, however, only two such sections appear and the third is lacking. It is very likely that even then this third section also exists but is located in the region of high velocities which are experimentally difficult to measure.•

The velocity of the electrons which are emitted during detachment [4] can give some idea as to the magnitude of the potential gradient in the electric double layer since these electrons are accelerated by the field existing in the space between the separated surfaces. Determining the velocity of the emitted electrons from the magnitude of the deflection of the electron bundle in a magnetic field and calculating the value of σ from the experimental data and the Paschen curve, it is possible to evaluate the work, A, of detachment and to compare this with the quantity A_0, experimentally determined by mechanical means (Table 1). It follows from the table that the higher the velocity of the emitted electrons, the greater is the adhesion in the system.

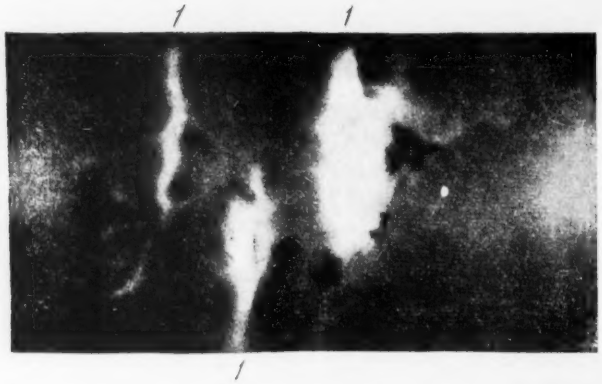

Fig. 1. Emission from the portions, (1), of a film of perchlorvinyl which were bound to a mechanically treated metallic (brass) surface, i.e., to the grooves in the metal.

In one of our most recent papers [5] it was shown that emission centers exist in a polymer film after detachment, so that those individual sections of the film emit which were in most intimate contact with the base. It is generally known that mechanical treatment of the base surface leads to an increase in the firmness of adhesion, a fact which is commonly attributed to an increase in the contact area••. Thus for us it is of definite interest to determine whether it is actually true that the intensity of emission from the detached polymer film will be high over those portions of the latter which were in contact with the mechanically worked surface. For this purpose grooves were made on a metallic (brass) surface with a file, after which a polymer solution was introduced onto the surface. Experiments were carried out in vacuum, using the rolling adhesiometer. In the photographs it is completely clear that the electron emission is more intensive in those

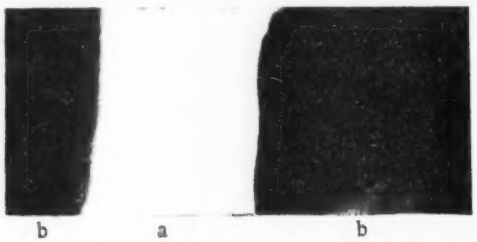

Fig. 3. The electron emission from rubber surfaces resulting from the detachment of gutta-percha films from them. a) rubber with kaolin filler, b) rubber with carbon black filler.

• Under the conditions of our experiments time intervals <0.01 sec. cannot be measured.

•• This phenomenon can, however, be explained in terms of other factors as well; for example, by the alteration of the surface properties of the mechanically worked surfaces or by the reduction of the depth of the oxide film.

TABLE 2

The Various Types of Adhesion Bonds

Character of the adhesion bond	Sign of the residual charge for detachment in air	Emitter for detachment in vacuum, $P = 1 \cdot 10^{-4}$ mm of Hg	Work of detachment at v = 1 cm/sec•	Type of detachment
Group I. Electrostatic interaction of the charges of the electric double layer which is formed at the surface of separation	Perchlorvinyl (–)–steel (+)	Perchlorvinyl	$1.04 \cdot 10^4$	Adhesional
	Perchlorvinyl (–)–glass (+)	"	$2.52 \cdot 10^4$	
	Polyethylene (–)–SKB rubber (+) (kaolin)••	Polyethylene	$4.45 \cdot 10^4$	
	Polyethylene (–)–SKN rubber (+) (kaolin)	"	$5.63 \cdot 10^4$	
	Gutta-percha(-)–glass(+)	Gutta-percha	$1.78 \cdot 10^5$	
	Polyvinylbutanal(–)–SKD rubber (+) (kaolin)	Polyvinyl-butyral	$2.02 \cdot 10^5$	
	Perchlorvinyl (–)–gelatin (+)	Perchlorvinyl	$2.82 \cdot 10^5$	
	Polyamide(-)–SKB rubber(+) (kaolin)	Polyamide	$3.01 \cdot 10^5$	
	Nitrocellulose (–)–SKB rubber (+) (kaolin)	Nitrocellulose	$3.16 \cdot 10^5$	
	Gutta-percha (–)–steel (+)	Gutta-percha	$3.98 \cdot 10^5$	
	BF-6 (–)–SKB rubber (+) (kaolin filler)	BF-6	$3.98 \cdot 10^5$	
	Perchlorvinyl (–)–SKB rubber (+) (kaolin)	Perchlorvinyl	$5.63 \cdot 10^5$	
	Polyurethan (–)–SKB rubber (+) (kaolin)	Polyurethan	$6.32 \cdot 10^5$	
	Gutta-percha (–)–SKB rubber (carbon black), treated with H_2SO_4 (+)	Gutta-percha	$6.52 \cdot 10^5$	
	Gutta-percha (–)–SKN rubber (+) (kaolin)	"	$1.05 \cdot 10^6$	
	Polyamide(-)–SKN rubber (+) (kaolin)	Polyamide	$1.12 \cdot 10^6$	
a. The role of the electrical phenomena is unclear	Polyethylene (–)–SKB rubber (+) (carbon black)	No emission	$4.45 \cdot 10^4$	
	Polyvinylbutyral (–)–SKB rubber (+) (carbon black)		$1.75 \cdot 10^5$	
	Polyamide(-)–SKB rubber (+) (carbon black)		$2.84 \cdot 10^5$	
	Nitrocellulose (–)–SKB rubber (+) (carbon black)		$3.04 \cdot 10^5$	
	Perchlorvinyl (–)–SKB rubber (+) (carbon black)		$5.41 \cdot 10^5$	
	BF-6 (–)–SKB rubber (+) (carbon black)		$3.87 \cdot 10^5$	
	Polyurethan (–)–SKB rubber (+) (carbon black)		$6.23 \cdot 10^5$	
b. Adhesion > cohesion	No charge:			Cohesional
	Nitrocellulose-SKN rubber (kaolin)		$3.0 \cdot 10^6$	(the rubber laminates)
	Perchlorvinyl-SKN rubber (kaolin)		$3.0 \cdot 10^6$	Ditto
	Polyurethan-SKN rubber (kaolin)		$3.0 \cdot 10^6$	
	BF-6-SKN rubber (kaolin)		$3.0 \cdot 10^6$	
	Perchlorvinyl-SKB rubber (carbon black), treated with H_2SO_4		$3.0 \cdot 10^6$	
Group II. Formation of the adhesive bond by diffusion of segments of the polymer chain	No charge:			
	Polyethylene-polyisobutylene		$1.19 \cdot 10^6$	Mixed
	Polyethylene-paraffin		$5.04 \cdot 10^5$	
	Gutta-percha-paraffin		$5.04 \cdot 10^5$	

• This velocity corresponds to the region in which electrical phenomena are usually observed in systems of Group I.

•• Kaolin and carbon black were used as fillers.

portions of the polymer film which have been detached from the grooves in the metal (Fig. 1).

Experiment shows that the systems investigated by us separate into two large groups (Table 2). The systems of the first of these groups are characterized by electrical phenomena accompanying rupture of the adhesive bond: luminescence in moderate vacuum, electron emission in high vacuum and the existence of residual charges on the separated surfaces. The charge sign was determined with the aid of a simple radiometer circuit, the following regularity being observed in each case: the surface which emits electrons on detachment has a negative residual charge; the surface which is opposed to it, and which does not show emission, carries a negative residual charge. Investigation of microscopic sections (Fig. 2, a and b) shows the presence of a clear cut boundary surface between two polymers of this group. In certain cases where the adhesion is particularly high, lamination occurs along the polymer film. In such a case there is neither electron emission nor a residual charge on the separated surfaces. The work of detachment is very high, the work of adhesion being obviously greater than the work of cohesion. Such systems are formed from components possessing strong polar groups (for example, BF-6 and acrylonitrile based rubber, perchlorvinyl and rubbers, the surfaces of which have been treated with concentrated H_2SO_4 and then washed).

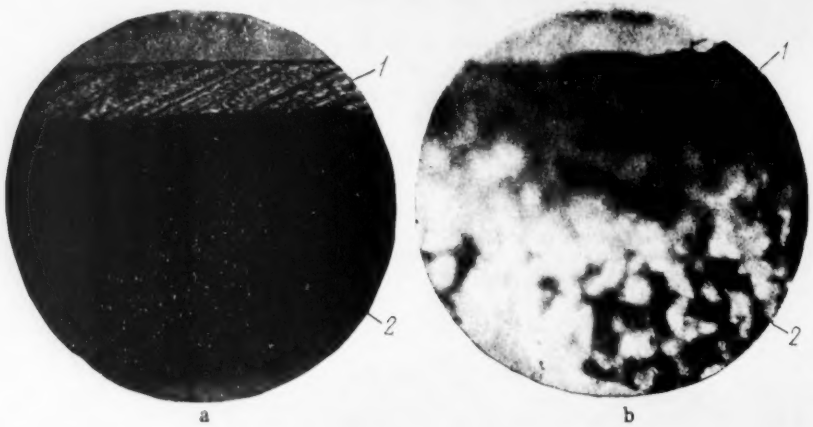

Fig. 2. Microphotographs of cross sectional cuts through the systems: a) perchlorvinyl (1) – SKN rubber (2); b) gutta-percha (1) – paraffin (2). 100 ×.

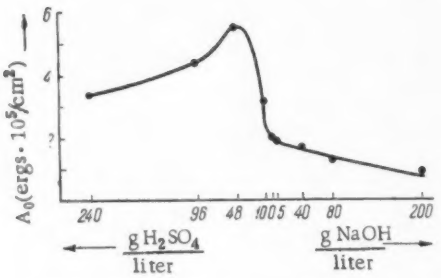

Fig. 4. The effect of treating a rubber (SKB) surface with acids and alkalis of various concentrations on the adhesion of perchlorvinyl.

Experiment shows that the character of the rubber filler plays a great role here. If one of the components is a SKB based rubber with a carbon black filler, electron emission is not observed on detaching a polymer film from it, although the separated surfaces carry residual charges of opposite sign. On detaching a polymer from a kaolin filled rubber of this same type, a very intense electron emission is observed (Fig. 3).

Fundamental differences are shown by systems of the second group (Fig. 2b) in which the components are nonpolar. On separating the components of these systems no electron emission is observed and the separated surfaces do not carry a charge.

Microscopic investigation of sections discloses diffuseness at the interfaces. It should be considered that

the adhesive bond in systems of the second group is formed by diffusion of the polymer chains in the contact zone.

A great role in the phenomena of adhesion is played by the reaction of the base, as is shown by our investigations of the adhesion of perchlorvinyl to the SKB rubber. It follows from Figure 4 that the maximum in the adhesion A_0 is shown with a rubber which has been treated with 1 N H_2SO_4.

On the separated surfaces residual charges are to be observed; negative on the polymer film and positive on the rubber.

The authors express their thanks to B. V. Deryagin, Corresponding Member of the Academy of Sciences of the USSR, for a number of valuable suggestions, to V. V. Karasev for valuable advice and continuing aid in the experimental part of the work and to V. R. Volpert for help in preparing the microsections.

Received December 17, 1956

LITERATURE CITED

[1] B. V. Deryagin and N. A. Krotova, Prog. Phys. Sci., 36, 387 (1948); B. V. Deryagin and N. A. Krotova, Adhesion (in Russian), Acad. Sci. USSR, Press, 1949; B. V. Deryagin, N. A. Krotova and Yu. M. Kirillova, Proc. Acad. Sci. USSR, 97, 475 (1954).

[2] D. Iosefowicz, H. Mark, Ind. Rub. World, 33, 106 (1942); S. S. Voyutsky and Yu. L. Margolina, Prog. Chem., 18, 449 (1947); B. V. Deryagin and N. A. Krotova, Adhesion (in Russian), Acad. Sci. USSR, Press, 1949, page 242; S. S. Voyutsky and V. M. Zamazy, Colloid J., 15, 407 (1953)*; S. S. Voyutsky and B. V. Shtarkh, Proc. Acad. Sci. USSR, 90, 573 (1953); S. S. Voyutsky, A. I. Shapovalova and A. P. Pisarenko, Proc. Acad. Sci. USSR, 105, 1000 (1955); B. V. Deryagin, S. K. Zherebkov and A. M. Medvedeva, Colloid. J.,* 18, 404 (1956).

[3] N. A. Krotova and Yu. M. Kirillova, Proc. 3-rd All-Union Conf. on Colloid. Chem.,** Acad. Sci. USSR, Press, 1956, page 329; N. A. Krotova, Gluing and Adhesion (in Russian), Acad. Sci. USSR, Press, 1956.

[4] V. V. Karasev, N. A. Krotova and B. V. Deryagin, Proc. Acad. Sci. USSR, 88, 777 (1953).

[5] V. V. Karasev and N. A. Krotova, Proc. Acad. Sci. USSR, 99, 715 (1954).

[6] S. S. Voyutsky, P. A. Rebinder, B. S. Khoroshaya and S. I. Shur, Proc. All-union Conf. on Colloid. Chem.,** Acad. Sci. USSR, Press, 1950, page 215.

* Original Russian pagination. See C.B. Translation.

** In Russian.

THE SUPEREQUIVALENT ADSORPTION OF CATIONS ON A NEGATIVELY CHARGED MERCURY SURFACE

Academician A. N. Frumkin, B. B. Damaskin and
N. V. Nikolaeva-Fedorovich

In the presentation of the theory of electrocapillarity it is usually assumed that among the inorganic ions only the anions possess specific adsorbability, the concentration of the inorganic cations in an electric double layer being completely determined by their charges [1]. There is, however, data in the literature which indicate the inadequacy of such an assumption. So, for example, through the work of Shtifman there was revealed a certain superequivalence in the adsorption of the cations of aluminum [2].

A direct indication of differences in the adsorbability of the cations of the alkali metals in 0.1 N solutions of their chlorides follows from the work of D. Grahame, who determined precise values of differential capacities in these solutions [3]. Actually, at potentials more negative than –0.7V (vs the 0.1 normal calomel electrode), there is an increase in the capacity in passing from lithium to cesium and, consequently, an increase of the surface charge. However, according to D. Grahame, this difference in surface charge, which is disclosed by comparing the differential capacities, is to be entirely attributed to a difference in the capacity of the Helmholtz portion of the double layers.• According to this interpretation of the experimental data of D. Grahame, to the large negative charges there should correspond the more negative values for the ψ_1-potential [5]. Such a conclusion agrees but poorly with the experimental data on the influence of the background cation radius on the rate of reduction of anions. It proves to be so that the rate of reduction of the anions $S_2O_8^{--}$ [6] and $S_4O_6^{--}$ [7] sharply increases in the sequence $Li^+ < Na^+ < K^+ < Rb^+ < Cs^+$, i. e., the observed rate dependence is the opposite of that which would be expected on the basis of the conclusions of D. Grahame. A more detailed elucidation of this matter has been given in the work of A. N. Frumkin and N. V. Nikolaeva-Fedorovich [5].

In order to avoid contradictions in the interpretation of the experimental data it is most simple to suppose a certain, although small, specific adsorbability of the cations of large radius. A study of the temperature coefficient of the reaction of anionic electroreduction leads to this same conclusion. Thus, in the case of the reduction of $S_2O_8^{--}$ against a 0.01 N NaCl background, the temperature coefficient of reaction has a small positive value, with a background of potassium anions at this same concentration the coefficient is practically equal to zero and with a background of cesium cations it has a negative value [5, 8].

In order to test the hypothesis of the existence of a specific cation adsorbability, measurements of differential capacities were carried out in 0.01 N solutions of the chlorides of the alkali metals. The impedance bridge circuit which was employed in these measurements did not essentially differ from that described in the papers of D. Grahame [9] and V. I. Melik-Gaikazyan [10]. The hanging mercury droplet served as the test electrode.

The data obtained are presented in Figure 1A in which there are sketched differential capacity curves as obtained in 0.01 N solutions of the chlorides of lithium, potassium and cesium. As is to be seen from this figure, differences in the differential capacities for cations of various radii are observed here, not only at high negative potentials, but also near the null charge point, where the capacity curves pass through a minimum. Actually, in

• In one of his works, D. Grahame pointed out that it was possible that his hypothesis was inadequate for the explanation of the experimental data on the adsorption of Cs^+ cations [4].

passing from lithium to cesium the difference in the values of the capacity near the null charge point amounts to 1 μf / cm².

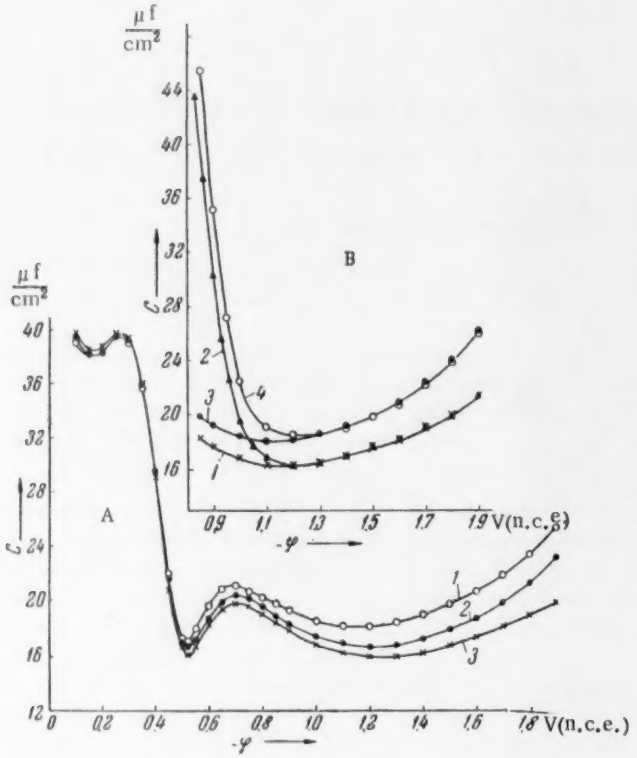

Fig. 1. Differential capacity curves. A) in 0.01 N solutions of CsCl (1), KCl (2) and LiCl (3); frequency, 400 cycles per second; 25°. B) in 0.1 N solutions of NaCl (1), NaI (2), CsCl (3) and CsI (4); frequency, 1000 cps; 25°.

The difference in the values of the electric double layer capacity in solutions of the chlorides of lithium and cesium is additional confirmation of the existence of a specific adsorbability for the cesium cation. It is, however, impossible to consider this conclusion as definitive since the experimental data obtained in solutions of the chlorides of the alkali metals are confused by the adsorption of Cl^-. We propose in the near future to carry out capacity measurements in solutions of the fluorides of sodium and cesium.

The most convincing data on the existence of a superequivalent adsorption for cations can be obtained through measurements of the differential capacity on negatively charged electrode surfaces in the presence of such anions as I^-, the surface layer adsorption of which has a considerable effect on the value of the differential capacity.

We have made measurements of differential capacities in 0.1 N solutions of NaCl, NaI, CsCl and CsI and also in solution of 1.1 N KCl, 1 N KI + 0.1 N KCl, 1 N KCl + 0.1 N $LaCl_3$ and 1 N KI + 0.1 N $LaCl_3$. The results obtained are presented in Figs. 1B and 2A. As is to be seen from the data shown, with sufficiently high negative polarization of the anion, the iodide ceases to exert an influence and the values of the differential capacity for the homologous chlorides and iodides are in agreement. For more negative potentials the magnitude of the capacity is determined only by the cations which are present in solutions. However, the potentials at which the difference between the capacity values for the homologous chlorides and iodides disappears, are not fixed and depend on the nature of the cation. Thus the action of iodine continues, in the case of solutions of NaCl and

NaI, to a potential $\varphi = -1.2$ V (vs the normal calomel electrode), and, in the case of solutions of CsCl and CsI, to a potential $\varphi = -1.3$ V (vs the normal calomel electrode), this pointing to a certain superequivalence in the adsorption of the Cs^+ cation which is lacking in the case of the Na^+ cation. A similar effect is also to be observed on the addition of 0.1 N $LaCl_3$ to 1 N solutions of KCl and KI. Thus the action of the I^- ion, which in

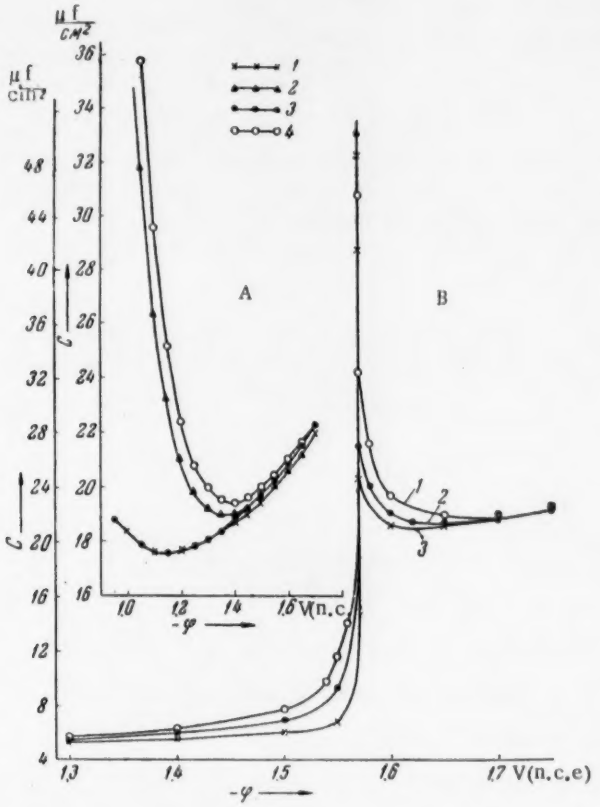

Fig. 2. Differential capacity curves. A) in solutions of 1.1 N KCl (1), 1 N KI + 0.1 N KCl (2), 1 N KCl + 0.1 N $LaCl_3$ (3), 1 N KI + 0.1 N $LaCl_3$ (4); frequency, 1000 cycles per second; 25°; B) in solutions of 10^{-3} N $[N(C_4H_9)_4]_2SO_4$ in the presence of 1 N KCl (1), 1 N KBr (2) and 1 N KI (3); frequency, 1000 cps; 25°.

solutions of 1.1 N KCl and 1 N KI + 0.1 N KCl continues to a potential $\varphi = -1.55$ V (vs the normal calomel electrode), is maintained in solutions of 1 N KCl + 0.1 N $LaCl_3$ and 1 N KI + 0.1 N $LaCl_3$ up to a potential $\varphi = -1.65$ V (vs the normal calomel electrode), thus indicating a definite superequivalence in the adsorption of the La^{+++} cation. The indicated phenomena could also be interpreted by supposing the presence of ion pairs in the electric double layer, for example, LaI^{++} and $LaCl^{++}$ in the case of lanthanum, the absorbability of the first of these complexes being greater than that of the second. As is seen from Figures 1B and 2A, the sharp rise in capacity, which is related to the penetration of anions into the electric double layer, is, in the presence of Cs^+ or La^{+++}, observed at more negative potentials than is the case with solutions containing Na^+ or K^+. In other words, even in this region of potentials, the adsorption of I^- is facilitated by the presence in the surface layer of the ions of Cs^+ or La^{+++} which, in all likelihood, are more easily adsorbed on a mercury surface which is overcharged by I^- ions than are the ions Na^+ and K^+.

From data on electrocapillary measurements L.M. Shtifman[2] also concluded that anions of iodine are adsorbed in the double layer in the presence of the cations Al^{+++}. Similar results have been obtained by us through the study of the interfacial tension of Hg in solutions 1 N KCl + 0.1 N $LaCl_3$ and 1 N KI + 0.1 N $LaCl_3$, although these data require further verification.

The fact that the superequivalent adsorption of cations can, even at negative potentials, lead to the entry of anions into the surface layer is expressed with particular clarity in the case of the adsorption of organic cations. This conclusion was reached earlier by one of us [11] on the basis of data obtained from electrocapillary measurements in solutions of $[N(C_3H_7)_4]Cl$, $[N(C_3H_7)_4]I$ and NH_4I. This phenomenon is also observed in measurements of the capacity of mercury electrodes in solutions which contain both surface active organic cations and inorganic anions. At sufficiently high negative potentials the cation $[N(C_4H_9)_4]^+$ desorbs from the mercury surface and a characteristic desorption peak is formed on the differential capacity curve [12].

In Fig. 2B there is presented data on the relationship between the differential capacity and the potential in 1 N solutions of KCl, KBr and KI in the presence of 10^{-3} N $[N(C_4H_9)_4]_2SO_4$. As is to be seen from this figure, the form of the desorption peak changes essentially on passing from Cl^- to I^-. The marked sharpening of the peak points to the fact that instead of a desorption over a narrow interval of potentials there is an abrupt destruction of the adsorption layer at a completely defined potential ($\varphi = -1.57$ V vs. the normal calomel electrode). The dependence of the desorption process on the nature of the anions definitely indicates an adsorption of anions in the surface layer when the mercury surface is negatively charged. The approach of the anions to the negatively charged surface is facilitated by those adsorbed cations which enter into the makeup of that face of the double layer which is turned toward the solution.

Received July 27, 1957

LITERATURE CITED

[1] D. Grahame, Chem. Rev., 41, 441 (1947).

[2] L. M. Shtifman, Proc. Acad. Sci. USSR, 63, 709 (1948).

[3] D. Grahame, J. Electrochem. Soc., 98, 343 (1951).

[4] D. Grahame, C. R. 3 Réunion Congr. Intern. Thermodyn. Cinét. Electrochim., Milano, 1952, p. 336.

[5] A. N. Frumkin and N. V. Nikolaeva-Fedorovich, Bull. Mos. State Univ., 1957.

[6] A. N. Frumkin, Progress in Chem., 24, 933 (1955).

[7] J. Zezula, Chem. Listy, 47, 492 (1953).

[8] S. I. Zhandov and V. I. Zykov, J. Phys. Chem., 31 (1957).

[9] D. Grahame, J. Am. Chem. Soc., 68, 301 (1946).

[10] V. I. Melik-Gaikazyan, J. Phys. Chem, 26, 560 (1952).

[11] A. N. Frumkin, Electrocapillary Phenomena and Electrode Potentials (in Russian), Odessa, 1919.

[12] N. V. Nikolaeva-Fedorovich and B. B. Damaskin, Proceed. Confer. on the Influence of Surface Active Substances on Electroprecipitation of Metals,* Vilnyus, 1957, page 33.

* In Russian.

STUDY OF THE MECHANISM OF THE ELECTROLYTIC FORMATION AND HYDROLYSIS OF PERSULFATE BY THE ISOTOPIC METHOD

Acad. Sci. USSR Corresponding Member A. I. Brodsky, I. F. Franchuk and V. A. Lunenok-Burmakina

The various mechanisms that have been proposed for the anodic formation of persulfates in the electrolysis of sulfates can be divided into two types. Persulfate, according to some widely held theories [1, 11], is formed by the direct recombination of the discharging sulfate (or bisulfate) ions, for example, $2SO_4^{--} \rightarrow S_2O_8^{--} + 2e$, or in two steps: $SO_4^{--} \rightarrow SO_4^{-} + e$; $2SO_4^{-} \rightarrow S_2O_8^{--}$. According to other theories [2, 3], the oxidation products of water (H_2O_2, OH, OH^-, surface oxides, etc.) are first formed at the anode or in the preanode layer of the electrolyte, which then oxidize the sulfate by the transfer of either electrons or oxygen atoms. In particular, the mechanism of Glasstone and Hickling [3], postulating the intermediate formation of hydrogen peroxide, has found wide acceptance:

$$2HO^- \rightarrow H_2O_2 + 2e; \quad 2SO_4^{--} + H_2O_2 \rightarrow S_2O_8^{--} + 2OH^-.$$

These authors extend this mechanism to anodic oxidation processes in general. Most of the other postulated mechanisms belong to one of the two types discussed, differing only in the details of the intermediate steps.

A. N. Frumkin and coworkers [4] found that when a solution of K_2SO_4 in H_2O^{18} is electrolyzed in either acid, neutral or weakly alkaline medium the oxygen of the obtained persulfate is devoid of excess heavy oxygen. This permits removing from discussion all of the mechanisms in which it is postulated that the oxygen of water participates in the formation of the persulfate.

We used the heavy oxygen isotope to elucidate the possible participation of hydrogen peroxide in the anodic formation of persulfate and to study the mechanism of its hydrolysis. From previous data [4, 5, 10] it is known that H_2O_2 and $K_2S_2O_8$ do not exchange oxygen with water.

For electrolysis we took solutions of 40 g of $KHSO_4$ in 200 ml of water, a current of 3 amps., platinum electrodes, and a temperature of 10-15°. To remove samples of anodic oxygen and for better stirring of the electrolyte the wire anode, having an area of 0.8 sq. cm., was inserted in a tube, open at the bottom, between two vertical cathode plates. The amount of O^{18} in the anodic oxygen was determined directly with an MS-2 mass-spectrometer, while that contained in the water was determined by a method developed in our laboratory [6], namely, as CO_2 after its exchange with the vapors of the investigated water. The sulfate was precipitated as $PbSO_4$, which was converted into CO_2 by ignition with hydrogen-deaerated carbon. The oxygen was liberated from the persulfate by heating. For its isotopic analysis the hydrogen peroxide was decomposed with $KMnO_4$ solution directly in the electrolyte after its degasification by evacuation, or if present in small amount, after extraction with ether. All of these methods were checked by running control experiments. The hydrogen peroxide was determined by titration with permanganate, while the persulfate was determined iodometrically in the presence of Cu^{++} as catalyst [7]. The formation of substantial amounts of Caro's acid during electrolysis was not observed. The results of the final experiments are given below.

1. In the experiments run without the use of isotopic indicators we added 10-20 g/liter of H_2O_2 to the electrolyte. Here the yield of persulfate dropped sharply when compared with the experiment run without the addition of H_2O_2 (Curve 1), and then it increased in measure with decrease in the residual amount of undecomposed

H_2O_2. In Fig. 1 Curves 2 show the increase in the $K_2S_2O_8$ concentration, while Curves 3 show the decrease in the H_2O_2 concentration in the electrolyte in two experiments a and b with an initial H_2O_2 content of 12 and 20 g/liter, respectively. In all three experiments the electrolysis was run until solid $K_2S_2O_8$ deposited. From these data it can be seen that both anodic processes – the decomposition of H_2O_2 and the formation of $K_2S_2O_8$ – apparently proceed independently of each other with a major predominance of the first if the H_2O_2 concentration is sufficiently great so that its presence interferes with the formation of the persulfate. This in itself places the theory of the intermediate formation of hydrogen peroxide in doubt. Qualitatively the same results and similar conclusions were obtained by Haissinsky [8] in the formation of percarbonate by the electrolysis of K_2CO_3 in the presence of H_2O_2. The independent nature of both anodic processes is supported by the following experiments on the electrolysis of a solution of $KHSO_4 + H_2O_2$ in H_2O^{18}, with isotopic analysis of the anodic oxygen (Table 1). At the start its O^{18} content was close to the amount present in the peroxide (natural: 0.20%), and

TABLE 1

Isotopic Composition of Anodic Oxygen in the Electrolysis of $KHSO_4 + H_2O_2$ in H_2O^{18} with 0.890% O^{18}

Time, min.	10	30	60	90	120
H_2O_2, g/liter	21.9	16.2	8.9	4.1	1.46
O^{18} in H_2O_2, %	0.309	0.353	0.495	0.679	0.851

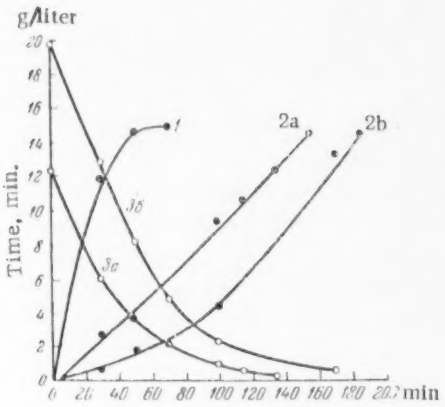

Fig. 1. The yield of persulfate as a function of the hydrogen peroxide concentration. 1) without H_2O_2 addition; 2a and 2b) with an initial H_2O_2 content of 12 and 20 g/liter, respectively; 3a and 3b) decrease in the H_2O_2 content in the electrolyte in the same experiments.

TABLE 2

Amount of O^{18} in H_2O_2 in the Electrolysis of $KHSO_4 + H_2O_2$ in H_2O^{18}

Expt. No.	Cat. Curr. density amp/cm²	Conc. H_2O_2, g/liter	O^{18} in H_2O_2, %	O^{18} in H_2O, %
I	0.05	0.26	0.459	0.831
		0.13	0.635	
II	0.10	0.78	0.209	0.745
		0.26	0.243	
		0.13	0.455	
III	0.17	0.42	0.229	1.100
		0.26	0.288	
		0.07	0.401	
IV	0.75	0.49	0.199	0.920
		0.26	0.204	
V	1.00	1.05	0.209	0.920
		0.42	0.213	
		0.16	0.213	

then it gradually approached the amount present in the water in accord with the curves shown in Fig. 1. From these data it can also be seen that the anodic oxidation of hydrogen peroxide proceeds without participation of the oxygen from water.

2. For conclusive direct proof of the nonparticipation of hydrogen peroxide in the anodic formation of persulfate we resorted to the method of isotopic dilution. In experiments, similar to those just described, we ran the isotopic analysis of the residual H_2O_2 in the electrolyte after its concentration had dropped below 1 g/liter. If H_2O_2 had been formed at the anode from the water, then it should have contained excess O^{18}, which should have found its way into the earlier added residual H_2O_2 and become mixed with it. With a cathodic current density of 0.05-0.17 amp./sq. cm. we actually did find a somewhat high O^{18} content in the residual H_2O_2, which became greater the lower the current density (Table 2). It was due to the cathodic formation of peroxide in

accord with the gross reaction $O_2 + 2H^+ + 2e \rightarrow H_2O_2$, which has no relation to the anodic process and, as is known, proceeds with a better yield the lower the cathodic current density. Actually, when we raised the current density to 0.75-1.0 amp./sq. cm., even the last H_2O_2 traces did not contain any excess O^{18}, since according to the mechanism of Glasstone and Hickling the amount of O^{18} in them should have approximated its content in the water.

TABLE 3

Hydrolysis of Persulfate in the Presence of $HClO_4$ at 70° (Amount of O^{18} expressed in percent)

Water	$K_2S_2O_8$	H_2O_2	$KHSO_4$
1.096	0.204	0.204	1.093
	0.204	0.207	1.088
0.204	0.733	0.736	0.313
	0.741	0.730	0.224

From all of these data it is clear that hydrogen peroxide cannot be an intermediate product in the formation of persulfate at the anode. Apparently, OH radicals also cannot be such (by the scheme $2SO_4^{--} + 2OH \rightarrow S_2O_8^{--} + 2OH^-$), since they quickly exchange oxygen with water [9] and easily recombine to form H_2O_2.

3. A mixture of 1.5-4 g of $K_2S_2O_8$ with either 1-3 g of 70% $HClO_4$ or 50% H_2SO_4 was hydrolyzed at 70° by passing water vapors through it at a pressure of 30 mm of Hg. The isotopic composition of the oxygen from the H_2O_2 in the distillate and from the bisulfate in the residue was determined in the same manner as indicated above. As can be seen from Table 3, in the experiments with $K_2S_2O_8 + H_2O^{18}$ and $K_2S_2O_8^{18} + H_2O$ (the heavy persulfate was obtained by the electrolysis of $KHSO_4^{18}$, which was prepared from $H_2SO_4 + H_2O^{18}$) the hydrogen peroxide had the composition of the water. Hydrolysis under the conditions of heating a $K_2S_2O_8$ solution with acid without distilling off the peroxide gave the same result. As a result, all of the peroxide oxygen originates from the oxygen of the persulfate without the oxygen of the water taking a part. These data are in accord with earlier studies on the decomposition of H_2O_2 and some other peroxides in water with a different isotopic oxygen content [11]. In all cases it was found that the peroxide bridge is not ruptured, and that the oxygen of the water is not introduced into the decomposition products of these peroxides (either other peroxide compounds or O_2). In part, this was found by Bunton and Llewellyn [10] to be true for the decomposition of Caro's acid.

A comparison of these data with the data obtained by us reveals that in the sequence of transformations $S_2O_8^{--} \rightarrow SO_5^{--} \rightarrow H_2O_2 \rightarrow O_2$ the peroxide group —O—O— passes through unchanged, failing to be cleaved from the persulfate in its final decomposition product, namely oxygen. Since under our experimental conditions the hydrolysis of persulfates proceeds with the intermediate formation of Caro's acid [12], then its simplest mechanism is as follows:

$$^-OS(O_2)OO\boxed{S(O_2)O^- + HO}H = {}^-OS(O_2)OO^- + H^+ + H\dot{O}S(O_2)O^-$$

$$H\boxed{\dot{O}H + {}^-OS(O_2)}OO^- + H^+ = H_2O_2 + H\dot{O}S(O_2)O^-.$$

In accord with this mechanism the bisulfate should contain $^3/_4$ oxygen from the persulfate and $^1/_4$ from the water. The oxygen from the decomposition of the persulfate had an isotopic composition that corresponded to this scheme, but in the bisulfate its composition was close to the composition of the water (Table 3), evidently due to a quite rapid exchange between the HSO_4^-, or the H_2SO_4 formed from it, and water. In order to eliminate this side exchange as much as possible we ran some experiments with the addition of $Pb(ClO_4)_2$, so that the formed sulfate immediately precipitated as $PbSO_4$. This greatly reduced the exchange, but did not eliminate it completely. In two experiments at 70° and an initial O^{18} content in the water of 1.17% the sulfate contained 0.412% (with a reaction time of 1 hour) and 0.492% (2 hours) of O^{18}, instead of the 0.44% or somewhat less required by the scheme, taking into consideration the initial dilution with light water, introduced with the $HClO_4$. On increasing the hydrolysis temperature to 100° the amount of O^{18} increased to 0.635%. These data show without doubt that a substantial amount of O^{18} is introduced into the formed bisulfate by way of secondary exchange. They are in agreement with the presented scheme, although they do not give conclusive quantitative support to it.

The L. V. Pisarzhevsky Institute
of Physical Chemistry
Academy of Sciences of the Ukrainian SSR

Received March 13, 1957

LITERATURE CITED

[1] K. Elbs, O. Schönherr, Zs. Elektrochem., 1, 417, 468 (1894); O. Essin, Zs. Elektrochem., 32, 267 (1926); W. D. Bancroft, Trans. Elektrochem. Soc., 71, 195 (1937).

[2] M. Le Blanc, Zs. phys. Chem., 8, 299 (1891); 12, 333 (1893); F. Foerster, Electrochemie nichtwasseriger Lösungen Leipzig, 1922; O. A. Esin and E. Alfimova, J. Phys. Chem. (USSR), 3, 439 (1932).

[3] S. Glasstone, A. Hickling, Electrolytic Oxydation and Reduction, London, 1935; Chem. Rev., 25, 407 (1939).

[4] A. N. Frumkin, R. I. Kaganovich, M. A. Gerovich and R. N. Vasilyev, Proc. Acad. Sci. USSR, 102, 981 (1955).

[5] E. R. S. Winter, H. V. A. Briscoe, J. Am. Chem. Soc., 75, 496, (1953); A. E. Cahill, H. Taube, J. Am. Chem. Soc., 74, 2312 (1952); P. Baertschi, Experientia, 7, 215 (1952).

[6] A. I. Brodsky, S. G. Demidenko, L. L. Strizhak and V. R. Lechekhleb, J. Anal. Chem. (USSR), 10, 256 (1955).•

[7] M. A. Bodin, Factory Labs., 11, 1248 (1938).

[8] M. Haissinsky. Trans. Farad. Soc., Discuss. No. 1, 254 (1947).

[9] O. R. Forscheimer, H. Taube, J. Am. Chem. Soc., 74, 3705 (1952); 76, 2099 (1954); I. A. Kazarnovsky, N. P. Lipikhin and M. V. Tikhomirov, J. Phys. Chem. (USSR), 30, 1429 (1956).

[10] C. A. Bunton, D. R. Llewellyn, Res., 5, 142 (1952).

[11] W. C. Schumb, Ch. N. Satterfield, R. L. Wentworth, Hydrogen Peroxide, N. Y., 1955.

[12] H. Palme. Zs. anorg. Chem., 112, 97 (1920).

[13] I. M. Kolthoff, I. K. Miller, J. Am. Chem. Soc., 73, 3055 (1951); L. S. Levitt, Canad. J. Chem., 31, 915 (1953).

• Original Russian pagination. See C.B. Translation.

ADSORPTION OF WATER ON QUARTZ, CRUSHED IN VACUUM

S. P. Zhdanov

(Presented by Academician M. M. Dubinin, March 21, 1957)

It is known that under ordinary conditions the surface of silica particles in the crystalline and amorphous states is hydrated and bears OH groups that are bound by valence forces to the surface silicon atoms. In view of this, when adsorption on SiO_2 is studied the matter of a variable hydration of the surface is a constant problem. More or less complete dehydration of the surface can be achieved only by ignition at elevated temperatures, of the order of 1100-1200°. However with such a treatment, together with removal of the residual hydroxyl groups, there can occur not only substantial modification of the surface layer structure (in the case of nonporous SiO_2 powders) but also a complete disappearance of the whole internally developed surface (in the case of silica gels and porous glasses).

A study of the adsorption of water on silica gel and porous glasses reveals that the magnitude of adsorption at low vapor pressures is very highly dependent on the degree of hydration shown by the surface. In the dehydrated state, obtained by the method of vacuum-ignition at 600-650°, the surface of amorphous silica proves to be quite inactive toward water vapors and adsorbs the latter very slightly at low P/P_S values [1]. It seemed of interest to obtain a SiO_2 surface, devoid of hydroxyls, without resorting to a thermal treatment at elevated temperatures, and to compare the adsorption properties of such a surface with the properties of a surface that had been dehydrated by ignition. Studies of such a nature could give some information bearing on the structure of a silica surface in different states.

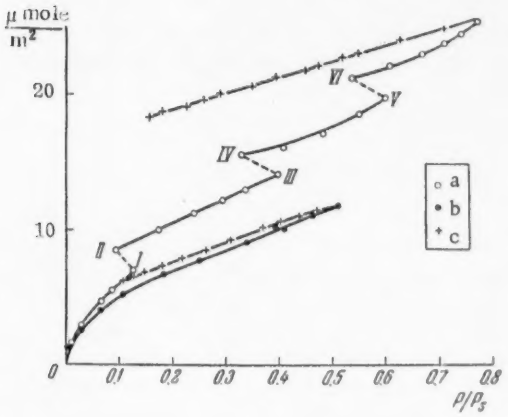

Fig. 1. Adsorption isotherms of water on an α-quartz surface, obtained by crushing in a vacuum. a) primary adsorption, b) repeated adsorption, c) desorption. I-II) 15 hrs., III-IV) 17 hrs., V-VI) 45 hrs.

One of the possible ways to obtain a silica surface free of hydroxyls, not requiring ignition, is the method of grinding in a vacuum. Under these conditions not only is hydration by atmospheric moisture excluded, but also the action of atmospheric gases on the freshly formed surface. In this paper we communicate the results obtained in studying the adsorption of water on low-temperature α-quartz powder, obtained by the method of crushing crystals of rock crystal in a vacuum, and we also compare the adsorption properties of variously prepared SiO_2 surfaces toward water vapors.

The crushing of the rock crystal was done with the aid of a solenoid in a jasper mortar, placed in a sealed glass cylinder, which was connected to a mercury diffusion pump through a trap cooled with liquid nitrogen, the latter serving to prevent the falling of any vacuum oil and mercury vapors on the freshly formed quartz surface. Evacuation was maintained during the whole crushing period, right up to

disconnecting the cylinder and mortar. After disconnecting from the pump the quartz powder was transferred (under vacuum conditions) from the mortar to a special ampul, which was unsoldered from the cylinder and soldered to the adsorption apparatus. With the aid of a small steel rod and solenoid the glass diaphragm was broken and the ampul contents came in contact with the measuring portion of the apparatus, which had been evacuated to a high vacuum.

The adsorption was measured by the volumetric method at 18°. The total surface of the powder was determined from the adsorption isotherm of argon at −195.6°, and from that of methyl alcohol at 18°. Close values were obtained in both cases: 16.0 sq. m. in the case of argon (ω_0 was taken equal to 15.5 A^2), and 15.5 sq. m. in the case of methanol (ω_0 = 23.7 A^2). The measurement of the Ar and CH_3OH adsorption was run after the water adsorption experiments.

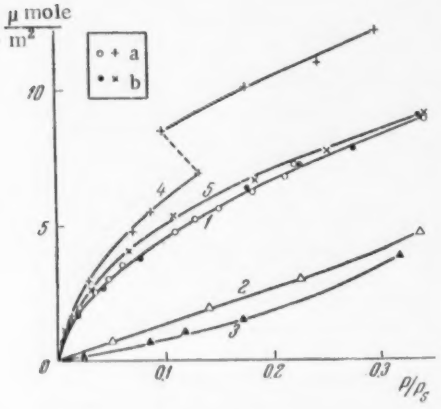

Fig. 2. Initial portions of the adsorption isotherms of water on an SiO_2 surface that had been obtained under various conditions. 1) α-quartz with a hydrated surface: a) primary adsorption, b) repeated adsorption; 2) silica gel that had been dehydrated by ignition in a vacuum at 650°; 3) porous glass, dehydrated in a vacuum at 600°; 4 and 5) α-quartz, crushed in a vacuum.

The isotherms of the primary and repeated adsorption and the desorption of water, obtained on α-quartz that had been crushed in a vacuum, are shown in Fig. 1. The isotherm of the primary adsorption is not entirely the usual shape and has characteristic steps, obtained in the prolonged exposure of the adsorbent to the water vapors at a given pressure•. The appearance of such steps is evidence that, in addition to purely physical adsorption with a quickly established equilibrium, a slow absorption process is present, evidently associated with chemical reaction between the water and the surface of the silica. This reaction should lead to hydration of the surface, i. e. it should be accompanied by the irreversible absorption of water, which finds confirmation in the position of the desorption branch of the isotherm, being situated considerably above the adsorption branch.

The repeated adsorption isotherm already has a more common appearance and is characterized by only slight hysteresis. However, the presence of the latter is evidence of continued chemical reaction between the water and the α-quartz surface. The hydration of the quartz is not complete, although the time that the adsorbent was exposed to the water vapors exceeded 17 days (the time elapsing between the start of the primary and the repeated adsorption experiment). At the same time the close proximity of this isotherm to the isotherm for the adsorption of water on α-quartz with a hydrated surface (see Fig. 2) indicates that prior to the start of the repeated adsorption experiment the surface, obtained by crushing in a vacuum, was for all practical purposes already nearly completely hydrated.

The initial portions of the isotherms for the adsorption of water on silica surfaces, obtained under various conditions, are compared in Fig. 2. Quartz with a maximum hydrated surface was obtained by the prolonged treatment of rock crystal powder with water at a temperature around 100°. The thermal dehydration of the SiO_2 surface was accomplished by ignition in a vacuum at 600-650°. The isotherms shown in Fig. 2 relate to the earlier studied specimens of porous glass and silica gel [1, 2]. Under such ignition conditions, as can be concluded from the water losses, there remains only about 15% of the amount of hydroxyl groups, found on the surface in the state of its maximum hydration, per unit of surface. In all cases the adsorption values are calculated on the basis of per unit of surface and the curves in Fig. 2 describe the properties of the adsorbents, depending only on the state and properties of their surface, but not on the magnitude of the specific surface.

Attention is attracted to the sharp differences in the surface properties of the SiO_2, obtained by ignition and by crushing in a vacuum. The hydroxyl-free SiO_2 surface, formed by crushing in a vacuum, proves to be

• The length of holding is indicated in Fig. 1.

much more active toward water vapors than does the surface dehydrated by ignition. These differences cannot be explained by the presence of residual hydroxyls on the surface dehydrated by ignition. Evidently, they are determined by other structural traits of the silica surfaces, obtained under the conditions of vacuum-crushing and by ignition. The state of the silica surface, dehydrated by ignition, was discussed in papers [1-4, 7].

It seems to us that the liberation of water during ignition at the expense of surface OH groups should, in the final analysis, lead to the formation of two types of electrostatically-and valence-saturated silicon oxide groups on the surface:

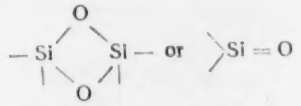

depending on whether a molecule of water is formed from the hydroxyls adjacent to two or only to one silicon atom. The formation of charges on the surface during thermal dehydration of a hydrated surface (silica gel, porous glasses), as is assumed in paper [3], is highly improbable [2, 4]. The liberation of water in this case apparently proceeds not by cleavage, but by redistribution of the bonds, assuring an electrical neutrality of the surface and a compensation of the valences, which is facilitated under heating.

When α-quartz is crushed in vacuum the state of the newly formed surface will depend on the direction of the cleavage plane relative to the boundaries and axes of the crystal. Since α-quartz is capable of cleavage [4, 5], then the splitting should be predominantly along the cleavage plane $(10\bar{1}1)$. Analysis of the α-quartz structure reveals that in this case one Si-O bond shows rupture for each pair connected by the apexes of the tetrahedrons, and charged groups of the type

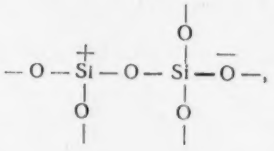

should be formed on the surface, in which the charges or places of Si-O bond rupture are localized, as is shown here and in Fig. 3*. Such an arrangement of the structure elements, bearing charges or free valences, is not favorable for saturation of the valences by the method of forming a second Si-O-Si bond, since for this is required not only a substantial deformation of the bonds, but also a reconstruction of the surface layer structure. It must be assumed that for rigid Si-O-Si bonds these processes are extremely difficult under room temperature conditions. Consequently, the charges and unsaturated valences, formed on a quartz surface when it is crushed in a vacuum, can remain uncompensated for a long period of time under vacuum conditions.

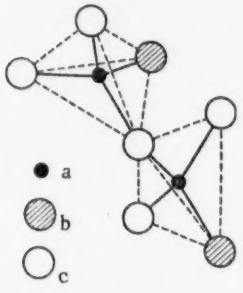

Fig. 3. Position of the places of rupture of Si-O-Si bonds on the surfaces of adjacent [$SiO_{2/2}$] tetrahedrons with cleavage along the plane of a rhombohedron $(10\bar{1}1)$; a) Si; b) apexes of the tetrahedrons, along which the Si-O-Si bonds rupture; c) apexes of the tetrahedrons, remaining connected.

Since the cleavage shown by quartz is extremely imperfect, then evidently other surfaces of cleavage, differing from the rhombohedral system of planes $(10\bar{1}1)$, are also possible. In all such cases silicon oxide groups can also be formed on the surface of cleavage, differing in their structure from those given above, for example $\gtrdot Si^{+}-O^{-}$ groups, later passing with compensation of the charges and valences into the more stable $\gtrdot Si = O$ groups [7].

* Evidently, the formation of like charges on adjacent silicon oxide groups is also possible.

The presence of charges and unsaturated valences on the surface of α-quartz, crushed in a vacuum, is one of the main structural traits of this surface, making it different from the surface structure of a silica that had been dehydrated by ignition. It is quite probable that the high activity shown by an α-quartz surface, formed by crushing in a vacuum, with respect to the adsorption of polar water molecules is specifically associated with this structural trait; it even exceeds that of a maximum hydrated hydrophilic quartz surface (Curve 1, Fig. 2). However, as can be seen from a comparison of isotherms 1 and 4 in Fig. 2, at low vapor pressures the activity per unit surface of α-quartz, crushed in a vacuum, is only slightly higher than the activity of a hydrated surface. This indicates that the amount of primary adsorption centers on a unit of surface is close in both cases. The faster increase in adsorption in the first case, with increase in the vapor pressure, even at the very beginning of the isotherm, is probably associated with the superimposition of chemical absorption, determined by hydration. The creation of charges on the freshly formed surfaces of mica when it was cleaved in a vacuum was observed by I. V. Obreimov [6].

In conclusion I consider it my pleasant duty to thank Acad. M. M. Dubinin and Prof. A. V. Kiselev for supporting this study and for the interest shown toward it.

Received March 20, 1957

LITERATURE CITED

[1] S. P. Zhdanov, Proc. Acad. Sci. USSR, 68, 99 (1949).

[2] Ibid., 100, 1115 (1955).

[3] W. A. Weyl, Res., 3, 230 (1950).

[4] W. Stöber, Koll. Zs., 145, 17 (1956).

[5] A. G. Betekhtin, Mineralogy, 1950.*

[6] I. V. Obreimov, Proc. Roy. Soc., A, 127, 805 (1930).

[7] S. P. Zhdanov and A. V. Kiselev, J. Phys. Chem. (USSR), 31, No. 10 (1957).

* In Russian.

FILM AND CAPILLARY-HELD WATER IN A POROUS MEDIUM

M. M. Kusakov and L. I. Mekenitskaya

(Presented by Academician A. V. Topchiev, February 13, 1957)

In papers [1-4] a study was made of the thickness of polymolecular layers of aqueous electrolyte solutions on the internal surface of a single capillary at various separation boundaries. To answer the question of the extent to which the conclusions relative to the properties of thin layers, obtained for single capillaries, can be considered valid when applied to a porous medium, and consequently can serve to characterize the state of the bound water in the gas-bearing and petroleum-bearing zones of a petroleum collector, these properties were studied on specimens of quartz sandstone from the Tuimazinsk deposits.

The water, remaining in a porous medium after displacing the water phase by nitrogen through a diaphragm of low permeability [5], served as a model for the bound water in the sandstone specimens (cores). The water phase was displaced at a pressure of $\underline{p}$ = 700 mm of mercury, which exceeded the capillary pressure in the very small pores of the core, and corresponded to that region in which the residual water-saturation capacity of the core was practically independent of the displacement pressure.

It was shown that the method of displacing water from cores through a diaphragm of low permeability can also be used to characterize the properties of thin layers of aqueous solutions in a porous medium.

If distilled water is taken as the residual water, then after displacement by nitrogen it is found in the cores not only in a capillary-held, but also in a film state, since distilled water on glass and on quartz at the boundary with a gas can exist in the form of thin layers showing equilibrium wetting [6, 7].

It could be expected that if the influence of the electrolyte concentration on the thickness of thin layers of water solutions in a porous medium bears the same character as in single capillaries (i.e. with increase in the concentration of the electrolytes the thickness of the thin layers decreases, and with a very high mineralization of the water it can even return to zero), then with increase in the electrolyte concentration the amount of liquid, displaced from the core through a low-permeability diaphragm, should increase.

The results of studying the influence of the concentration of NaCl on the residual water-saturation capacity (expressed in percent of the volume of the pores) shown by three cores of differing permeability are presented in Fig. 1. From the graph (Fig. 1) it can be seen that the amount of liquid remaining in the core decreases with increase in the concentration of NaCl.

In this connection, beginning with a certain concentration C' (different for cores with different permeability), the amount of liquid remaining in the core is practically without change with further increase in the amount of electrolyte (5N NaCl solution is nearly the limiting salt concentration, corresponding to the formation of a saturated solution at room temperature). A similar picture was also observed in the displacement of $AlCl_3$ solutions of variable concentration.

A reduction in the residual water-saturation capacity shown by cores, caused by the addition of an electrolyte and increase in its concentration, is evidently associated with the fact that for that portion of the residual water, which is found in a film state, the thickness of the thin layers decreases with increase in the electrolyte concentration. In this connection the amount of liquid displaced from the cores increases. At high electrolyte concentrations, due to the desolvating action shown by the ions [6, 7], the thin layers break [1, 2]. This circumstance permits understanding why, beginning with a certain concentration of the electrolyte, there is practically

no further change in the residual water-saturation capacity shown by the cores. Apparently, in this case nearly all of the liquid remaining in the core is found in a capillary-held state (in very fine, subcapillary pores, completely filled with water, in ring-shaped meniscuses, formed in the narrow points of contact of the grains, and in blind pores), and also in the form of individual droplets, remaining after rupture of the film.

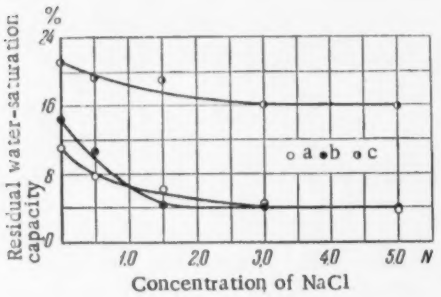

Fig. 1. The residual water-saturation capacity of cores as a function of electrolyte (NaCl) concentration: a) K = 860 mda., b) K = 430 mda., c) K = 39 mda.

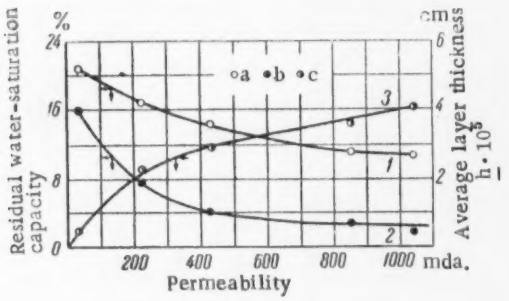

Fig. 2. The residual water-saturation capacity and the average film thickness as functions of the core permeability: a) 5N NaCl solution, b) distilled water, c) thickness of a thin layer of distilled water.

Consequently, it can be assumed that if the electrolyte concentration is less than C*, then the liquid is found both in the capillary-held and partially in the film states. A decrease in the residual water-saturation capacity of the cores with increase in the electrolyte concentration cannot be associated with the presence of clay particles in the cores or with a change in the contact angle of wetting.

The presence of clay particles in the cores could not produce these changes, since their amount is small (the sandstone contains 97% quartz and 3% of clay minerals), and in addition, this is evidenced by the experiments run on cores practically free of clay particles. A reduction in the residual water-saturation capacity of the cores could not have been caused by a change in the contact angle of wetting shown by electrolyte solutions, since on the basis of the experiments run in the Z. V. Volkova apparatus [8, 9] on the impregnation of cores with distilled water and with 5N NaCl solution it was established that in both cases the values of the kinetic contact angles of wetting practically coincide, reaching a value of 89°. The values of the contact angles of wetting, measured under static conditions (on paraffin), also proved to be practically the same for both liquids, being equal to 108-110°.

As a result, on the basis of the data obtained in studying the influence of the electrolyte concentration on the residual water-saturation capacity of cores (as a result of which the character of the influence of the amount of electrolyte in the solution on the thickness of thin layers was established, established earlier [1, 2] for single capillaries) the amount of liquid remaining in a porous medium in a capillary-held state was determined.

The curves, expressing the residual water-saturation capacity for distilled water and for 5N NaCl solution as a function of the core permeability, are depicted in Fig. 2. From Fig. 2 it can be seen that with a permeability of 800-1000 mda. and higher for a porous medium the amount of liquid remaining is independent of the permeability*. Curve 2 in Fig. 2 shows the amount of capillary-held liquid in a porous medium as a function of its permeability. From Table 1 it can be seen that the amount of capillary-held liquid in a porous medium is practically independent of the nature of the electrolyte.

Distilled water in the form of residual liquid in a porous medium consists of both film and capillary-held water. The average thickness $\bar{h}$ of films of distilled water in cores of variable permeability can be estimated by the difference between the total amount of residual liquid in the cores and the amount of capillary-held liquid, and also by the value of the specific surface of the cores.

* As was established in paper [10], the residual water-saturation capacity as a function of the core permeability is different for different deposits.

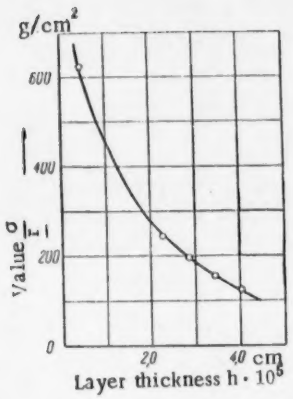

Fig. 3. The average thickness of a film of distilled water in a porous medium as a function of the value σ/r.

TABLE 1

The Amount of Capillary-Held Liquid in a Porous Medium as a Function of the Electrolyte Nature

Core No.	Permeability K, mda.	Residual water-saturation capacity S,%			
		5N NaCl solution	4N KCl solution	5N $CaCl_2$ solution	5N $AlCl_3$ solution
13	39	15.7	15.0	15.0	13.3
27	430	4.0	3.8	4.0	3.9
29	850	3.2	3.3	3.0	4.0

• A 4N solution is the limiting KCl concentration, above which a saturated solution is formed.

The P. Carman method [11] was used to calculate the values of the specific surface from the permeability and porosity of the cores. From literature data it is known that the values of the specific surface, calculated by this method, are below the actual values [12-14]. Proceeding from these considerations it must be assumed that the results of calculating the film thicknesses in a porous medium should be somewhat lower, and then they will agree with the results, obtained earlier for equilibrium layers on simple geometric systems [6, 7]. A plot of the function $h = f(k)$ is also depicted in Fig. 2.

From Fig. 3, where the average thickness of a film of water (distilled) in a porous medium is shown as a function of the value σ/r•, proportional to the cleaving pressure of a thin cylindrical layer, it can be seen that in a porous medium, the same as had been shown on a flat solid surface [6, 7] and in capillary systems [1-4], the average layer thickness, with other conditions constant, is determined by the cleaving pressure of the layer.

The influence of the valence of the electrolyte cations on the thickness of thin layers of water solutions in a porous medium was also checked on the basis of the value of the residual water-saturation capacity of the cores.

When a comparison was made of the residual saturation capacity of similar cores for the same concentrations of water solutions of salts with univalent and with trivalent cations (NaCl and $AlCl_3$) it was established that at comparatively low solution concentrations, with equal values for both, the residual saturation capacity of the cores is less for $AlCl_3$ solutions than for NaCl solutions. Evidently, this result is associated with the fact that for that portion of the residual liquid which at comparatively low electrolyte concentrations is found in the state of a film, the thickness of the thin layers of the $AlCl_3$ solutions is less than for the NaCl solutions. A difference in the residual degree of saturation of $AlCl_3$ and NaCl solutions was practically not observed at high concentrations of these salts, which can be explained by the above mentioned complete destruction of the thin wetting layers at high electrolyte concentrations.

The above discussed experimental results show that the properties of thin layers, studied in single capillaries at the separation boundary: air|aqueous electrolyte solution| glass or quartz, are also completely retained in porous media. Consequently, the earlier made conclusion [1, 4] that the state of the bound water, in particular that found in gas-bearing collectors, representing solutions of electrolytes, is determined by the physicochemical properties of the liquid, remains valid.

The I. M. Gubkin Moscow
Petroleum Institute

Received February 11, 1957

• As the value of the radius r of the pores we took the average radius, calculated from the ration $r = 8K/m$, where m is the porosity of the cores.

LITERATURE CITED

[1] M. M. Kusakov and L. I. Mekenitskaya, Report at the 4th World Petroleum Congress in Rome, Acad. Sci. USSR Press, 1955; Proc. 4th World Petr. Congr., Rome, Sec. II, p. 593 (1955); 4th World Petr. Congr., Moscow, 3, p. 261 (1956).*

[2] M. M. Kusakov and L. I. Mekenitskaya, Proc. Acad. Sci. USSR, 107, No. 4 (1956).

[3] M. M. Kusakov and L. I. Mekenitskaya, Proc. Acad. Sci. USSR, 107, No.5 (1956).

[4] M. M. Kusakov and L. I. Mekenitskaya, Trans. Moscow Petroleum Inst., No. 16, 39 (1956).

[5] O. F. Thornton, D. L. Marshall, Trans. AIME, Petr. Dev. Techn., 172, 69 (1947).

[6] B. V. Deryagin and M. M. Kusakov, Bull. Acad. Sci. USSR, Div. Math. and Natural Sciences, 5, 741 (1936).

[7] B. V. Deryagin and M. M. Kusakov, Bull. Acad. Sci. USSR, Div.Math. and Natural Sciences, 5, 1119 (1937); Acta Physicochim. URSS, 10, 25 (1939); 10, 153 (1939).

[8] Z. V. Volkova, Mineral Raw Materials, 7, 34 (1934).

[9] Z. V. Volkova, Koll. Zs. 67, 280 (1934).

[10] J. C. Calhoun, Oil and Gas J., 47, No.3, 241 (1948).

[11] P. C. Carman, J. Soc. Chem. Ind., 57, No.5, 225 (1938).

[12] B. V. Deryagin, N. N. Zakhavaeva and M. V. Talalaev, Proc. Acad. Sci. USSR, 61, 653 (1948).

[13] G. I. Logginov and O. M. Khusynova, Informal Commun. Sci.-Res. Inst. Cement, 27, 29 (1956).

[14] G. I. Logginov and O. M. Khusiinova, Trans. Inst. Phys. Chem., Acad. Sci. USSR, Monograph "New Study Methods" (1957).*

* In Russian.

THE INFLUENCE OF ADSORPTION LAYERS ON THE DISPERSION OF GRAPHITE

L. A. Feigin and V. N. Rozhansky

(Presented by Academician P. A. Rebinder, March 14, 1957)

The questions of the physicochemical influence of the medium on the processes for the dispersion of graphite have been studied quite inadequately, which is first of all associated with the difficulties of making a dispersion analysis in the region of colloidal particle dimensions. In our work we used the method of low-temperature nitrogen adsorption [1], our earlier developed x-ray method [2] and investigation with an electron microscope to measure the specific surface.

The vibration grinding of graphite [2, 3] permits obtaining very highly dispersed colloidal graphite preparations with an average size of 100 A and less for the primary particles; the specific surface in these cases reaches a value of 600 sq. m./ g. In this connection the very fine grinding of dry graphite proceeds at a rate that is 10-20 times more intense than the grinding in a water medium.

It is important to mention that in the vibration grinding of a number of solids (quartz, cement, etc.) it is impossible to exceed the value of the specific surface by a matter of several tenths of a sq. m./ g. Consequently, it is natural to associate such a high dispersion degree of ground graphite powders with the (scale) lamellar structure of the graphite lattice. Substantial distances between the layers of carbon atoms (3.37 A) when compared with the corresponding distance in the plane of the base (1.41 A) determine the small energy of the layer bonds, which explains the perfect cleavage shown by graphite, the sharp anisotropy of the bond forces, and the ease of dispersion along the planes of the base. This is supported by x-ray and electron microscope studies, which show that the graphite particles are scales, the size of which in the plane of the base is considerably greater than their height. The semitransparent (for electronic radiation) graphite particles are clearly visible in Fig. 1.

To elucidate the mechanism for the dispersion of graphite we ran some experiments in which small amounts of water, and also some other substances, were added during grinding. The experiments were run mainly in a laboratory mill•, which permitted running simultaneous grinding under completely identical conditions in 4 chambers-drums with a capacity of 100 cc. each. The drums were thoroughly sealed. It was shown [4] that a very slight average pressure is created in a vibration mill, so that the process of dispersion proceeds mainly as the result of surface abrasion of the particles during their relative movements, and consequently the force of the friction between particles determines to a large degree the degree of grinding.

The curves for the growth of the specific surface of graphite as a function of the time of grinding in the presence of various amounts of water are shown in Fig. 2. From these data it can be seen that the dispersion of dry graphite proceeds with the greater intensity; the specific surface increases at a constant rate of 30 sq. m./ / g. min, right up to a value of 300 sq. m./ g. (The indicated rate was determined by the choice of the vibration mill parameters, and variation of these parameters within quite wide limits is essentially without influence on the established rules; in this connection the dispersion intensity shows a ten-fold variation). On the other hand, when water of the order of 3% with respect to the graphite is added, the growth of the specific surface with time also shows a linear progress, but at a rate that is $\sim$10 times slower, i. e. about 2 sq. m./ g · min. With

• The mill was designed by M. I. Aronova and L. M. Morgulis.

smaller additions of water it is possible to distinguish two portions, differing sharply in the formation rate of new surface graphite particles.

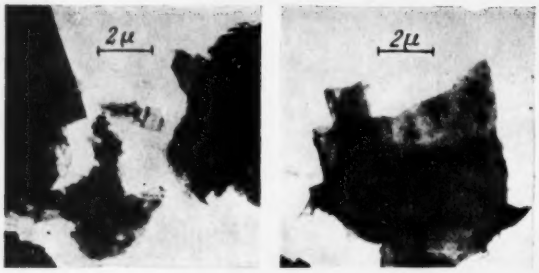

Fig. 1. Thin semitransparent scales of graphite, ground in a water medium. Electron microphotographs.

Knowing the true value of the specific surface permitted us to calculate the number of saturated monolayers of water, formed on the surface of the graphite particles, and also to estimate the reduction in the number of these layers during the process of dispersing the powder with a definite amount of water. (In view of the hydrophobic nature of graphite to speak of layers possesses sense only when their number does not exceed 3-4; however, as will be made clear later, it is specifically this case that is of greatest interest to us.) In this connection it was revealed that a change in the growth rate of the graphite surface occurs when the amount of water corresponds to the formation of a saturated adsorption monolayer. This circumstance must be regarded as being due to the sharp increase in the friction coefficient of the pure freshly formed surfaces of the graphite particles when

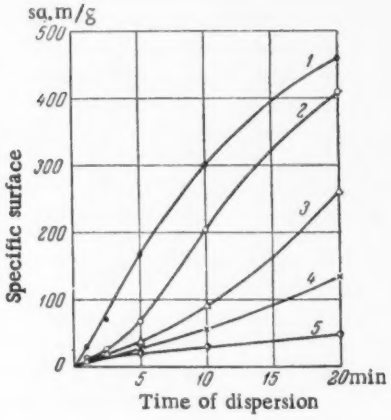

Fig.2. Kinetics for the dispersion of graphite in the presence of small amounts of added water. 1) dry dispersion, 2) 0.35% water, 3) 0.7% water, 4) 1% water, 5) 3% water.

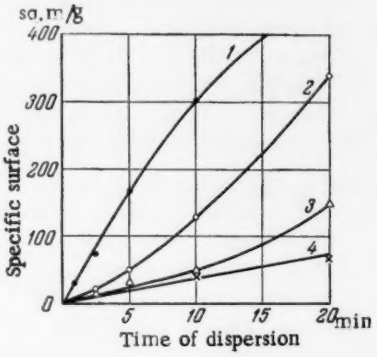

Fig. 3. Kinetics for the dispersion of graphite in the presence of added butyl alcohol. 1) dry dispersion, 2) 0.8% alcohol, 3) 2.4% butyl alcohol, 4) 8% butyl alcohol.

compared with the friction shown by graphite surfaces covered with adsorption moisture. In the light of this the kinetics for the dispersion of graphite in the presence of small amounts of water can be explained as follows. At the start of the dispersion process the surface of the graphite particles is small, so that even extremely small additions of water assure a sufficient number of layers of adsorption moisture (in this connection the water molecules are adsorbed from saturated steam), and the rate of grinding corresponds to the "wet" dispersion regime.

Then, in measure with increase in the surface area, the number of water layers decreases, and after the existing amount of water becomes less than that required to form a saturated monolayer, the rate of grinding approaches that for the case of "dry" grinding.

From our experiments it is quite obvious that small amounts of moisture or other substances, always present in the surface layer of the original graphite sample, can influence the dispersion process only in the very initial stages, since in the vibration grinding of graphite the specific surface of the latter increases hundreds (and even thousands) of times, and the impurities, contained in the graphite, will possess an insignificant surface density during the grinding process. In particular, we verified this circumstance by subjecting the graphite sample to variable drying prior to grinding. Drying the graphite at 100°, heating the drum with graphite to 200° directly before the experiments, and drying the graphite at 300° in a stream of nitrogen, all failed to show a noticeable difference in the shape of the grinding curves, whereas the introduction of 1% water reduced the dispersion rate several times.

TABLE 1

Influence of Small Additions of Water on Acceleration of the Process for the Dispersion of Mica (Specific Surface in sq. m./g)

Amount of water, %	Time of grinding, min.			
	1	2	4	6
0.0	7.0	14.5	21.0	23
2.5	9.3	14	22	—
5.0	11.2	16	30	34

The data on the kinetics of grinding graphite in the presence of small amounts of added butyl alcohol are shown in Fig. 3, which data reveal the same shape for the curves as in the case of water. Calculation reveals that the formation of a butyl alcohol monolayer is also sufficient for a sharp reduction in the coefficient of friction. The experiments with the introduction of benzene vapors qualitatively confirm the same picture. Our results showed an identity of the influence exerted by water additions on the grinding of both natural graphite and of synthetic graphite, obtained from anthracite at elevated temperature.

The obtained results agree with the data of Bowden and coworkers [5], establishing a smooth growth of the coefficient of friction for the graphite-graphite system with elevation of the graphite degasification temperature (in a high vacuum) to 1000°, and also with the data, obtained in studying the increased wear shown by carbon and graphite brushes of electrical machines under conditions of a highly reduced moisture content of the atmosphere [6, 7].

For comparison we ran similar experiments on the dispersion of mica (hydrophilic material), the crystal lattice of which also possesses a lamellar structure. In this case we found, on the contrary, an increase in the rate of grinding in the presence of added water (Table 1), which is in accord with the general phenomenon of an adsorption reduction in the strength of solids, discovered by P. A. Rebinder [8, 9]. A change in the picture in the transition from graphite to mica is analogous to the inversion effect — a transition from a lubricating action to wear with increase in the pressure during rubbing in a surface-active medium.

Very recently Eichborn [11], in studying the grinding of cement, quartz and marble, revealed that the dispersion process is facilitated in the vapors of adsorption-active substances. A similar phenomenon was also observed by I. L. Ettinger and M. M. Protodyakonov [12]. As a result, the results obtained by us testify to a well defined specificity of graphite dispersion, and to an adsorption lubricating action by monomolecular layers.

In conclusion the authors wish to sincerely thank P. A. Rebinder, A. A. Zhukhovitsky, V. I. Likhtman and D. S. Sominsky for their discussion of the results and valuable advice.

The All-Union Institute of New Problems
on the Production of Construction Materials
and the Chair of Colloidal Chemistry of the
Moscow State University

Received March 2, 1957

LITERATURE CITED

[1] S. Brunauer, Adsorption of Gases and Vapors, Moscow, 1948.•

[2] L. A. Feigin and V. N. Rozhansky, Proc. Acad. Sci. USSR, 113, No. 5, 1102 (1957).••

• In Russian.

•• Original Russian pagination. See C. B. Translation.

[3] L. A. Feigin, Chemical Science and Industry, 1, p. 210 (1956).•

[4] P. D. Lesin, Scientific Communication of VNIITISM, No. 25, (1957).

[5] F. P. Bowden, J. E. Young, G. Rove, Proc. Roy. Soc., A, 212, 485 (1952).

[6] D. Ramadanoff, S. W. Glass, Electr. Eng., 11, 825 (1944).

[7] R. H. Savage, J. Appl. Phys., 19, 1 (1948).

[8] P. A. Rebinder, Papers at the 6th Convention of Russian Physicists, Moscow, 1928. •

[9] P. A. Rebinder, Jubilee Collection, Dedicated to the 30th Anniversary of the Great October Socialistic Revolution, Vol. I, p. 533 (1947). Acad. Sci. USSR Press. •

[10] P. A. Rebinder and N. N. Petrova, Monograph Friction and Wear in Machines, Vol. I, (1940). Acad. Sci. USSR Press. •

[11] J. L. Eichborn, Koll. Zs., 149, 128 (1956).

[12] I. L. Ettinger and M. M. Protodyakonov, Proc. Acad. Sci. USSR, 84, 1235 (1952).

• In Russian.

THE ANODIC SOLUTION OF THORIUM IN SALT MELTS

L. D. Yushina and M. V. Smirnov

(Presented by Academician A. N. Frumkin, March 13, 1957)

Papers devoted to a study of the processes for the anodic solution of metals in salt melts, which are of interest relative to the theory and practice of the electrolysis of fused salts, are absent in the literature. The main results obtained in studying the process for the anodic solution of thorium metal in a melt composed of the alkali metal chlorides are presented in this communication.

The experiments were run in a cell, the design of which is schematically depicted in Fig. 1. The cell was a wide quartz test tube with an airtight closure on top. A molten equimolar mixture of sodium and potassium chlorides served as the electrolyte. It was prepared by melting the pure salts in a dry hydrogen chloride atmosphere, which was blown through the melt for some time. In order to remove dissolved gases the salt melt, prior to experiment, was kept under a reduced pressure of about 0.1 mm of Hg, and all of the measurements were run in an atmosphere of pure argon. The thorium anode, having a geometric surface of about 1 sq. cm., was fastened to a molybdenum lead. A molybdenum wire served as the cathode, and it was inserted inside a quartz test tube so as to prevent penetration of the alkali metal at the anode. The bottom of the test tube had a small opening. The cell was contained in a massive metal block, heated in an electric resistance furnace with automatic control of the temperature, which was maintained constant with an accuracy of ± 1°.

The experiments reduced to measurement of the thorium anode in a wide range of current densities (calculated on the geometric surface of the electrode), ranging from $2 \cdot 10^{-3}$ to 8 amp./sq. cm., at 710 and 815°. The anode was polarized in a matter of 3-4 seconds at a given strength. As preliminary experiments revealed, this time was sufficient to establish a stationary potential. A train oscillograph was used to measure the values of the potential of the thorium anode, with the chlorine electrode as the reference standard, at the moment of breaking the electrolysis by a special time relay, which connected the oscillograph to the cell at the same time that the polarizing current was disconnected. The reference chlorine electrode represented a tube made of spectrally pure carbon, through which chlorine, obtained by the electrolysis of molten lead chloride [1], was passed continuously. To prevent the chlorine from coming in contact with the thorium anode the chlorine electrode was placed in a quartz test tube with a small opening on the bottom, which was covered with an asbestos diaphragm.

Measurement of the polarization was begun after the thorium electrode in the starting molten equimolar mixture of sodium and potassium chlorides had assumed a constant potential, equal to –2.558 v at 710° and –2.524 v at 815°. The results of the measurements at the indicated temperatures are plotted in Fig. 2, using the semilogarithmic coordinates (log i vs. φ).

As can be seen, at $D_a < 0.05$ amp./sq. cm. the potential of the thorium anode changes but slightly with change in the current density, and in value is close to the potential of the thorium electrode in a melt of alkali metal chlorides in the absence of polarization. Above 0.05 amp./sq. cm. the potential of the anode shows linear increase with the logarithm of the current density: $\varphi = a + b \log i$. The slope of the polarization curves (coefficient b before the logarithm of the current density), equal to 0.095 at 710° and 0.105 at 815°, within the limits of possible measurement error is close to 2.3 RT/2F. Such a shape for the polarization curves is observed up to approximately 1 amp./sq. cm. At higher current densities they deviate toward more positive potentials. When the current density exceeds 4 amp./sq. cm. at 710° and 6 amp./sq. cm. at 815°, the potential of the

thorium anode remains practically constant with further increase in the strength of the electrolysis current. In value it approaches the value of the equilibrium potential of thorium in melts with a high concentration of $ThCl_2$.

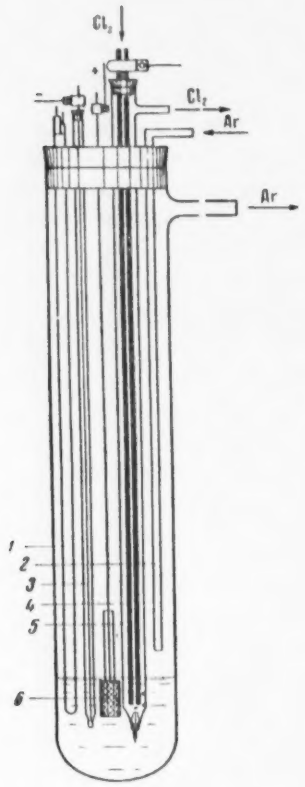

Fig. 1. Cell. 1) thermocouple; 2) tube for the introduction of argon; 3) cathode; 4) reference chlorine cell; 5) quartz test tube; 6) thorium anode.

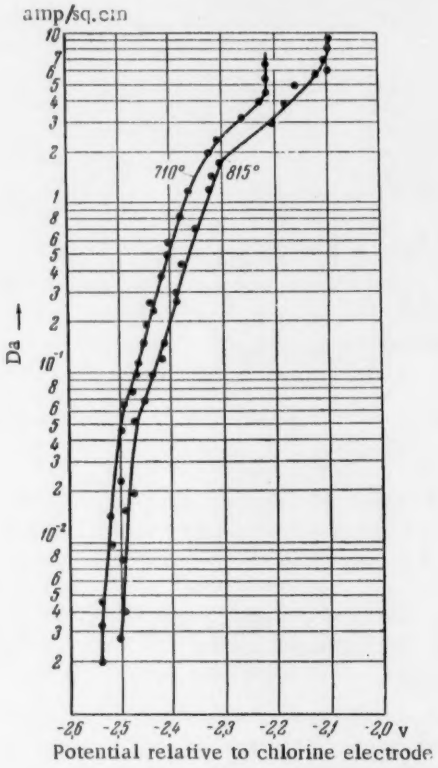

Fig. 2. Polarization of a thorium anode in a melt of an equimolar mixture of potassium chlorides at 710 and 815°.

The same as in the case of cathodic polarization [2], it can be assumed that the thorium anode is found in equilibrium with the adjacent layer of the salt melt. In a melt of alkali metal chlorides, not containing thorium ions, the potential of the thorium electrode becomes established when equilibrium is reached between the surface layers of the metal and the electrolyte:

$$x\,Th\,(т) + 2\,Na^+\,(melt) \rightleftarrows Na_2Th_{x-1}\,(т) + Th^2\,(melt),$$
$$Th\,(т) + 4\,Na^+\,(melt) \rightleftarrows 2\,Na_2^+\,(melt) + Th^{2+}\,(melt),$$
$$2\,Th^{2+}\,(melt) \rightleftarrows Th\,(т) + Th^{4+}\,(melt).$$

The contacting surface layers of the electrode and electrolyte are not found in equilibrium with the interior layers of the corresponding phases. Consequently, the formed Th^{2+} and Na_2^+ ions diffuse into the depth of the salt melt, while the liberated alkali metal diffuses into the interior of the electrode, where their concentrations are practically equal to zero. In the absence of electrolysis the diffusion current of the thorium ions is compensated by the current of the discharge and overcharge of the alkali metal ions.

Replacement of the discharge and overcharge of the alkali metal ions by the direct ionization of metallic thorium is essentially what happens when the electrolysis is run at anodic current densities below the values of this diffusion current for Th^{2+} ions. In this connection the potential of the thorium anode changes within the limits of the difference in the potentials between the alloy Na_2Th_{x-1} and Th (approximately by 0.058 v at 710° and by 0.049 v at 815°).

The diffusion of thorium ions begins to exert an influence on the polarization of the anode at higher current densities (D_a > 0.05 amp./sq. cm.), when the reaction for the displacement and reduction of the alkali metal ions by metallic thorium is suppressed. In our previous studies it was shown that in the equilibrium with metallic thorium there may be found melts, which contain Th^{2+} ions in overwhelming amount. If in this connection it is also considered that in chloride melts Th^{4+} ions form with anions less mobile complex groupings than do Th^{2+} ions, then it can be assumed that the thorium that passes into the electrolyte shows diffusion into the interior of the melt essentially as bivalent ions. In particular, this is supported by the formation in the electrolyte of a fine suspension of metallic thorium, observed in the electrolysis run with a thorium anode in a closed electrolyzer, excluding the admittance of atmospheric oxygen. Evidently, the suspension of the metal is formed as the result of the partially progressing disproportionation reaction (proceeding up to the attainment of an equilibrium concentration of Th^{4+} ions):

$$2Th^{2+}(\text{melt}) \rightleftarrows Th^{4+}(\text{melt}) + Th\,(\text{т}).$$

As a result, the anodic current density can be expressed by the equation

$$i = \frac{2F}{\delta} D_{Th^{2+}} [Th^{2+}]_S,$$

where δ is the thickness of the diffusion layer, $D_{Th^{2+}}$ is the diffusion coefficient of the Th^{2+} ions in the salt melt and $[Th^{2+}]$ is the stationary mole-fraction concentration of these ions in the electrolyte layer adjacent to the electrode, determining the value of the anodic potential:

$$\varphi = E^{\circ}_{Th/Th^{2+}} + \frac{RT}{2F} \ln f_{Th^{2+}} [Th^{2+}]_S,$$

where $f_{Th^{2+}}$ is the activity coefficient of the Th^{2+} in the melt. As our studies revealed, the activity coefficient of thorium dichloride, and consequently of Th^{2+} ions in molten mixtures with alkali metal chlorides, changes but slightly with the concentration right up to the pure salt. Therefore, without great error it can be assumed

$$\varphi = E^{\circ}_{Th/Th^{2+}} + \frac{RT}{2F} \ln [Th^{2+}]_S.$$

Substituting here the expression $[Th^{2+}]S$ through the diffusion current i, we obtain

$$\varphi = \text{const} + \frac{2{,}3\,RT}{2F} \log i,$$

where

$$\text{const} = E^{0}_{Th_s/Th^{2+}} + \frac{2{,}3\,RT}{2F} \log \frac{\delta}{2F D_{Th^{2+}}}.$$

With elevation of the temperature the polarization curves are shifted toward more positive values of the potential, since the value $E^0 Th / Th^{2+}$, entering into the constant, has a large positive temperature coefficient ($\sim 1.0 \cdot 10^{-3}$ v./deg.).

Above 1 amp./sq. cm. at 710° and above 1.5 amp./sq. cm. at 815° the anodic potential, having respectively reached a value of −2.375 v and −2.130 v, begins to rise with the current density at a considerably faster rate than would be expected from the equation derived by us, if it is assumed that the thickness of the diffusion layer remains unchanged with increase in the concentration of thorium ions in the electrolyte layer adjacent to the anode. Actually, as experiment reveals, such an assumption is justified only at relatively low concentrations, the upper limit of which can be estimated from the experimental data.

Earlier we had found the equilibrium potential of a thorium electrode with a molybdenum lead (including the thermal electromotive force between the molybdenum and the carbon), relative to the chlorine electrode, as a function of the temperature and mole-fraction concentration of Th^{2+} ions in a molten equimolar mixture of sodium and potassium chlorides. It is expressed by the equation:

$$E = -3.199 + 10.60 \cdot 10^{-4} T + 0.992 \cdot 10^{-4} T_{\log} [Th^{2+}].$$

With this equation it is possible to calculate the limiting mole-fraction concentration of thorium ions in the electrolyte layer adjacent to the anode, in which connection a linear dependence of the potential on the logarithm of the current density is still observed. It is obtained equal to $5.81 \cdot 10^{-3}$ at 710° and $3.59 \cdot 10^{-3}$ at 815°.

Apparently, in the region of higher concentrations the thickness of the diffusion layer ceases to be a constant value and begins to increase rapidly with the current density, and this in turn leads to a reduction in the diffusion rate, i. e. to an increase in the concentration of thorium ions in the electrolyte layer adjacent to the electrode and a corresponding increase in the anodic potential.

When the concentration of thorium chloride in the layer of the melt adjacent to the anode approaches 100% the potential of the anode reaches values that are very close to the equilibrium potential of thorium in its chloride melt, respectively equal to −2.204 v at 710° and −2.089 v at 815°.

As a result, in the electrolysis of mixed chloride melts with a metallic thorium anode it is practically only Th^{2+} ions that migrate into the electrolyte, even at relatively high current densities (of the order of 10 amp./sq. cm.). In this connection concentration polarization is observed. We have a different picture in the case of the electrolysis of molten thorium tetrachloride, which shows an essentially anionic conductance. Here even at relatively small anodic current densities (~0.1 amp./sq. cm.) the reduction reaction

$$Th + Th\,Cl_4 (melt) \rightleftarrows 2\,Th\,Cl_2 (melt)$$

is suppressed, and the dissolving of the metal proceeds as the result of forming Th^{4+} ions without noticeable polarization. We made use of this phenomenon in one of our studies to determine the decomposition potential of molten thorium tetrachloride [3].

Ural Branch of the
Academy of Sciences of the USSR

Received March 13, 1957

LITERATURE CITED

[1] M. V. Smirnov, S. F. Palguev and L. E. Ivanovsky, J. Phys. Chem.(USSR), 29, 774 (1955).

[2] M. V. Smirnov and L. D. Yushina, Bull. Acad. Sci. USSR, Div. Chem. Sci., 1956, 1285.*

[3] M. V. Smirnov and L. E. Ivanovsky, J. Phys. Chem. (USSR), 31, 140 (1957).

* Original Russian pagination. See C.B. Translation.

ON THE MECHANISM OF ACTION OF REAGENTS IN THE FLOTATION PROCESS

V. I. Klassen and L. P. Starchik

(Presented by Academician P. A. Rebinder, March 25, 1957)

Already in the early researches on the theory of flotation attention has been drawn to the specific role played by the linear zone of contact between the three phases. P. A. Rebinder pointed out that it is in this zone that one must look for the elucidation of the molecular mechanism of action of flotation reagents on the adhesion of mineral particles to air bubbles [1]. Ostwald suggested that collector-reagents are preferentially absorbed along the boundary line between the three phases; particularly suitable for this purpose are reagents the molecules of which possess a "triphilic" structure, i. e. groups which possess an affinity, respectively, for the mineral, water and air [2]. Such molecules would be expected to undergo preferential fixation in the boundary separating the three phases. Bradley has disucussed the phenomena of linear tension and linear adsorption in three-phase boundaries, and D. Talmud established experimentally that non-polar reagent-oils form a thin thread along the phase boundary [3].

None of these theories have ever been confirmed experimentally, especially with reference to froth flotation, and have therefore never been given practical consideration by most workers in the field.

Fig. 1. Trace of a drop of an aqueous xanthate solution on the surface of a galena particle.

Among other things, if it were possible to show that there is an increase in concentration of the collector-reagent molecules in the three-phase boundary, it would be possible to explain largely the mechanism of fixation of mineral particles on air bubbles, the cause of the molecular hysteresis of wetting [1], as well as the fact that flotation can take place at very low reagent concentrations. The experimental proof of the above theories may, thus, provide a positive contribution to the development of the theory of flotation processes and, consequently, of flotation practice.

Previous investigations carried out by I. N. Plaksin and ourselves [4] have proved that part of the hypothesis which concerned the behavior of reagents which are difficultly soluble in water. When the surface of a given mineral is sufficiently hydrophobic, droplets of such reagents instantly distribute themselves along the three-phase boundary forming a continuous thread. This leads to a considerable increase in the force of adhesion of the mineral particles to air bubbles. The presence of such reagents markedly increases the upper size limit of particles of bituminous coal, native sulfur and like minerals which can pass into the froth during flotation.

The experiments described here have proved that the more important collector-reagents the molecules of which possess a heteropolar structure, are likewise present in increased concentration in the three-phase boundary.

As a representative of this type of reagents we have chosen potassium ethyl xanthate labeled with the radioactive sulfur isotope S^{35}, while the mineral used was galena • Microautoradiography was used as the principal method of investigation [5].

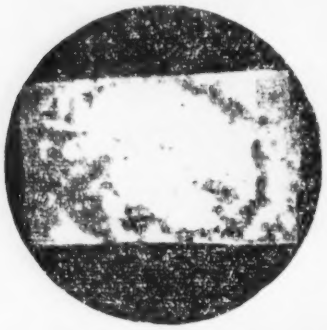

Fig. 2. Trace of an air bubble which adhered to a galena particle immersed in an aqueous solution of a xanthate.

In the first series of experiments large galena crystals with well-formed planes of adhesion were placed in such a way that one of the planes was exactly horizontal. Droplets of an aqueous solution of the xanthate (concentration 50 mg/l) were placed on this plane by means of a pipette. After 2 minutes the droplet was removed by means of filter paper. The mineral particle was then placed on the sensitized side of a photographic film, and after exposure for a determined period the film was developed. In nearly all cases it was possible to observe the appearance of a dark border along the former contour line of adhesion of the droplet (see Fig. 1), which is evidence for the preferential concentration of xanthate molecules in that zone.

The second series of experiments still more corresponded to conditions of the flotation process. The galena particle was immersed in the same xanthate solution. After 1-2 seconds an air bubble was placed on a face of the particle. After 1 to 2 minutes the particle was removed from the solution and dried carefully and an autoradiograph of its treated surface was then taken. The experiments showed that under these conditions the molecules of the radioactive xanthate were again concentrated along the three-phase boundary (Fig. 2).

From these experiments it may therefore be concluded that the concentration of molecules of collector-reagents is higher in the three-phase boundary zone than on other parts of the surface of the mineral particles; this should be taken into account in future investigations of the theory of flotation processes.

Institute of Mining
Academy of Sciences of the USSR

Received March 14, 1957

LITERATURE CITED

[1] P. A. Rebinder et al., Physical Chemistry of Flotation Processes, Moscow, 1933; P. A. Rebinder, Bull. Acad. Sci. USSR, Dept. Math. and Nat. Sci, Ser. Chem. 5, 703 (1946)

[2] W. Ostwald, Koll. Zs., 1, 58, H. 2, 179 (1932).

[3] D. Talmud, J. Phys. Chem., 22, No.8, 812 (1931).

[4] V. I. Klassen and I. N. Plaksin, Proc. Acad. Sci. USSR, 95, No. 4 (1954).

[5] I. N. Plaksin, R. Sh. Shafeev and S. P. Zaitseva, Proc. Acad. Sci. USSR 108, No. 105 (1956).

• Experiments with the droplets were carried out by V. V. Troitsky.

PASSIVATION AND DEPASSIVATION OF THE LEAD ANODE IN CONCENTRATED HYDROFLUOSILICIC, PERCHLORIC AND HYDROFLUOBORIC ACIDS

M. M. Nikiforova and Z. A. Iofa

(Presented by Academician A. N. Frumkin, March 28, 1957)

In recent years a number of investigations have been reported in the literature concerning the electrochemical system PbO_2/ acid/ Pb with fairly concentrated perchloric, hydrofluosilicic and hydrofluoboric acids as the electrolyte [1]. Such cells work at low temperatures and generate high discharge currents. However, the behavior of the lead anode and the conditions under which it is passivated in the acids mentioned have not been investigated in detail.

In the investigation of the passivation of lead (C-O) described here we used distilled perchloric acid, hydrofluosilicic acid containing 47% of H_2SiF_6, 0.14% of SiO_2, 0.01% of SO_4 and traces of As. Hydrofluoboric acid was prepared from chemically pure H_3BO_3 and HF and had the following composition: HBF_4 49.5%, H_3BO_3 3.04%, Pb 0.1%. The experiments were conducted in polystyrene cells kept in special thermostats (temperature variation did not exceed ± 0.5°). The anode potential was measured by the compensation method or by means of a cathode voltmeter with reference to a non-polarizing PbO_2 electrode in the same acid solution.•

In solutions of acids at the concentration given, and at constant temperature, the lead anode remains active and undergoes little polarization if the anodic current density (i_a) does not exceed a certain definite critical value (i_{cr}) which depends on a number of factors. The experiments showed that the period at the end of which the anode begins to undergo passivation (t_p) depends on the density of the passivation current selected and can be expressed over the time interval, t_p, of from a few seconds to $1\frac{1}{2}$ hours sufficiently accurately by the well-known equation $\log t_p = A - B \log i_a$, where A and B are constants.

Lowering the temperature in all cases sharply decreases the value of i_a at which the anode undergoes passivation in the same period. When the concentration of the acid is considerably lowered this current density increases markedly. Lead undergoes passivation most easily in H_2SiF_6. In $HClO_4$ and HBF_4 at $t > -20°C$ and $i_a < 100$ ma / cm^2 no passivation of lead takes place.

The initial stage of passivation is, undoubtedly, a diffusion process. From this it follows that, other things being equal, mixing of the electrolyte (by rotation of the disc-shaped electrode) should increase the time interval which elapses before passivation sets in. For example, in 7.9 N H_2SiF_6 at a current density of $i_a = 40$ ma/cm^2 and at a temperature of $t = -20°$ the following results were obtained:

No. of revs./ min.	No mixing	300	450	520	650	800
t_p, min.	0.86	3.26	7.25	13.3	34	60

At current densities greater than the critical density ($i_a > i_{cr}$) the rate of ionization of lead is greater than the rate of transport of Pb^{2+} ions and their rate of diffusion into the solution under the influence of the concentration gradient set up. As a result, the concentration of Pb^{2+} ions increases and there is formed a porous layer

• The potential of the PbO_2 electrode as measured in 7.9 N H_2SiF_6 at 25° is equal to 1.774 v, referred to the normal hydrogen electrode.

of the poorly conducting divalent lead salt of the given acid. The current density and the potential in the pores of the layer increase sharply and a passivating layer of PbO_2 is formed on these parts of the electrode.

In Fig. 1 is shown a typical curve representing the variation of the potential with time during passivation of a Pb anode in 7.9 N H_2SiF_6 at a current density of 40 ma/cm² and at a temperature of –10°, in the absence of mixing. In the initial stage of passivation the potential rises sharply on account of the resistance of the salt layer, while the current drops from 40 to 5 ma/cm². Subsequently, as a result of the formation in the pores of PbO_2 which exhibits good electric conductivity [2], the passage of the current can go on with the evolution of oxygen. The potential drops and the current increases to its initial value. The layer of PbO_2 which brings

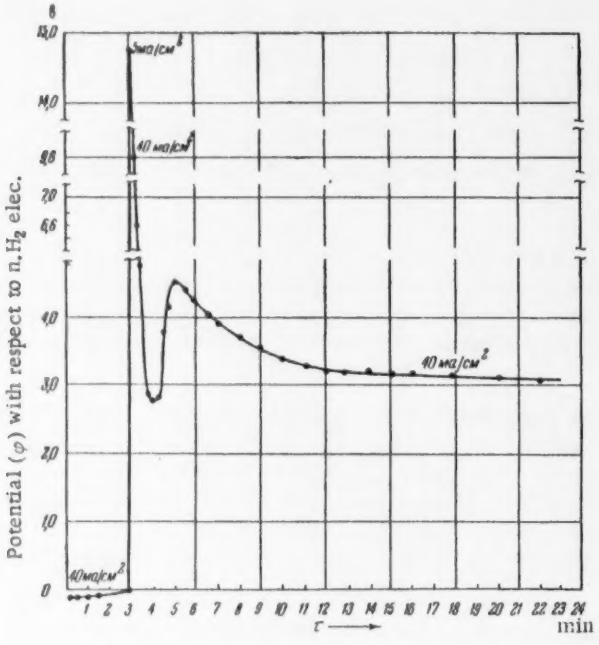

Fig. 1. Variation of the potential with time during passivation of a lead anode in 7.9 N H_2SiF_6 at t = – 10°.

about passivation, rapidly spreads over the entire area of the electrode while the layer of the lead salt as it is not replenished, dissolves rapidly in the acid and a potential is set up which corresponds to the oxygen overvoltage on PbO_2 at the given current density $i_a > i_{cr}$.

In Fig. 2 are plotted depassivation curves obtained after elimination of the passivation current of a lead anode which has been passivated in 7.9N H_2SiF_6 at a current density of i_a = 40 ma/cm² and at a temperature of t = – 10° and kept, after passivation, at the same current density for periods of 1, 2, 4, 6 and 8 minutes. From this diagram it follows that after elimination of the passivation current the potential drops rapidly to a value of φ = 0.70 to 0.66 v, referred to the normal hydrogen electrode. This value, which is characteristic of the potential of the passivated lead, is maintained for periods which increase with increasing length of time during which the current was passed through the passivated anode.

Rotation of the electrode shortens the time required for depassivation; for example, at 700 revs./min. the time of depassivation is shortened by approximately one half.

If, after passivation, currents of low density ($i_a < i_{cr}$) are passed through the lead anode, the potential is maintained for some time at the value indicated (φ = 0.70–0.66 v referred to the normal hydrogen electrode); for example, when a current at a density of 40 ma/cm² was passed through the anode for four minutes the state of passivation was subsequently maintained at the potential mentioned for periods of 15, 27, and 40 minutes when the current density was, respectively, 1, 4 and 5 ma/cm².

At current densities $i_a > 6$ ma/cm² the potential increases to a value which corresponds to evolution of oxygen (~2.2 v).•

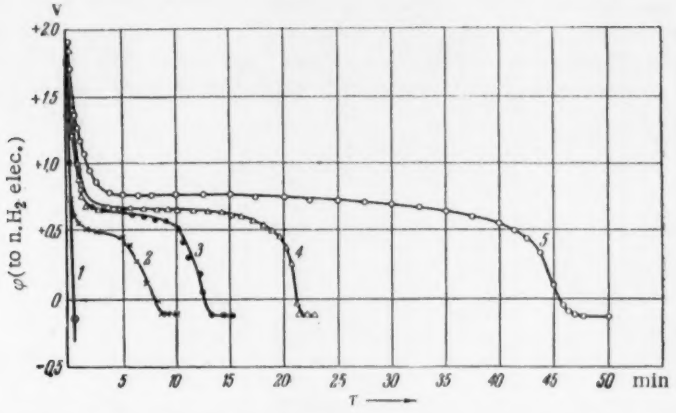

Fig. 2. Variation of potential with time during depassivation of a lead anode in 7.9 N H_2SiF_6 at a temperature of t = – 10° after the passivated anode has been maintained under a current density of 40 ma/cm² for different periods: 1) 1 min., 2) 2 min., 3) 4 min., 4) 6 min., 5) 8 min.

The potential of passivated lead indicated above is close to the value of 0.666 v quoted by Lander [4] for the reaction $Pb + 2H_2O = PbO_2 + 4H^+ + 4e$. If we accept this reaction for the system with lead in the passivated state we have to assume that it is the porous layer of PbO_2 in contact with the pure surface of lead metal which is responsible for the passivation. On this basis depassivation consists of the discharge of the short-circuited galvanic cell PbO_2/ acid/ Pb, the corresponding reactions being: at the anode, $Pb + SiF_6^{2-} \longrightarrow PbSiF_6 + 2e$; at the cathode, $PbO_2 + 2e + SiF_6^{2-} + 4H^+ \longrightarrow PbSiF_6 + 2H_2O$.

From results of these experiments it is possible to conclude that as the period during which the passivated anode is maintained under constant current density ($i_a > i_{cr}$), is increased, the thickness of the PbO_2 layer increases, as does the length of the pores while their diameter decreases, as a result of which diffusion of the reaction products in the pores becomes more difficult and the time necessary for depassivation of the anode increases (see Fig. 2).

When the density of the anodic current is less than the critical density ($i_a < i_{cr}$), the rate of depassivation is slowed down, which, apparently, is due to the slower rate of reduction of PbO_2 at the cathode, as also due to the increased ohmic resistance of the working galvanic cell resulting from the increase in the concentration of lead ions in the pores of the passivating layer.

Potentiostatic determinations of the current have also been carried out at constant potential. The lead anode was passivated in 7.9 N H_2SiF_6 at a current density of 40 ma/cm² at a temperature of – 10°, and was then maintained under the same current density for different lengths of time (4, 8 and 12 mins.). By a corresponding reduction of the current density the voltage was decreased to about 0.75 v and was then increased gradually and at the same time the current was measured when stationary conditions were reached. The results of these measurements are plotted in Fig. 3. From these curves it follows that in order to maintain the previously passivated anode

• Before the potential attains the value corresponding to that at which oxygen begins to evolve (~2.1 v) under the conditions of experiment, the current density being equal to 6 ma/cm², a horizontal portion appears on the curve $\varphi(\tau)$ at a potential of $\varphi = 1.15$ v. According to Lander [4] the potential of the system $PbO + H_2O = PbO_2 + 2H^+ + 2e$ is equal to 1.100 v; it may, therefore, be assumed that before the potential attains the value corresponding to the evolution of oxygen, under conditions when $i_a > i_{cr}$, metallic lead within the pores becomes coated with a layer of PbO or the bivalent lead salt, both of which are rapidly transformed to PbO_2.

at a constant potential within the range of from 0.8 to 2.2 v it is necessary to have a constant anodic current. At potentials less than 0.8 v the current tends to decrease as a result of depassivation, while at potentials greater than 2.2 v oxygen begins to evolve and the current increases sharply with increasing potential. Since the constant current observed over the range of potentials from 0.8 to 2.2 v prevents depassivation, it may be identified with the corrosion current from the galvanic pair PbO_2-Pb. Decreasing the corrosion current and lengthening the period during which the passivated electrode is kept in the system under high current densities ($i_a > i_{cr}$) results in an increase in the thickness of the passivating layer and in greater resistance of the galvanic pair (see Fig. 3). The fact that the corrosion current remains constant over a wide range of potentials is, evidently, also due to a proportional increase in the thickness of the passivating layer and in the length of the pore channels with increasing potential in the range stated.

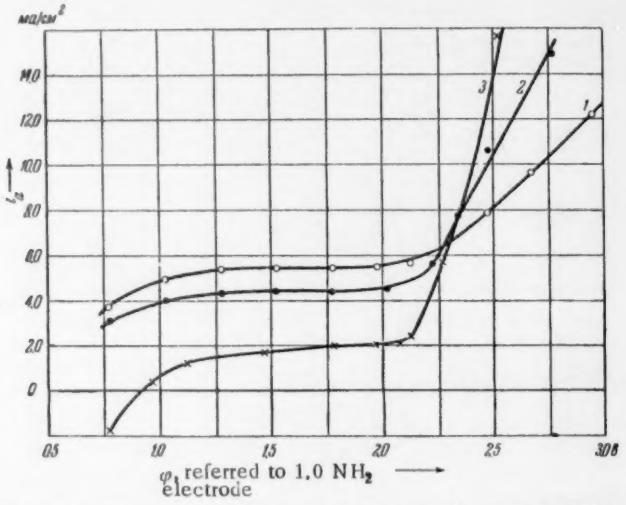

Fig. 3. Current density, determined by the potentiostatic method, as a function of the potential of passivated lead in 7.9 N H_2SiF_6 at $-10°$ after it has been maintained, under a current density of 40 ma/cm² for different periods following passivation: 1) 4 minutes; 2) 8 minutes; 3) 12 minutes.

Passivation of lead in concentrated H_2SiF_6 resembles, to some extent, the passivation of iron in sulfuric or nitric acids described by Bonhoeffer and coworkers [3, 5]. However, as follows from this investigation, the mechanism by which the passive state of the lead anode is maintained and the process of its passivation are different. The difference lies, in the first instance, in the fact that in the case of iron the steady anodic current necessary to maintain the state of passivation is three orders of magnitude lower than in the case of lead in H_2SiF_6 and is used up to form iron oxide which dissolves at a constant rate, and not to counteract the work of the galvanic pair consisting of the porous layer of lead dioxide, acid and metallic lead.

Research Institute for Electrochemistry

Received March 28, 1957

LITERATURE CITED

[1] J. P. Schrodt, W. J. Otting, J. O. Schoeger, D. N. Craig, Trans. Electrochem. Soc., 90, 405 (1946); J. C. White, W. H. Power, R. L. McMartrie, R. T. Rierce, Trans. Electrochem. Soc., 91, 73 (1947); G. W. Vinal, Primary Batteries, N. Y., 1950, p. 282-303; A. B. Garrett, J. Welsh et al., J. Phys. and Coll. Chem., 53, No. 4, 505 (1949).

[2] U. B. Thomas, Trans. Electrochem. Soc., 94, No. 2, 43 (1948).

[3] K. Bonhoeffer, U. Franck, Zs. Elektrochem., 55, 80 (1951).

[4] J. J. Lander, J. Electrochem. Soc., 103, No. 1, 1 (1956).

[5] U. F. Franck, K. Weil, Zs. Elektrochem., 56, 814 (1952); A. M. Sukhotin, Prog. Chem. 25, No.3, 314 (1956).

INVESTIGATION OF THE KINETICS OF SHEAR DEFORMATION IN AQUEOUS SOLUTIONS OF GLYCERINE, SACCHAROSE AND XYLITOL

L. V. Khailenko

(Presented by Academician P. A. Rebinder, March 28, 1957)

In 1953 we had demonstrated [1] that the flow curves $\epsilon = \varphi(\tau, P)$ for aqueous glycerine do not correspond to a Newtonian liquid, but rather resemble those of solutions of high molecular compounds [2]. The existence of an elastico-viscous region on the flow curve of glycerine has been confirmed by the work of A. Korotkova and D. Sandomirsky who in 1955 observed this effect when investigating glycerine in the Veiler-Rebinder elastometer [3].

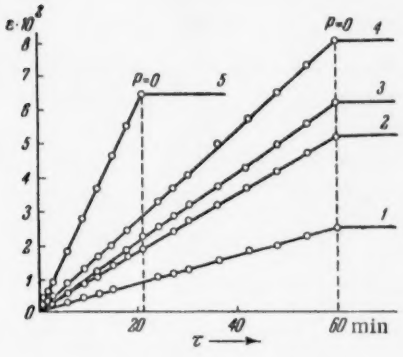

Fig. 1. Dependence of shear deformation on the shearing period for 100% glycerine. 1) P = 0.0002; 2) P = 0.0004; 3) P = 0.0006; 4) P = 0.0008; 5) P = 0.002 dynes/cm².

Since the results obtained were rather unexpected, it was of interest to investigate in greater detail the rheological properties of glycerine and of its aqueous solutions over a sufficiently wide range of concentrations, as well as the behaviour of aqueous solutions of hydroxyl-containing compounds, because the hydroxyl group may be responsible for the above-mentioned anomaly in the properties of these solutions owing to hydrogen bonding. As our objects of investigation we have chosen aqueous solutions of saccharose and of the pentahydric alcohol, xylitol.

The elastico-viscous properties of anhydrous and aqueous glycerine as well as those of the solutions mentioned were investigated in the highly sensitive Shvedov elasto-viscosimeter which permits experimentation at shear stresses of 0.0002 dynes/cm² and above [1, 4].

The experiments showed that pure, anhydrous glycerin behaves over the given range of shear stress as a true Newtonian liquid. The flow curves $\epsilon = \varphi(\tau, P)$ are illustrated graphically by straight lines which show no reversal after the load is taken off (Fig. 1). When glycerine is diluted with water its visco-elastic properties change sharply. Already in the case of the 95% solution is there a distinct elasticity in the system. On further dilution the visco-elastic constants increase, reaching a maximum in the case of the 70% solution.

In Fig. 2 are represented flow curves $\epsilon = \varphi(\tau, P)$ obtained for the 80% solution which are typical for the system glycerine-water in the concentration range investigated.

The equilibrium modulus $E = \frac{P}{\epsilon_m}$, calculated from the corresponding curves $\epsilon = \varphi(\tau, P)$, varies with the concentration of the solution as follows:

Concentration, %	80	70	60
E, dynes/cm²	0.03	300.0	80.0

Flow curves $\epsilon = \varphi(\tau, P)$ were recorded for a 50% aqueous saccharose solution at shear stresses of from P = 0.0002 to 0.002 dynes/cm^2 (see Fig. 3).

The curves representing shear deformation as a function of the shearing period, shown in Fig. 3, indicate that the solution in question exhibits elasticity characteristic of solutions of high molecular compounds and observed by us in the system glycerine-water.

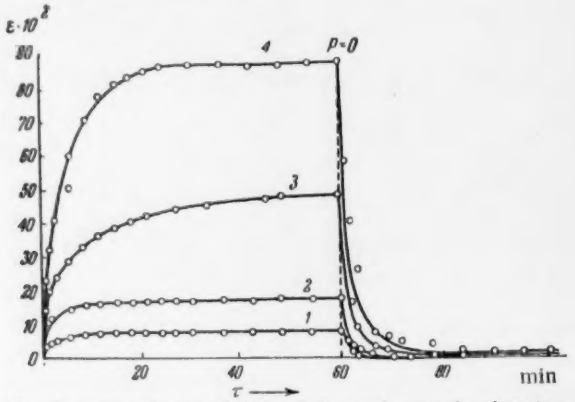

Fig. 2. Dependence of shear deformation on the shearing period for 80% aqueous glycerine solution. 1) P = 0.0021; 2) P = 0.0043; 3) P = 0.0064; 4) P = 0.0085 dynes/cm^2.

On heating the solution to 100° the continuous structural network which is responsible for the visco-elastic properties of the system is destroyed, but is restored when the solution is again cooled to 20°.

In a similar manner the 50% aqueous solution of xylitol was investigated. The flow curves were plotted at different shear stresses varying from 0.002 to 0.008 dynes/cm^2 at a temperature of 20°.

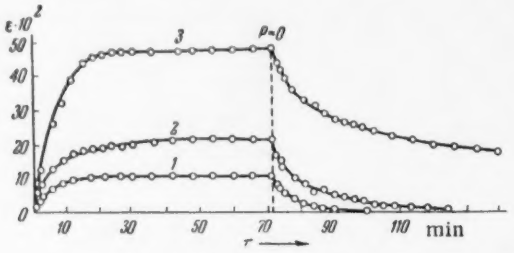

Fig. 3. Dependence of shear deformation on the shearing period for 50% aqueous saccharose solution. 1) P = 0.0002; 2) P = 0.0004; 3) P = 0.0007 dynes/cm^2.

In all cases the curves obtained are similar to those recorded for aqueous solutions of glycerine and saccharose (Fig. 4).

From the data obtained it is possible to draw the following conclusions:

(1) Concentrated aqueous solutions of glycerine, saccharose and xylitol are not true Newtonian liquids as has been thought hitherto, but exhibit elasticity characteristic of solutions of high molecular compounds.

(2) The formation, in the solutions investigated, of mechanically rigid and elastico-viscous structures may be explained as being due to hydrogen bonding in these systems, with the formation of long quasi-polymeric macromolecules which are characterized by time-dependent highly elastic deformation – a behavior necessitating the concept of an equilibrium or limiting modulus of elasticity.

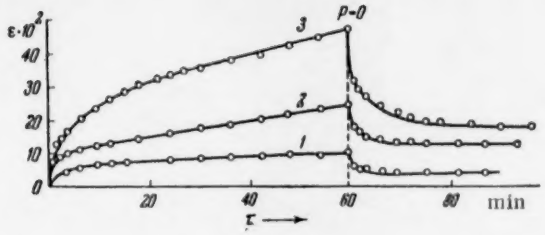

Fig. 4. Dependence of shear deformation on the shearing period for 50% aqueous xylitol solution. 1) P = 0.0021; 2) P = 0.0043; 3) P = 0.0085 dynes/cm².

(3) The structures formed in the liquids investigated are thixotropic and visco-elastic in nature, the forces of cohesion between individual elements of the structures being small. The structures appear to occupy an intermediate region between coagulation and condensation structures which form the subject of investigation of contemporary colloid chemistry [5, 6].

(4) The application of highly sensitive viscometric methods, realized by means of the Shvedov viscosimeter, permits the investigation of extremely subtle features of intermolecular interaction which in this case manifests itself in the formation of a mechanically rigid structural framework.

Institute of General and Inorganic Chemistry
Academy of Sciences of the Ukrainian SSR

Received January 14, 1957

LITERATURE CITED

[1] I. A. Dumansky and L. V. Khailenko, Colloid J. 15, 426 (1953). •

[2] A. S. Kolbanovskaya and P. A. Rebinder, Colloid J., 12, 194 (1950).

[3] A. Korotkova and D. Sandomirsky, Colloid J., 17, 264 (1955). •

[4] F. N. Shvedov, J. Phys., 8 (2), 341 (1889).

[5] P. Rebinder, Disc. Farad. Soc., No. 18 (1954); Proc. Third All-Union Conference on Colloid Chemistry, (1957)••

•Original Russian pagination. See C.B. Translation.
••In Russian.

PROCEEDINGS OF THE ACADEMY OF SCIENCES OF THE USSR

Section: PHYSICAL CHEMISTRY

Volume 115, Issues 1-6

July-August, 1957

TABLE OF CONTENTS

(Continued)

TABLE OF CONTENTS (Continued)

GLASS AND CERAMICS

in complete English translation:

WHAT IS IT ? It's a cover-to-cover translation of "Steklo i Keramika", the Soviet monthly journal published for their glass and ceramics researchers, technologists and production workers. It's your open sesame to the latest technical advances fresh from the laboratories and factories of the USSR . . . over 500 pages of important reports on up-to-the-minute research . . . significant developments in new techniques . . . latest production methods . . . new theories . . .

DON'T WASTE PRECIOUS MAN- AND EQUIPMENT HOURS in costly duplication of research. Scientists returning from international conferences report the Soviets are forging ahead in all fields of research. Find out for yourself how they are upgrading products and improving processes . . . how they are solving refractory corrosion . . . grinding away their melting problems . . . designing unique, improved equipment . . . breaking production records and reducing costs. Take advantage of the intensified Soviet research program.

CAN YOU AFFORD TO BE WITHOUT GLASS AND CERAMICS ? Don't underestimate the importance of being informed on how these and other problems are being solved in the Russian counterparts of your own laboratories and factories. GLASS AND CERAMICS, completely and accurately translated by the C. B. staff of bilingual scientists, puts this information at your fingertips. A yearly subscription – 12 complete issues – costs far less than individual ordered translation of only two or three articles.

BE ASSURED OF COMPLETE HOLDINGS OF GLASS AND CERAMICS– place your order now! This "must" for your library will maintain the same superior standards for which C. B. translations have become known the world over – translation by scientists for scientists – reproduced from typewritten copy by the multilith process – all photographs, charts and tabular material accurately reproduced – each issue staple-bound with durable paper cover. Each issue will be mailed to subscribers immediately upon publication. Your investment for an annual subscription, 12 issues, is a moderate . . . . . $ 80.00

Single issues 20.00
Individual articles 7.50

CONSULTANTS BUREAU INC.
227 West 17th Street, New York, N. Y.